

**Characterization of Large Earthquakes on the San
Andreas Fault in the Carrizo Plain: Implications
for Fault Mechanics and Seismic Hazard**

Thesis by
Lisa Baugh Grant

In Partial Fulfillment of the Requirements
for the Degree of
Doctor of Philosophy

California Institute of Technology
Pasadena, California
1993

(Defended May 18, 1993)

© 1993

Lisa Baugh Grant

All rights reserved

For Stanley
with love and thanks

"The heavens are telling the glory of God;
and the firmament proclaims his handiwork."

Psalm 19:1, RSV

Acknowledgments

I would never have made it to this point in my career and thesis without the help of many fine people. To thank each of them *properly* would require writing an entire chapter entitled "Thank You!". This is a shortened version of the chapter I would write if time and space permitted. I apologize for inevitable omissions.

I have learned much scientifically, professionally and personally from my thesis and research advisor, Kerry Sieh. I thank him for his guidance, enthusiasm and support, especially regarding my adventures with pregnancy and motherhood. By allowing me the freedom to juggle my time and work arrangements in unorthodox ways, he helped me to complete my thesis without changing my original 4-year goal. I hope that he shares some of my satisfaction in accomplishing this!

My academic advisor, Lee Silver, provided excellent advice as well as abundant enthusiasm and support at critical times. Such important contributions cannot be overestimated.

My first thesis advisor, Norman Brooks, convinced me to do graduate work at Caltech. I greatly appreciated his empathy, advice and support of my decision to pursue a Ph.D. in geology rather than environmental fluid mechanics. I also thank him for teaching me lots of environmental engineering.

Experiences and encounters with Bob Sharp have been highlights in my education at Caltech. His field trips reminded me of the real motivation behind my research: love of geology! Bob's example of unselfish service to others is a quality that I have rarely seen outside of churches, and not often enough there. Mahalo!

Thanks to Prof. Leigh Royden for leading the discussion series on women in science, for practical advice (get a babysitter!) and for Erika's crib and port-a-crib. I especially appreciated her willingness to share her personal experiences, positive and negative, with other women trying to juggle the same tasks.

The Caltech faculty, as a group, have enriched my life by teaching me interesting things, opening my mind to new possibilities, and occasionally forcing me to grow by requiring that I perform tasks which I thought were impossible. Thanks are due to many faculty members in all options of the Division of Geological and Planetary Sciences, Environmental Engineering, and Civil Engineering. Ron Scott, of civil Engineering, deserves special mention for helping me prepare for my candidacy exam in geology, and allowing me to audit his soil mechanics classes.

Thanks to my thesis committee for constructive comments and being generally supportive of my progress. Critical reviews by Ray Weldon, Steve Wesnousky, John Sims and Judy Zachariasen are also appreciated.

The competent, cheerful assistance of numerous Caltech staff members is acknowledged and appreciated. Special thanks to Kerry Etheridge and Mary Mellon for fielding long distance requests for help, to Ann Freeman for supportive gestures and prayers, to Marilee Manley-Wagner for taking care of unusual field requirements (e.g., petty cash reimbursement for shower curtains, no questions asked), to Anne Lilje for getting me out of numerous computer jams, to Meg Garstang, Russ Giambelluca and Terry Gennaro for help with field logistics, and *especially* to Jan Mayne for help with figures and supportive words in the homestretch.

The field data was collected with the assistance of Heidi Anderson, Manuel Berberian, Stefanie Brachfeld, Steve Bryant, Stanley Grant, Greg

Holk, Ken Hudnut, Linda Maepa, Sally McGill, Elizabeth Nagy, Carol Prentice, Jeff Ritchie, Theresa Roberts, Kerry Sieh, Mike Slates, Rob Spieler, Andy Thomas, Tim Wacholz, Katryn Wiese and D.J. Wood. I thank them all for their hard work, talent, friendship and support. Extra thanks to Heidi and Mike for persevering with good humor and sharing the delights of "tea time" in the August inferno. Research with Andrea Donnellan was a nearly perfect example of how scientific collaboration is supposed to work. I learned a lot and enjoyed it. Thanks!

I thank Leonard Bidart of Bidart Brothers, and Arthur J. Phelan, for permission to excavate and explore their property. The Nature Conservancy and BLM provided valuable information. Larry Vredenburgh of the Bakersfield/Caliente BLM told me about the 1855 surveys in the Carrizo Plain, and compiled some maps with dates and locations of early surveys. Thanks to Jay Satalich and Paul Dunham of Caltrans for their time and the loan of two GPS receivers. Thanks to Mike McGee of McGee Surveying, and the San Luis Obispo County Surveyor's office. Backhoe operators from D&L Construction did precision digging and helped with shoring.

Most radiocarbon samples were dated by the NSF Acelerator Facility at the University of Arizona and were partially funded by NSF grant EAR85-12761. Thanks to Doug Donahue, Larry Toolin, Tim Jull and Rosemary Maddock for answering questions. I thank M. Stuiver at the University of Washington Quaternary Isotope Lab for a high precision radiocarbon date. Thanks also to the University of Toronto IsoTrace lab for dating one sample.

This research was funded primarily by USGS grants 14-08-0001-G1370, 14-08-0001-G1789 and 1434-93-G-2331. The Wild TC2000 Total Station used to survey all the trenches and to collect elevations for topo maps was purchased with a grant from the W.M. Keck Foundation. Wildsoft surveying software

was donated by Wild. Additional support was provided by an Anthony Fellowship, F. Beach Leighton Fellowship and a grant from the Caltech Earthquake Research Associates. Thanks also to Woodward-Clyde Consultants for allowing me to work just a few hours a week during the last months of writing this thesis.

The support of family and friends has been invaluable throughout my adventures at Caltech. My office mates were good company and tolerated my eccentricities and baby pictures without complaint. Many friends cheered me on, propped me up, and entertained me. Special thanks to Jonathan Fay, Yigal and Osnat Erel, Laura Jones, Sally McGill, Sandra Carmel Katz, Eme Burt, and Andrea Donnellan. Grandpa taught me the value of hard work and education. Nana offered numerous prayers for health, happiness and progress. Mom and Dad were always there when I needed them (which was frequently!). Mark visited often, and Ken and Susan donated carloads of baby clothes and paraphernalia. Maudie cooked sumptuous feasts for family gatherings and provided emergency lodging when needed. George and Donna were supportive of career and parenting efforts, and trusted me enough to follow me down the Grand Canyon on a mule. Sofia Eodinger provided surrogate grandmothering for Erika which freed me mentally and physically for this task, until her very last hour. She is greatly missed. Erika motivated me to work as efficiently as possible, reminding me of her imminent arrival with swift kicks whenever I wasted time. She has added joy and balance to my life.

This thesis would not have been possible without the love, support and assistance of my husband, Stanley. I especially appreciate the gifts of time and babysitting in the last few weeks. His contributions to this work are too numerous to count. I am deeply grateful.

Abstract

Despite the widespread use of geomorphic offset measurements for calculating earthquake probabilities, little attention has been paid to either the uncertainties in the interpretation of offset geomorphic features, or the effects of these uncertainties on fault models and estimates of seismic hazard.

Interpretation of offsets along the San Andreas fault in the Carrizo Plain have been the basis of hypotheses of a strong Carrizo fault segment which regularly breaks in great earthquakes several centuries apart with dextral surface slip on the order of 10 m per event.

The smallest geomorphic offset measurements along a 6 km stretch of the fault southeast of Wallace Creek vary between ~6.5 m and ~10 m. A 3-D excavation of alluvial deposits at the Phelan fan shows that at least 6.6 to 6.9 m of dextral slip occurred during the 1857 Fort Tejon earthquake, and that the penultimate earthquake occurred several centuries prior to 1857. Thus, either the amount of surface slip varied several meters over a 2-3 km stretch of the fault in 1857, or 2 to 3 meters of slip in a penultimate earthquake was followed by ~7 m of slip in 1857.

Two monuments from an 1855 survey which spans the San Andreas fault in the Carrizo Plain have been displaced 11.0 ± 2.5 m right-laterally by the great earthquake of 1857. This magnitude of offset is consistent with geomorphic indications that slip across the fault during the 1857 earthquake and associated foreshocks and aftershocks varied from 6.6 to 10 m over 2.6 km along this section. Comparison of recent geodetic measurements with the late Holocene slip rate at Wallace Creek shows that fault slip rates determined from short-term wide aperture measurements are indistinguishable from rates determined from long-term narrow aperture measurements. Using

radiocarbon dates of the penultimate large earthquake and measurements of slip in 1857, we calculate an average slip rate for the last complete earthquake cycle that is at least 25% lower than the late Holocene slip rate on the main fault trace. This suggests that variation in fault slip during the 1857 earthquake left a slip deficit in at least the upper 1km of crust at Wallace Creek. Slip in future earthquakes may compensate this deficit.

Three trenches across the San Andreas fault on the Bidart fan in the Carrizo Plain record evidence of 7 previous earthquakes. Radiocarbon dating indicates five earthquakes, including the 1857 earthquake, have occurred since A.D. 1218. The penultimate earthquake, event B, occurred between 1405 and 1510 A.D. Several centuries before 1857, events B, C, D and E occurred in a temporal cluster after approximately 1218 A.D. and prior to 1510 A.D. The average recurrence interval within this cluster ranges from 73 to 116 years, depending on assumptions. Events B and D may correlate with prehistoric earthquakes recorded in sediments elsewhere along the southern San Andreas fault. Events C and E appear to have ruptured locally in smaller magnitude earthquakes. Surface slip from either event B, or events B and C combined, totals 7 to 11 m.

If fault strength is defined by long earthquake repeat time, then the Carrizo segment of the San Andreas is not inherently stronger than the Mojave segment. The temporal and spatial distribution of large earthquakes on the San Andreas fault is difficult to reconcile with slip-based theories of segmentation of strike-slip faults. Temporal patterns of seismicity may be more robust than spatial trends. Clusters of large earthquakes analogous to sequences of foreshocks, mainshocks and aftershocks may occur on longer time scales of seismic "supercycles."

Table of Contents

Title Page.....	i
Copyright.....	ii
Dedication.....	iii
Acknowledgments.....	iv
Abstract.....	viii
Table of Contents.....	x
List of Figures, Tables and Plates.....	xii
Chapter 1: Introduction.....	I-1
Purpose.....	I-1
The Study Area.....	I-3
Organization of the Thesis.....	I-3
References.....	I-8
Chapter 2: Stratigraphic Evidence for Seven Meters of Dextral Slip on the San Andreas Fault During the 1857 Earthquake in the Carrizo Plain.....	II-2
Abstract.....	II-2
Introduction.....	II-2
Site Description.....	II-11
Excavation.....	II-11
Stratigraphy.....	II-14
Correlation of Channels.....	II-19
Measurements of Offset.....	II-20
Number of Faulting Events.....	II-23
Dating of Units and Faulting.....	II-27
Discussion.....	II-32
Acknowledgments.....	II-37

References.....	II-38
Chapter 3: 1855 and 1991 Surveys of the San Andreas Fault: Implications for Fault Mechanics.....	III-1
Abstract.....	III-2
Introduction.....	III-2
The Rectangular Survey System.....	III-5
Survey and Error Analysis.....	III-8
Results.....	III-13
Implications.....	III-13
Acknowledgments.....	III-21
References.....	III-22
Chapter 4: Paleoseismic Evidence of Clustered Earthquakes on the San Andreas Fault in the Carrizo Plain, California.....	IV-1
Abstract.....	IV-2
Introduction.....	IV-3
Site Selection.....	IV-6
The Bidart Fan.....	IV-7
Methods.....	IV-11
Trench 2 : The Penultimate Earthquake.....	IV-16
Structure and Stratigraphy.....	IV-16
Evidence of Earthquakes.....	IV-21
Event A: The Fort Tejon Earthquake.....	IV-21
Event B: The Penultimate Earthquake.....	IV-22
Event C.....	IV-28
Radiocarbon Dating of Event B.....	IV-29
Trenches 3 and 4: Older Events.....	IV-32
Structure and Stratigraphy.....	IV-33

Evidence of Earthquakes.....	IV-41
Event A.....	IV-41
Event B.....	IV-56
Event C.....	IV-57
Event D.....	IV-63
Event E.....	IV-64
Graben Growth During Events A - E.....	IV-65
Event F.....	IV-66
Event G.....	IV-67
Radiocarbon Dating of Beds and Earthquakes.....	IV-67
Average Recurrence Intervals.....	IV-70
Correlation of Earthquakes.....	IV-76
Discussion.....	IV-80
Acknowledgments.....	IV-86
References.....	IV-86
Appendix A: Notes on Plants in the Carrizo Plain and Temblor Range.....	A-1
Appendix B: Description of Section Corner Monuments, and Distances Between Selected Monuments.....	B-1
Appendix C: Photographs.....	C-1
Appendix D: Legend for Plates.....	D-1

List of Figures, Tables and Plates

Figure 1-1: Earthquake probabilities from WGCEP (1988).....	I-4
Figure 1-2: Location map.....	I-6
Figure 2-1: Phelan fan location map.....	II-5
Figure 2-2: Contour map of ~7m offset channel.....	II-7

Figure 2-3: Contour map of ~7 m and ~21 m offset channels.....	II-9
Figure 2-4: Contour map of the Phelan fan.....	II-12
Figure 2-5: Plan view of fan-head channels, Phelan fan.....	II-15
Figure 2-6: Cross-section of trenches 3 and 4, Phelan fan.....	II-17
Figure 2-7: Piercing line and restoration.....	II-21
Figure 2-8: Lithologic and interpretive logs of trench 5, Phelan fan.....	II-24
Table 2-1: Radiocarbon analyses of samples from the Phelan fan.....	II-28
Figure 2-9: Measurements of offset geomorphic features, Carrizo Plain.....	II-33
Figure 3-1: Location map.....	III-3
Figure 3-2: Township map.....	III-6
Table 3-1: Length, displacements, GPS errors.....	III-11
Figure 3-3: Model configuration.....	III-17
Figure 3-4: Results of elastic dislocation modeling.....	III-19
Figure 4-1: Location map.....	IV-4
Figure 4-2: The Bidart Fan.....	IV-8
Figure 4-3: Trench 2 site topographic map.....	IV-12
Figure 4-4: Trenches 3 and 4 site topographic map.....	IV-14
Figure 4-5: Simplified cross-section of trench 2.....	IV-17
Figure 4-6: Stratigraphic column of trench 2.....	IV-19
Figure 4-7a: Portion of the log of trench 2.....	IV-23
Figure 4-7b: Portion of the log of trench 2.....	IV-25
Figure 4-7c: Portion of the log of trench 2.....	IV-26
Table 4-1: Radiocarbon analyses of samples from Bidart fan trenches.....	IV-30
Figure 4-8: Simplified cross-section of trench 3.....	IV-34
Figure 4-9: Simplified cross-section of trench 4.....	IV-36
Figure 4-10: Correlation of beds between trenches 3 and 4.....	IV-38
Figure 4-11a: Portion of the southeast wall of trench 4, Bidart fan.....	IV-42

Figure 4-11b: Portion of the northwest wall of trench 4, Bidart fan.....	IV-44
Figure 4-11c: Portion of the southeast wall of trench 4, Bidart fan.....	IV-46
Figure 4-11d: Portion of the northwest wall of trench 4, Bidart fan.....	IV-48
Figure 4-11e: Portion of the southeast wall of trench 4, Bidart fan.....	IV-50
Figure 4-11f: Portion of the northwest wall of trench 4, Bidart fan.....	IV-52
Figure 4-11g: Portion of the southeast wall of trench 4, Bidart fan.....	IV-54
Figure 4-12a: Portion of the southeast wall of trench 3, Bidart fan.....	IV-58
Figure 4-12b: Portion of the northwest wall of trench 3, Bidart fan.....	IV-60
Figure 4-12c: Portion of the northwest wall of trench 3, Bidart fan.....	IV-61
Figure 4-12d: Portion of the southeast wall of trench 3, Bidart fan.....	IV-62
Figure 4-13: Plot of radiocarbon samples from trench 4.....	IV-68
Figure 4-14: Visual representation of recurrence interval calculations.....	IV-71
Table 4-2: Summary of radiocarbon dates of earthquakes, Bidart fan.....	IV-73
Figure 4-15: Hypothesized correlation of earthquakes	IV-77
Photo C-1: Channel A-B, trench 4, Phelan fan.....	C-2
Photo C-2: Channel across Elkhorn Road, March 1991.....	C-4
Photo C-3: Piercing line excavation and fire scar.....	C-6
Photo C-4: Piercing line excavation.....	C-8
Photo C-5: Piercing line excavation.....	C-10
Photo C-6: Fault zone, trench 5, Phelan fan.....	C-12
Photo C-7: Monument D.....	C-14
Photo C-8: Monument E.....	C-16
Photo C-9: Monument H and surroundings.....	C-18
Photo C-10: Monument J.....	C-20
Photo C-11: Offset channel near trench 2, Bidart fan.....	C-22
Photo C-12: Paleosol, surface of unit 8, Bidart trench 2.....	C-24
Photo C-13: Fresh debris flow, Bidart fan, March 1991.....	C-26

Plate I: Phelan fan trenches 1 and 2.....P-I
Plate II: Phelan fan trenches 3, 4 and 5.....P-II
Plate III: Logs of Bidart fan Trench 2.....P-III
Plate IV: Logs of Bidart Fan trench 3.....P-IV
Plate V: Logs of Bidart Fan trench 4.....P-V

Chapter 1: Introduction

Purpose

The San Andreas fault traverses coastal California, from Cape Mendocino near the northern border of the state to the Salton Trough, near the southern border, skirting the densely populated San Francisco Bay area and southern California metropolis. In south-central and southern California the San Andreas fault accommodates most of the relative motion between the Pacific and North American plates (Argus and Gordon, 1991; Lisowski and others, 1991; Sieh and Jahns, 1984) via episodic, seismic slip. Destructive, great earthquakes occurred in 1857 and 1906 along the southcentral and northern reaches of the fault, respectively. Because of its threat to urban areas, historic earthquakes and proximity to research centers, the San Andreas is one of the best studied faults in the world. As such, models of active faulting worldwide have been greatly influenced by the development of models for the San Andreas. Nonetheless, the properties which determine the timing and size of great earthquakes on the San Andreas are poorly understood. The goal of this study is to use a small section of the San Andreas fault in the Carrizo Plain as a natural laboratory to examine the recurrence patterns of large earthquakes and the strain release, or slip, associated with them to test models of earthquake recurrence.

In southern California, the San Andreas fault has not generated a large earthquake since 1857. Elastic strain accumulates at rates that average 25 mm/yr to 35 mm/yr (Weldon and Sieh, 1985; Sieh and Jahns, 1984; Lisowski

et al., 1991) since the 1857 earthquake. To estimate the likelihood of large earthquakes on the San Andreas fault in the next 30 years, the Working Group on California Earthquake Probabilities (1988) divided the San Andreas fault into several segments for theoretical modeling and the creation of probabilistic hazard maps (Figure 1-1). Each segment was assumed to break in a "characteristic" manner.

The probability calculations are based on models of fault segmentation, characteristic fault-segment properties, estimated dates of prehistoric earthquakes, late Quaternary fault slip rates, estimates of the amount of slip generated per earthquake, and a time-predictable model of the relationship between the amount of slip in previous earthquakes and the time interval between earthquakes. Even with simple models of elastic strain accumulation and release, large uncertainties in the input parameters create large uncertainties in probabilistic hazard calculations (Wesnousky, 1986; Savage 1991). Some data and models suggest that patterns of large earthquakes may be irregular, or even chaotic (Rundle, 1988; Thatcher, 1989; Jacoby and others, 1988; Sieh and others, 1989; Scholz, 1990; Huang and Turcotte, 1990; King, 1991), and therefore difficult to predict. The Carrizo segment of the San Andreas, however, was thought to rupture infrequently, in large-slip, semi-regularly spaced "characteristic earthquakes" (Schwartz and Coppersmith, 1984) which control the occurrence of great earthquakes on the southcentral section of the fault (Sieh and Jahns, 1984; Sykes and Seeber, 1985; Sieh *et al.*, 1989). I chose a short stretch of the San Andreas fault in the Carrizo Plain for detailed study because of its hypothesized simplicity, importance, and textbook examples of geomorphic expression (Wallace, 1990).

The Study Area

The study area extends for approximately 6 km along the fault from Wallace Creek to slightly southeast of the Bidart alluvial fan, southwest of the Temblor Range, on the McKittrick Summit and Painted Rock 7 1/2 minute USGS topographic quadrangle maps (Figure 1-2). In dry weather, the area can be reached from state highway 152 by turning south on 7 Mile Road and then turning southeast (left) on Elkhorn Road a few hundred yards from the highway.

The Carrizo Plain is undeveloped, sparsely populated, and vegetated with annual grasses and a few drought tolerant shrubs. A seven-year drought and overgrazing denuded the vegetation in the study area during collection of most of the field data, providing unusually good opportunities to observe and map subtle geomorphic features (see photo C-11).

Organization of the Thesis

This thesis consists of three separate projects (chapters 2, 3 and 4) organized as self-contained papers. Supporting data is presented in the appendices and plates. Chapters 2 and 3 investigate the amount of slip from past large earthquakes in the study area. Chapter 4 presents paleoseismic evidence of previous surface ruptures, estimates the dates of those events, and examines the recurrence patterns. The relationship between earthquake recurrence and strain release is explored in chapters 3 and 4.

The first paper is co-authored with my thesis adviser, Dr. Kerry Sieh. He suggested the topic and assisted with field data collection. The paper is in press in the *Bulletin of the Seismological Society of America*. Field data

Figure 1-1: Results of conditional earthquake probability calculations for the San Andreas fault (from Working Group on California Earthquake Probabilities, 1988). Probabilities were calculated for several hypothesized segments of the fault. The name of each segment (e.g., Carrizo) is printed above the bar representing its estimated conditional probability.

(Working Group on Calif. Earthquake Probabilities, 1988)

CONDITIONAL PROBABILITY OF MAJOR
EARTHQUAKES ALONG SEGMENTS OF THE
SAN ANDREAS FAULT
1988-2018

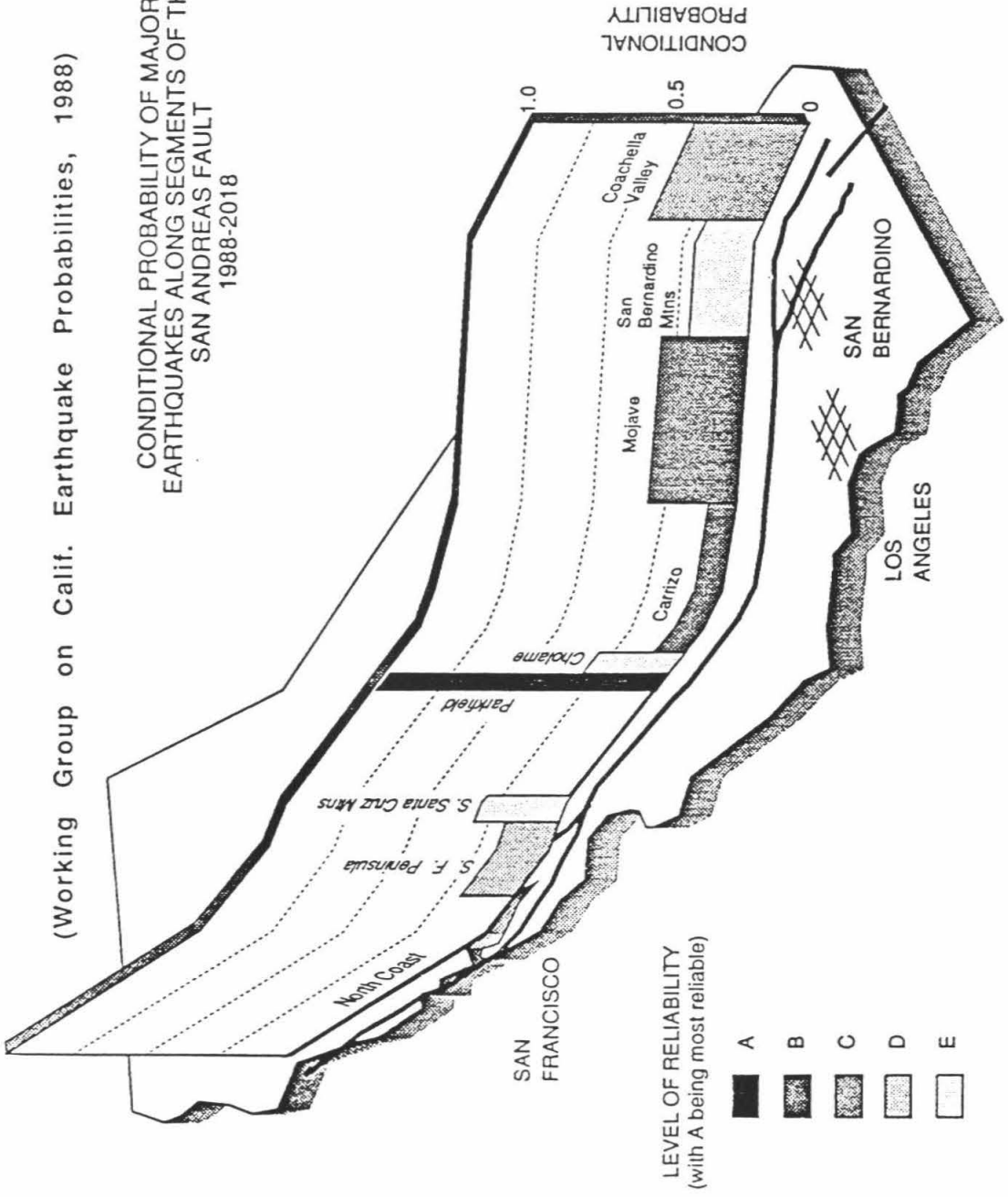
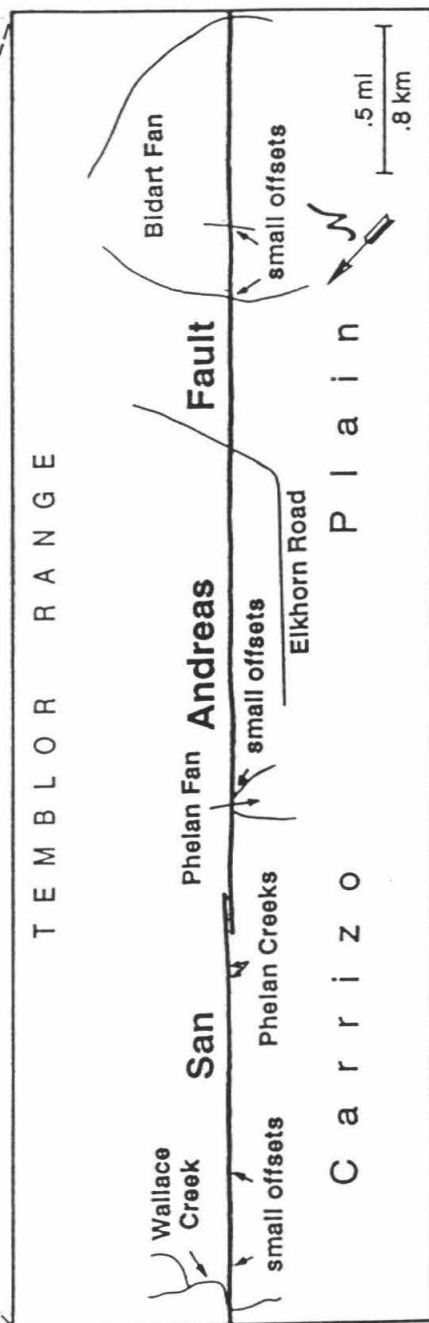
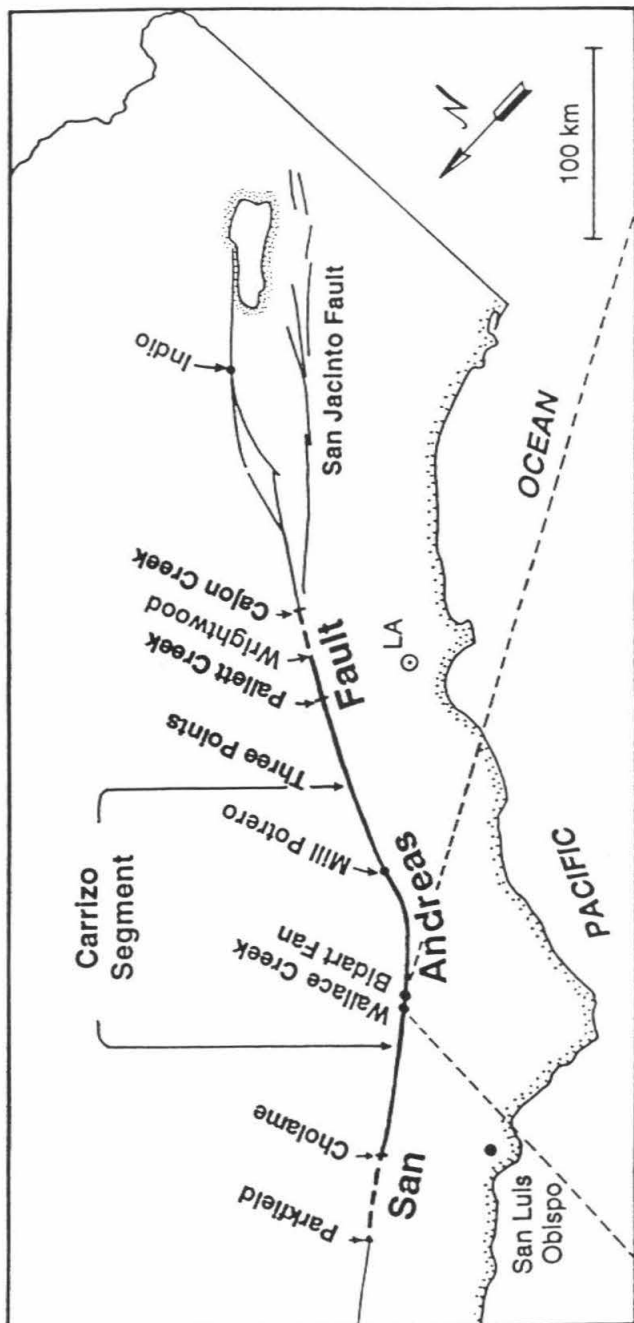


Figure 1-2: Location map of the study area.



collection, analysis and write-up of the second paper were executed jointly with Dr. Andrea Donnellan with support from Profs. Kerry Sieh and Hiroo Kanamori. Chapter 3 will be submitted to *Bulletin of the Seismological Society of America*. Supporting data is presented in appendices B and C. The research in chapter 4 was supported and supervised by my thesis advisor and co-author, Kerry Sieh. The paper will be submitted to *Journal of Geophysical Research*.

References

- Argus, D. F. and R. G. Gordon (1991). Current Sierra Nevada-North America motion from very long baseline interferometry: Implications for the kinematics of the western United States, *Geology*, **19**, 1085-1088.
- Huang, J. and D. L. Turcotte (1990). Evidence for chaotic fault interactions in the seismicity of the San Andreas fault and Nankai trough, *Nature*, **348**, 234-236.
- Jacoby, G., P. Sheppard and K. Sieh (1988). Irregular recurrence of large earthquakes along the San Andreas fault - Evidence from trees, *Science*, **241**, 196-199.
- King, C. (1991). Multi-cycle slip distribution along a laboratory fault, *J. Geophys. Res.*, **96**, 14377- 14381.
- Lisowski, M., J. C. Savage and W. H. Prescott (1991). The velocity field along the San Andreas fault in central and southern California, *J. Geophys. Res.*, **96**, 8369-8389.
- Rundle, J. B. (1988). A physical model for earthquakes 2. Application to Southern California, *J. Geophys. Res.* **93**, 6255-6274.
- Savage, J. C. (1991). Criticism of some forecasts of the National Earthquake

- Prediction Evaluation Council, *Bull. Seism. Soc. Am.*, **81**, 862-881.
- Scholz, C. H. (1990). Earthquakes as chaos, *Nature*, **348**, 197-198.
- Schwartz, D. P. and K. J. Coppersmith (1984). Fault behavior and characteristic earthquakes: Examples from the Wasatch and San Andreas fault zones, *J. Geophys. Res.* **89**, 5681-5698.
- Sieh, K. E. and R. H. Jahns (1984). Holocene activity of the San Andreas fault at Wallace Creek, California, *Geol. Soc. Am. Bull.* **95**, 883-896.
- Sieh, K. E., M. Stuiver and D. Brillinger (1989). A more precise chronology of earthquakes produced by the San Andreas fault in Southern California, *J. Geophys. Res.* **94**, 603-623.
- Sykes, L. R. and L. Seeber (1985). Great earthquakes and great asperities, San Andreas fault, southern California, *Geology*, **13**, 835-838.
- Wallace, R. E. (1991). The San Andreas fault system, California, Geomorphic expression, *U.S. Geol. Surv. Prof. Paper 1515*, 15-58.
- Weldon, R. J. and K. E. Sieh (1985). Holocene rate of slip and tentative recurrence interval for large earthquakes on the San Andreas fault in Cajon Pass, southern California, *Geol. Soc. Amer. Bull.*, **96**, 793-812.
- Wesnousky, S. G. (1986). Earthquakes, Quaternary faults, and seismic hazard in California, *J. Geophys. Res.* ,**91**, 12587-12631.
- Working Group on California Earthquake Probabilities (1988). Probabilities of large earthquakes occurring in California on the San Andreas fault, *U. S. Geol. Surv. Open File Report* , **88-398**.

Chapter 2

Stratigraphic Evidence for Seven Meters of Dextral Slip on the San Andreas Fault During the 1857 Earthquake in the Carrizo Plain

by

Lisa B. Grant and Kerry Sieh

Seismological Laboratory 252-21
California Institute of Technology
Pasadena, CA. 91125

In Press

Bulletin of the Seismological Society of America

Abstract

The smallest geomorphic offsets along a 35 km section of the San Andreas fault in the Carrizo Plain vary from 7 to 10 m. Our three-dimensional excavation of alluvial deposits a few km southeast of Wallace Creek confirms that at least 6.6 to 6.9 m of dextral slip occurred there during the latest large earthquake, in 1857. Dates on detrital charcoal suggest that the last event prior to the 1857 earthquake occurred before a date within the range A.D. 1305-1623. The 3-m range in smallest offsets along this portion of the fault may reflect either a 3-m variation in slip along the San Andreas in 1857, or 2 to 3 m of slip during an event prior to 1857. Observations made after the recent Landers earthquake are compatible with the hypothesis of large, local variations in slip during a single earthquake, but do not explain the cause of such variations. Off-fault dextral rotations would be one plausible explanation. However, paleoseismic data in the Carrizo Plain are too sparse to allow rejection of the alternative hypothesis that slip in the event prior to 1857 was only 2 to 3 m, an amount of slip which would be several times too small to fit a time-predictable model.

Introduction

The San Andreas fault has been the primary laboratory in which modern probabilistic seismic hazard analysis has been formulated (Sykes and Nishenko, 1984; Bakun and Lindh, 1985; Wesnousky, 1986; Working Group on California Earthquake Probabilities (WGCEP), 1988). Geological determinations of late Holocene slip rates, dates of paleoseismic earthquakes, and geomorphologic estimates of slip per event have been the raw data from which segmentation models have been created, recurrence intervals

calculated and deviations from the average estimated (Bakun and McEvilly, 1984; Schwartz and Coppersmith, 1984; Sykes and Nishenko, 1984; WGCEP, 1988; Sieh and others, 1989; Scholz, 1990). At this time, however, these critical data are sparse and thus, models of fault behavior are still primitive.

In this paper, we attempt to improve the quality of one piece of data: the amount of dextral slip that occurred in the Carrizo Plain during the great 1857 earthquake. Sieh and Jahns (1984) reported that dextral offsets of ephemeral stream channels cluster around 10, 22 and 33 m near Wallace Creek. Thus, they interpreted the latest three earthquakes along this section of the San Andreas fault to have produced about 10, 12 and 11 m of slip, respectively. That interpretation, coupled with an estimated 34 ± 3 mm/yr rate of late Holocene slip at Wallace Creek, was their basis for estimating the recurrence interval at between 240 to 450 years along this section of the San Andreas. These observations and interpretations have now been used in estimates of long-term earthquake probabilities (Sykes and Nishenko, 1984; Wesnousky, 1986; Working Group on California Earthquake Probabilities, 1988), mechanical models of fault behavior (Schwartz and Coppersmith, 1984; Stuart, 1986; Rundle, 1988; Huang and Turcotte, 1990), and in rupture correlation models (Sieh and Jahns, 1984; Sieh and others, 1989).

Despite the widespread use of the interpretation, little attention has been paid either to the uncertainties in the interpretation of offset geomorphic features, or the effects of these uncertainties on current fault models and estimates of hazard. Such an assessment is important to seismic hazard analysis and our understanding of fault mechanics. For example, if seismic offsets in the Carrizo Plain are typically about 10 m, then recurrence intervals must average about 300 years, more than twice the current 136 year

interval of dormancy. This implies very low probabilities for repetition of the 1857 earthquake in the near future (Figure 2-1). Alternatively, if slip is typically less than 10 m during Carrizo Plain earthquakes, then the San Andreas may be much closer to failure than previously considered. Finally, the recurrence characteristics of large earthquakes within the Carrizo Plain must be explained by any fault model designed to describe the mechanical behavior of the fault.

Here, we attempt to evaluate the reliability of the geomorphic data, using stratigraphic information. Without historic measurements or stratigraphic control on the number of events per offset, it is very difficult to determine how many earthquakes formed each geomorphic offset and how much slip occurs per earthquake.

Our first suspicion that the 9.5 m offsets documented by Sieh (1978) were not completely representative of offsets in the Carrizo Plain arose when we found several dextral offsets that were closer to 7 m in value. Two of these are shown in Figures 2-2 and 2-3. Other measurements by Sieh (1978) include three additional sites along the same stretch of the fault with substantially less than 9.5 m of offset. Were these representative of slip in 1857? If so, could the 9.5 m offsets represent the 1857 earthquake *plus* an earlier, smaller offset?

To address this uncertainty, we excavated in three dimensions an active alluvial fan at its intersection with the San Andreas fault at the Phelan Ranch to obtain stratigraphic evidence of the amount of slip which occurred in the most recent, or 1857 Fort Tejon, earthquake and its predecessor.

Figure 2-1: The San Andreas fault in southern California last ruptured in 1857, along a 350-400 km stretch from Parkfield to near Cajon Creek. Wallace Creek and the Phelan fan site are located along the Carrizo segment of the San Andreas in the northwestern Carrizo Plain. Numerous small offsets are well preserved in the northern half of the Carrizo fault segment. The Carrizo segment of the fault sustained at least 6 m of slip during the 1857 earthquake. In this paper, we discuss 7-10 m geomorphic offsets along the 35 km portion of the San Andreas fault that extends approximately 25 km southeast and 10 km northwest of Wallace Creek. Modified from Sieh *et al.*, 1989.

1857 Rupture

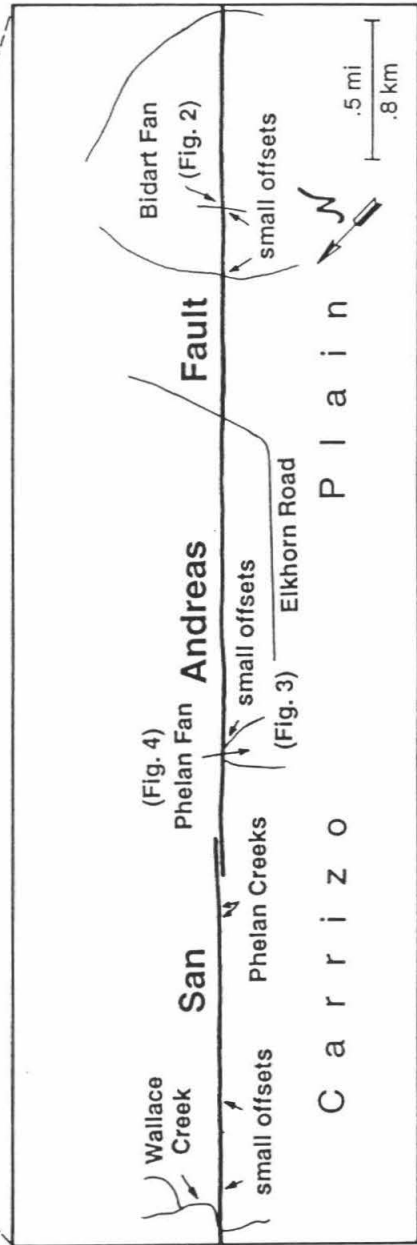
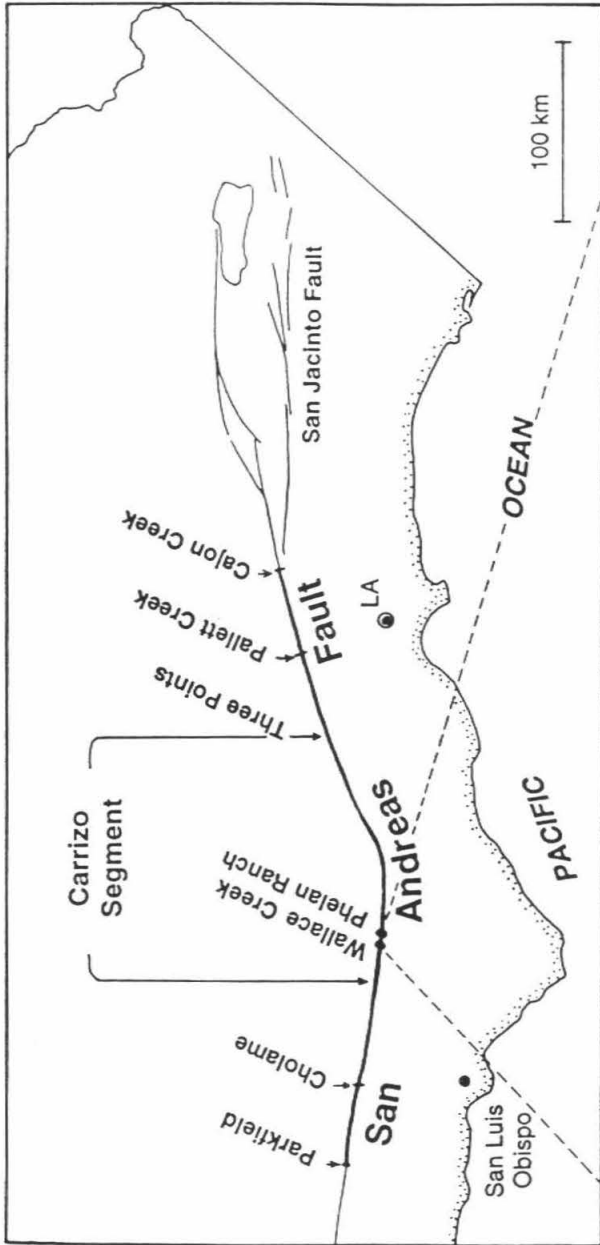


Figure 2-2: Contour map (0.1m contour interval) of an incised ephemeral stream channel on the Bidart Ranch alluvial fan 5.6 km southeast of Wallace Creek and 3.0 km southeast of the Phelan fan excavation site. The San Andreas fault extends between brackets. The channel is offset about 7.2 m in a right-lateral sense across the fault. The offset is measured by projecting the parallel trends of the channel (thick lines) to the middle of the fault zone from just outside the fault zone. Elevation datum in this and other figures is arbitrary.

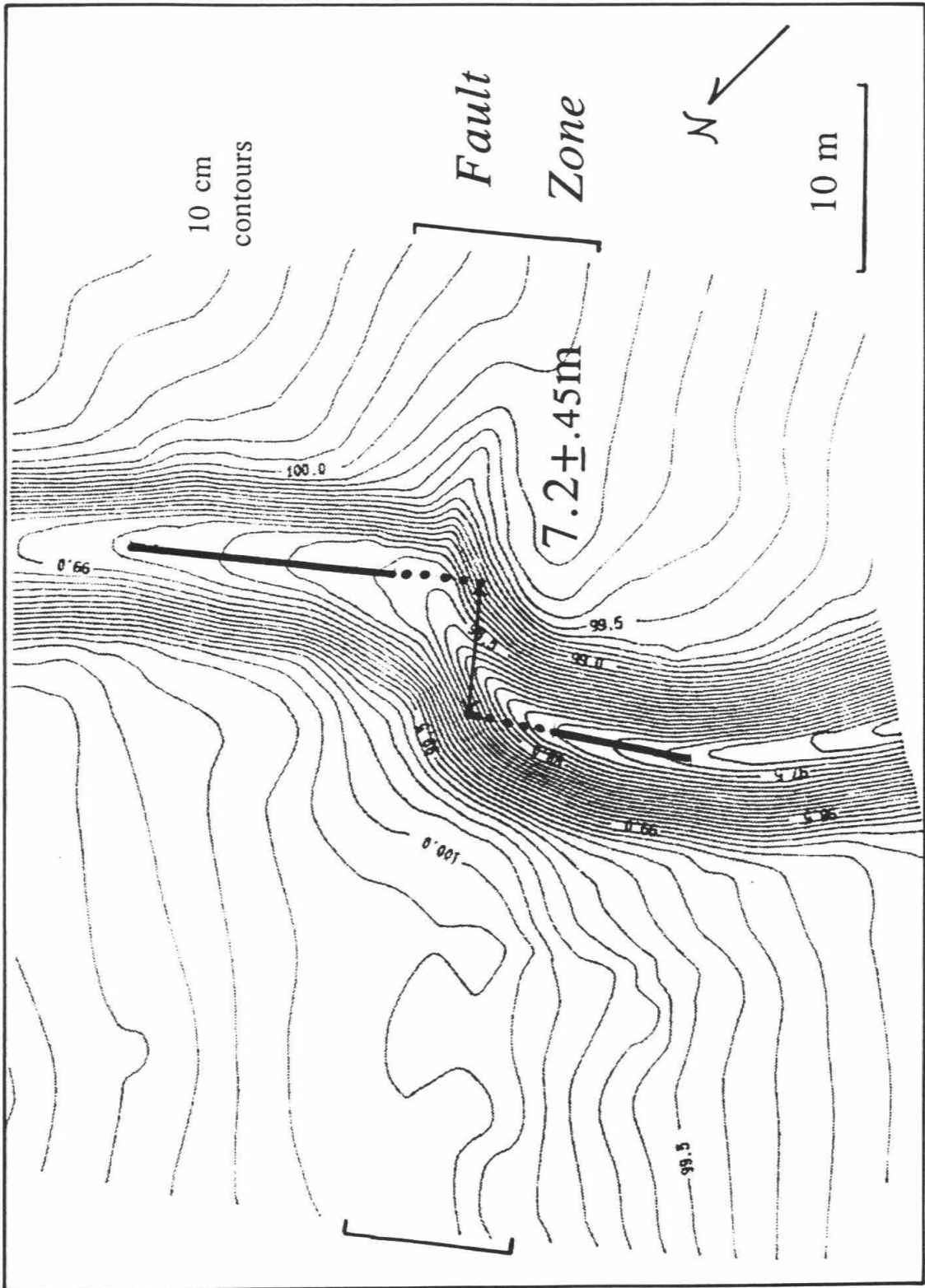
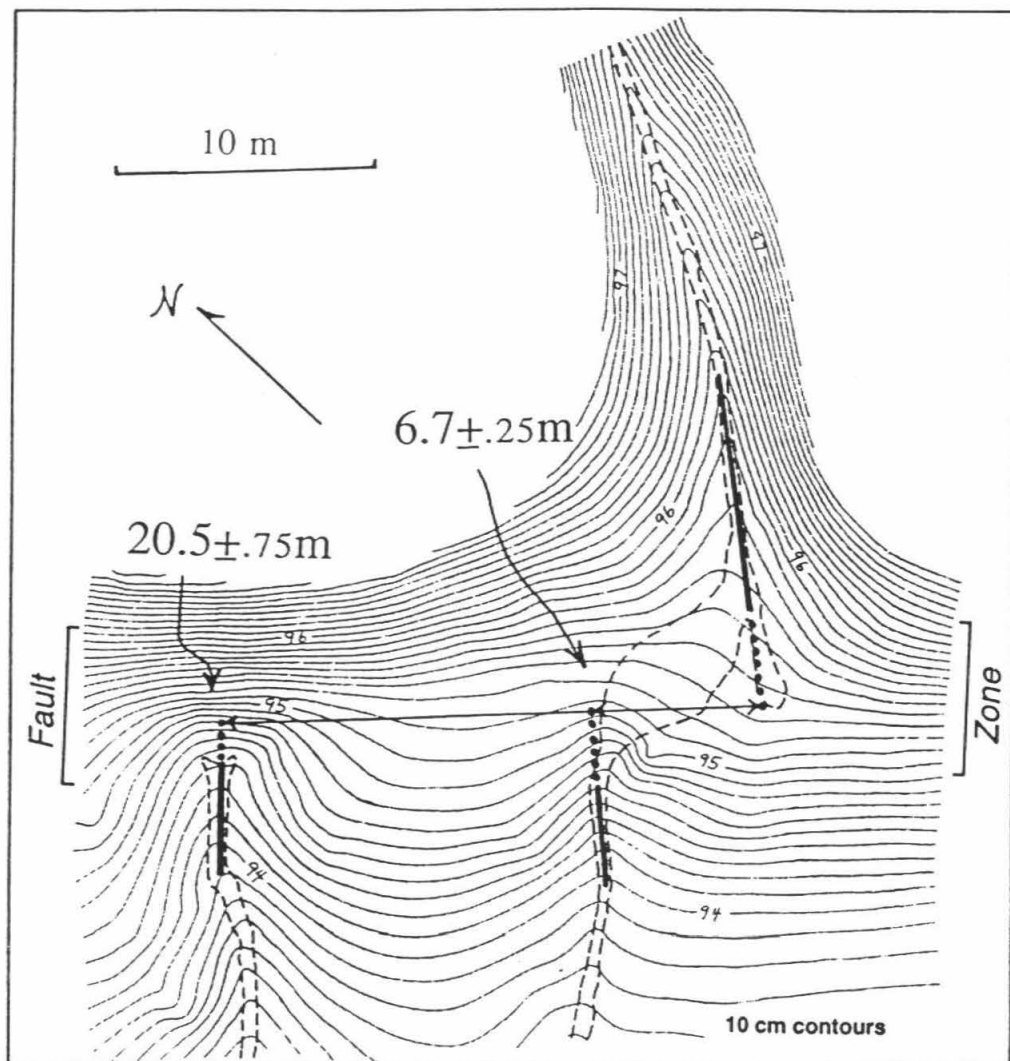


Figure 2-3: Contour map (0.1m contour interval) of two stream gullies 0.1 km southeast of the Phelan fan excavation site. The San Andreas fault extends between the brackets. The channels are dextrally offset across the fault approximately 6.7 and 20.5 m. Offset is measured by projecting the trend of each gully (thick lines) to the fault zone.



Site Description

The Phelan fan site is on the San Andreas fault in the Carrizo Plain 2.6 km southeast of Wallace Creek (Figure 2-1). At the site, a stream channel that extends upstream to the crest of the Temblor Range debouches onto an alluvial fan, the apex of which buries the fault (Figure 2-4). Northeast of the fault is a 10-to 15-m high scarp underlain by dissected late Pleistocene alluvial fan deposits. Southwest of the fault are deposits of the alluvial fan and colluvial slope deposits.

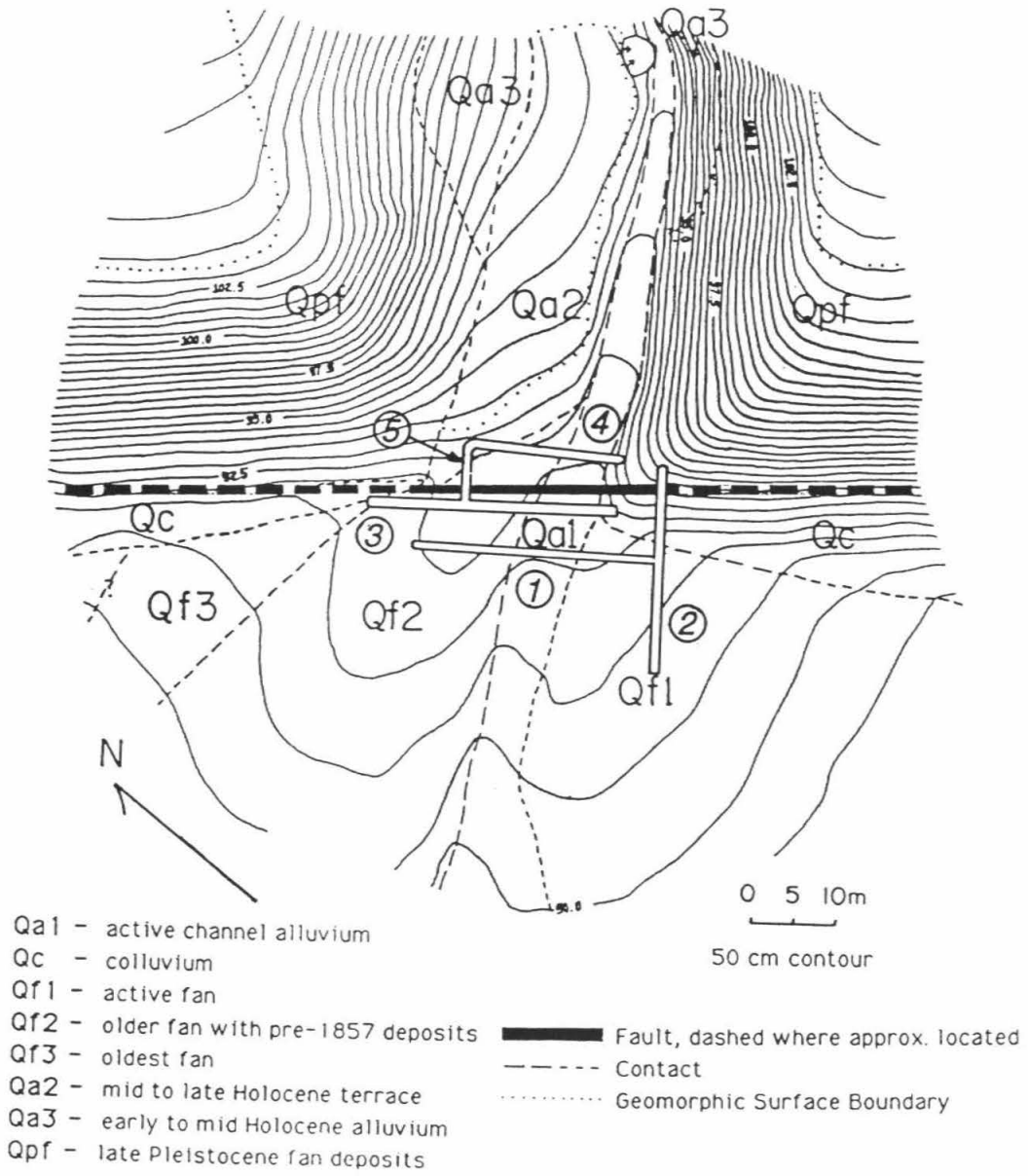
The Phelan fan has two geomorphically mappable lobes, Qf1 and Qf2 (Figure 2-4). The active fan channel, nearly filled with alluvium (labelled Qa1), supplies sediment to the southeastern lobe of the fan, Qf1. The Qf2 lobe of the fan, northwest of the active channel, is topographically higher than the Qf1 lobe, suggesting that it was constructed principally prior to 1857 and offset to the northwest during the 1857 earthquake. This was confirmed by excavations

Excavation

We excavated five trenches parallel and perpendicular to the fault to determine the precise location of the fault zone, and to identify stratigraphic features that are offset by the fault to use as piercing lines for measuring slip. We cleaned off, surveyed, and mapped the trench walls in detail, at a scale of 1:20.

After describing, mapping and correlating units in the trenches, we chose a piercing line for detailed 3-D excavation. Beginning at the walls of trenches 3 and 4, and moving toward the fault, we excavated the entire length of the piercing line by hand and cleaned it off with brushes. We then dug out the piercing line past trenches 3 and 4, moving away from the fault zone. We placed nails approximately every 10-20 cm along the top of the exposed

Figure 2-4: Contour map (0.5m contour interval) of an alluvial fan on the Phelan Ranch 2.6 km southeast of Wallace Creek. Stream channel alluvium (Qa1) crosses the San Andreas fault. Indurated late Pleistocene siltstone and sandstone beds (Qpf) are in fault contact with Recent alluvial fan deposits (Qf1, Qf2). A blanket of colluvial slope wash (Qc) lies at the base of a scarp. Fluvial terraces are mapped as Qa2 and Qa3. Locations of five trenches (numbered) are shown.



piercing line, and surveyed the nail locations using a Wild TC2000 Total Station. When we encountered small faults and the main fault zone, we nailed and surveyed them in the same manner. We also excavated the Qa1 alluvium of the active channel between trenches 3 and 4 and found that the sedimentary fill was not broken by any faults.

Stratigraphy

The trenches revealed several buried fanhead channels and the subsurface expression of the active fanhead channel, Qa1. The channels exposed in the trench walls were visually prominent features with sharp contacts. Distinctive coarse sand and gravel deposits with imbricated clasts, scour and fill structures, and sparse matrix filled the scoured channels. In the upper levels of each channel, up to the surface of the alluvial fan, debris flows and gravel deposits interfingered and spread out laterally above the elevation of the channel banks, producing the surficial fan morphology.

Three fanhead channels (A', B',C') existed in trenches 1 and 3, on the downstream (southwest) side of the fault. These are labelled A', B' and C' in figures 2-5 and 2-6. Two channels labelled A-B and C, existed in trench 4, on the upstream (northeast) side of the fault. In trench 3, channels A', B' and C' cut poorly sorted, poorly indurated, colluvial slope wash deposits (Qc) that display no bedding or other sedimentary structures. We hypothesize that these deposits were shed off the 10-15 m scarp to the southeast of the alluvial fan apex, and transported northwest by faulting, prior to channel incision.

Upstream from the fault, in trench 4, channel A-B cut indurated, well-bedded siltstone, mudstone, and sandstone (Qpf) which we interpret as the mid-to-distal facies of deposits of much older alluvial fan beds (Table 2-1). The southeastern margin of channel C also cut the same lithified beds. The base and northwestern margin of channel C cut burrowed, layered and

Figure 2-5: A plan view of the channels and fault zone was constructed from their exposure in the trench walls, locations from 3-D excavations, and projections of stratigraphic features. Channels B' (circles) and C' (crosses) are offset from their sources. Channel A' (dots) extends across the fault to its source, channel A-B (circles and dots). The channel-bank piercing line at the northern margin of offset channels C and C' was exposed by excavation. Bold dots mark the endpoints of piercing lines (dashed) projected beyond the trench walls. *Projected Offsets* (P-P' etc.) are inferred from projection of piercing lines to the fault. P and P' are the projected locations of the southern bank of channel C-C', at the fault zone. S-S' is the estimated offset of the southern bank of channel B-B'. Lines Q-Q' and R-R' are different projections of the thalweg of channel B-B'. The *Observed Offset* was determined by excavating the piercing line to the fault (arrows). Numbered circles refer to trench numbers.

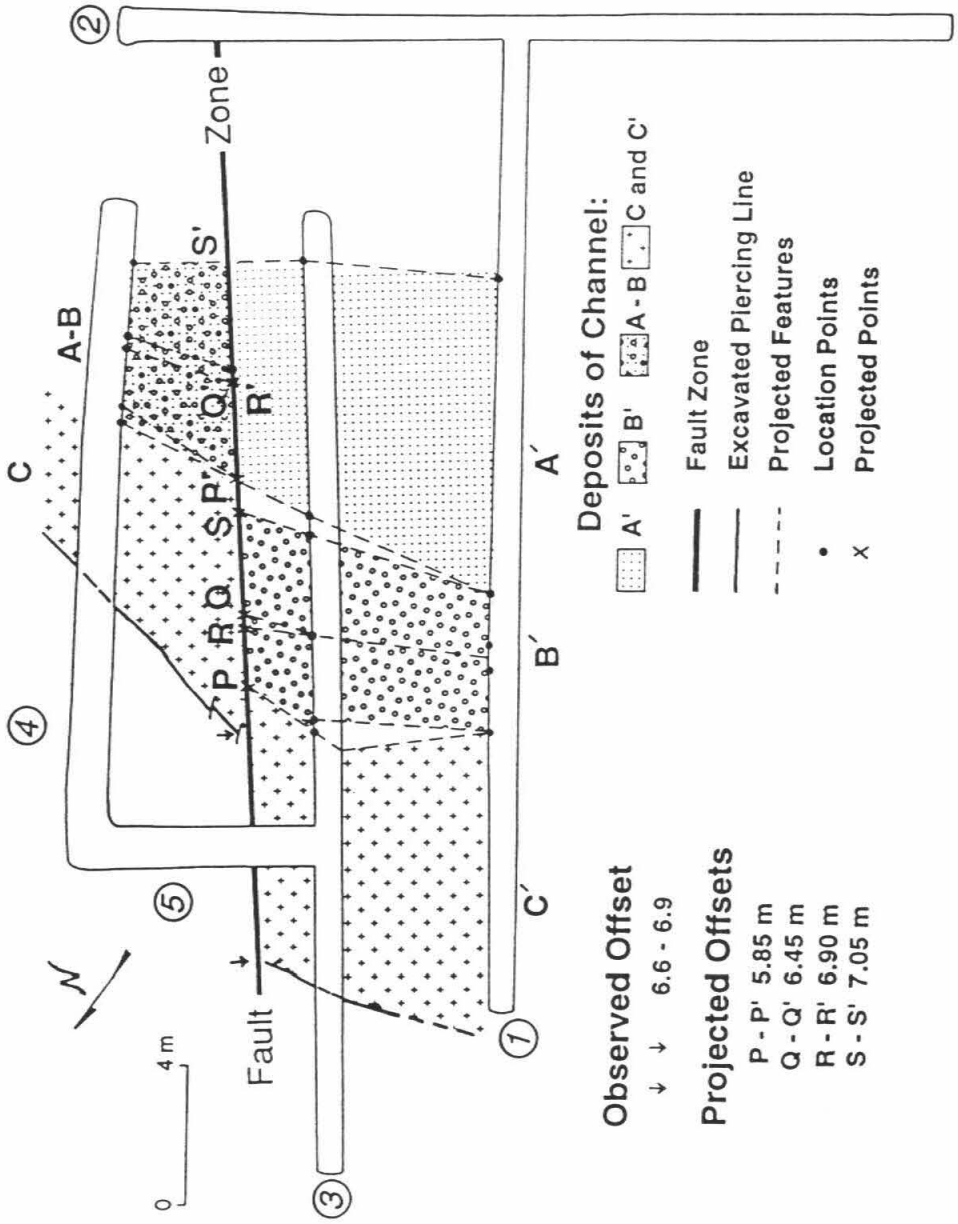
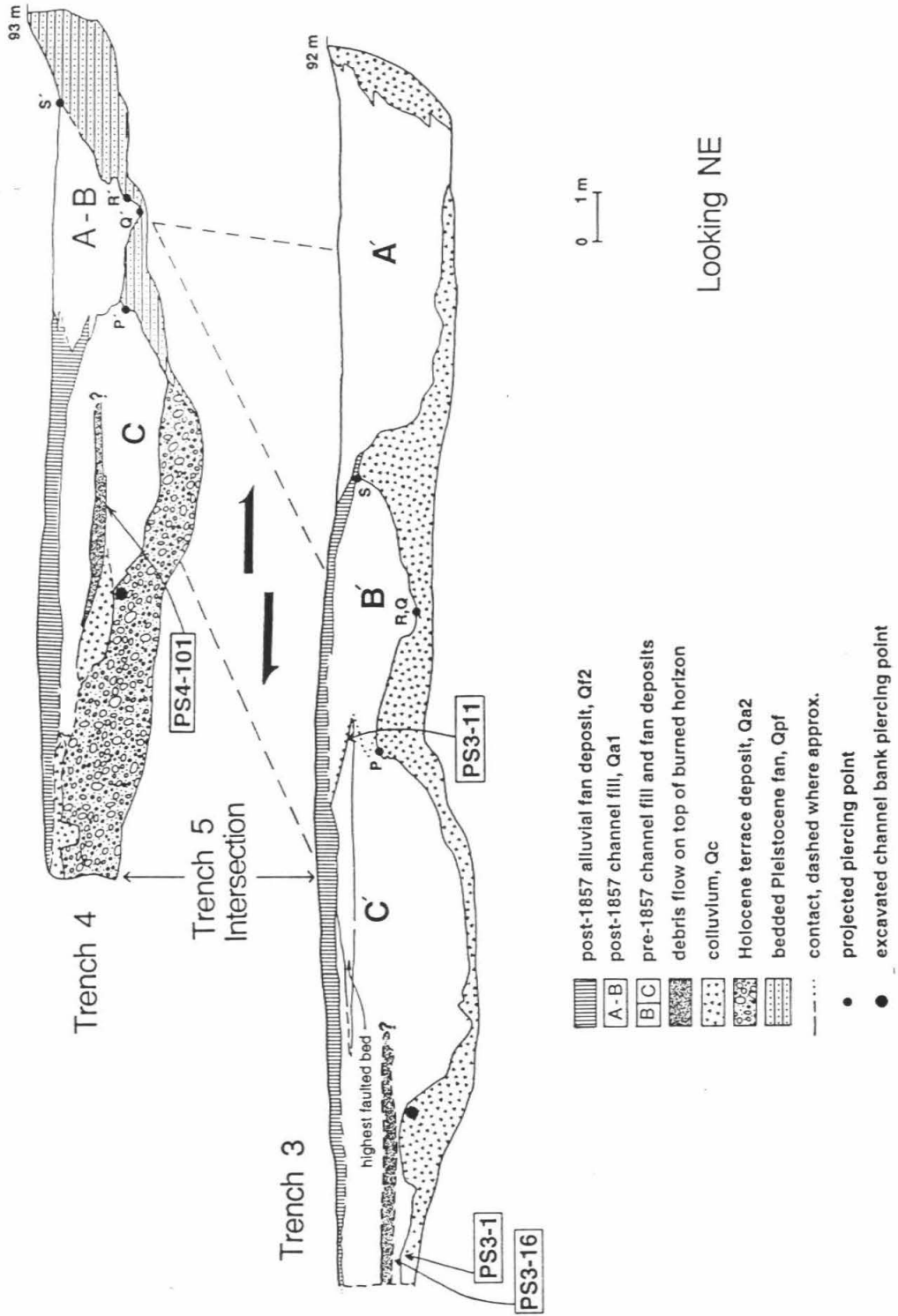


Figure 2-6: Cross-sectional map of generalized stratigraphy of trenches 3 and 4 reveals a set of three fanhead channels. Channels B' and C' have been offset from channels A-B and C, respectively. Channel A-B,A' is the currently active channel. The location of the excavated channel bank piercing line is marked with a large dot on the northwest bank of channel C-C'. A fire scar is prominent in the sediments between trenches 3 and 4, but does not crop out in either of the trench walls. A laterally extensive debris flow bed deposited on top of the burned horizon and correlated between the trenches is shown with dark stipple. Locations of piercing line projections from figure 5 are marked with corresponding letters. Radiocarbon samples PS3-1, PS3-11 and PS3-16 were collected from the locations shown. Sample PS4-101 was collected from the fire scar between trenches 3 and 4, at the horizon shown. Sample PS2-3 was collected from unit Qpf, in trench 2 (not shown). Detailed lithologic logs of the trenches are in Plates I and II.

Stratigraphy of Trenches 3 and 4



channelized beds of gravel and debris flows. These beds are correlated with terrace Qa2 because they underlie the surface of this terrace (Figure 2-4). The upper contact of the Qa2 deposits in trench 4 (Figure 2-6) is irregular due to the presence of burrows. In trenches 4 and 5, unit Qa2 grades upward into bioturbated colluvium.

A baked, reddish black, fire scar formed an important time-stratigraphic marker in the upper sediments of channels C and C' (see photo C-3, appendix C). In gravel beds, the fire scar was a red and black rind around pebble clasts. At the surface of debris-flow beds, it was a reddish horizon. Charcoal clasts were locally abundant within the burned horizon and, in one place, were entrained in the base of a debris flow bed on top of the fire scar. Due to its patchy areal extent, the fire scar was not observed in the walls of trenches 3 and 4. It was well developed in the sediments between the trenches, in the beds just above the piercing line.

Correlation of Channels

Excavation of the Qa1 deposits between trenches 3 and 4 demonstrated that the sedimentary fill of channel A-B in trench 4 is continuous with the fill of channel A' in trench 3 (Figure 2-6). Both the upstream and downstream parts of active channel A-B,A' therefore, formed and filled after the last major earthquake. Channel B' is inferred to have been fed by source channel A-B, and then offset by the San Andreas fault (Figure 2-5). Because channel A-B now contains the younger, unfaulted Qa1 sediments, individual beds cannot be matched between channel B' and channel A-B to prove the correlation hypothesis. However, no other plausible hypothesis exists.

We interpret the sizes, locations, stratigraphic positions, sedimentary structures and individual beds of channels C and C' displayed in trenches 1, 3

and 4 to suggest that they correlate across the San Andreas fault and are offset (Figures 2-5, 2-6 and 2-8). This correlation was confirmed during the piercing line excavation.

Measurement of Offset

The amount and sense of offset of channels B' and C' west of the fault can be estimated from projections of several piercing lines (Figure 2-5). The estimates range from 5.85 m to 7.05 m, depending on the piercing line projection used. The projections of individual piercing lines differ between different trenches, so offset estimates vary. To measure the offset accurately, it is necessary to trace a single piercing line to the point where it intersects each side of the fault.

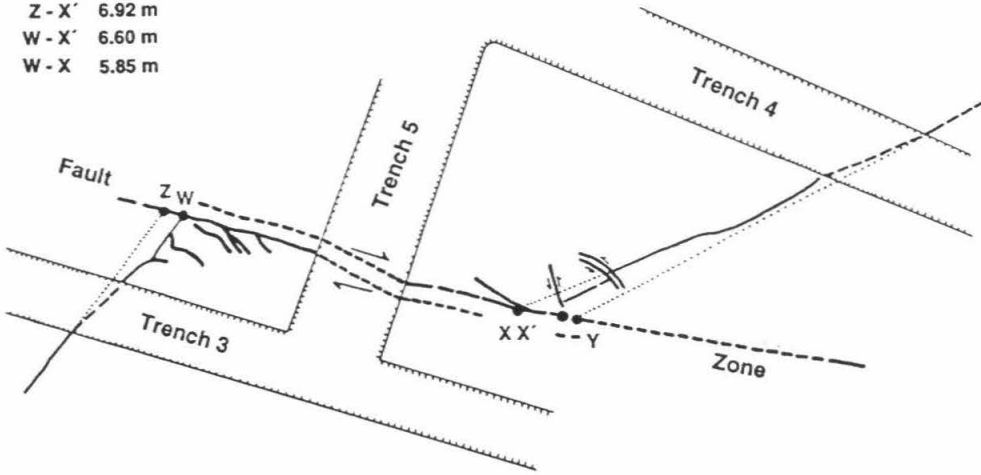
We examined channels C and C' for features that were identifiable on both sides of the fault, to use as a piercing line. We chose the intersection of the top of the northwestern channel bank with overlying debris flows and gravel lenses, on each side of the fault as the piercing line. We excavated and surveyed the top of the channel bank. Figure 2-7a is a map view of the piercing line and the faults that cut it. The channel bank has an irregular shape, as expected for a natural fluvial feature, and is slightly disrupted by small faults outside the main fault zone. On the west side of the fault, the piercing line intercepts the main fault zone at point W. Two small faults with less than a centimeter of displacement each cut the piercing line between W and trench 3. No faults were observed west of trench 3 (see photo C-5, appendix C), although some minor faults might have been removed by excavation of trench 3. If we project the piercing line toward the fault, from the unfaulted region west of trench 3, it intersects the fault zone at Z.

Figure 2-7:A) The excavated top of the northern bank of channel C-C' forms a piercing line which was surveyed to measure offset. Maximum offset is obtained by projecting the piercing line to the fault zone from beyond trenches 3 and 4 to points Z and Y. Point W is at the intersection of the piercing line and the main fault zone. Point X is projected to the main fault from just outside the maximum observed width of the fault zone. Point X' is the best estimate of the intersection of the piercing line and the main fault zone, after restoration of slip on the smaller faults (See text.). **B)** Restoration of slip along the faults reveals the best match in trends of the piercing lines at WX' and ZX', indicating 6.6-6.9 m of offset.

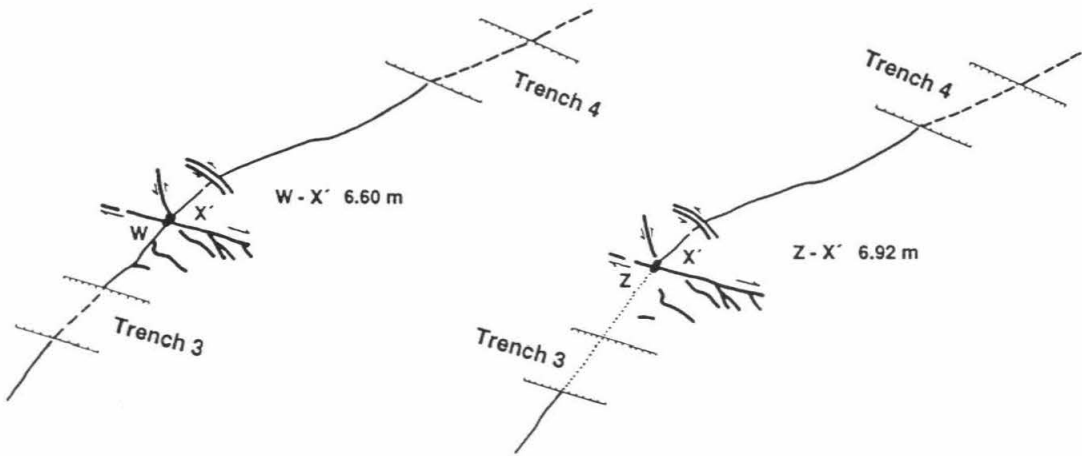
a Piercing Line Offset

OFFSETS
 Z - Y 7.15 m
 Z - X' 6.92 m
 W - X' 6.60 m
 W - X 5.85 m

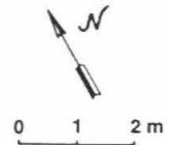
6.6 - 6.9 m



b Slip Restoration



- — — Fault, dashed where approx. located at edge of fault zone
- — — Piercing line, dashed where approx. located
- Projected piercing line
- Trench wall
- Piercing point



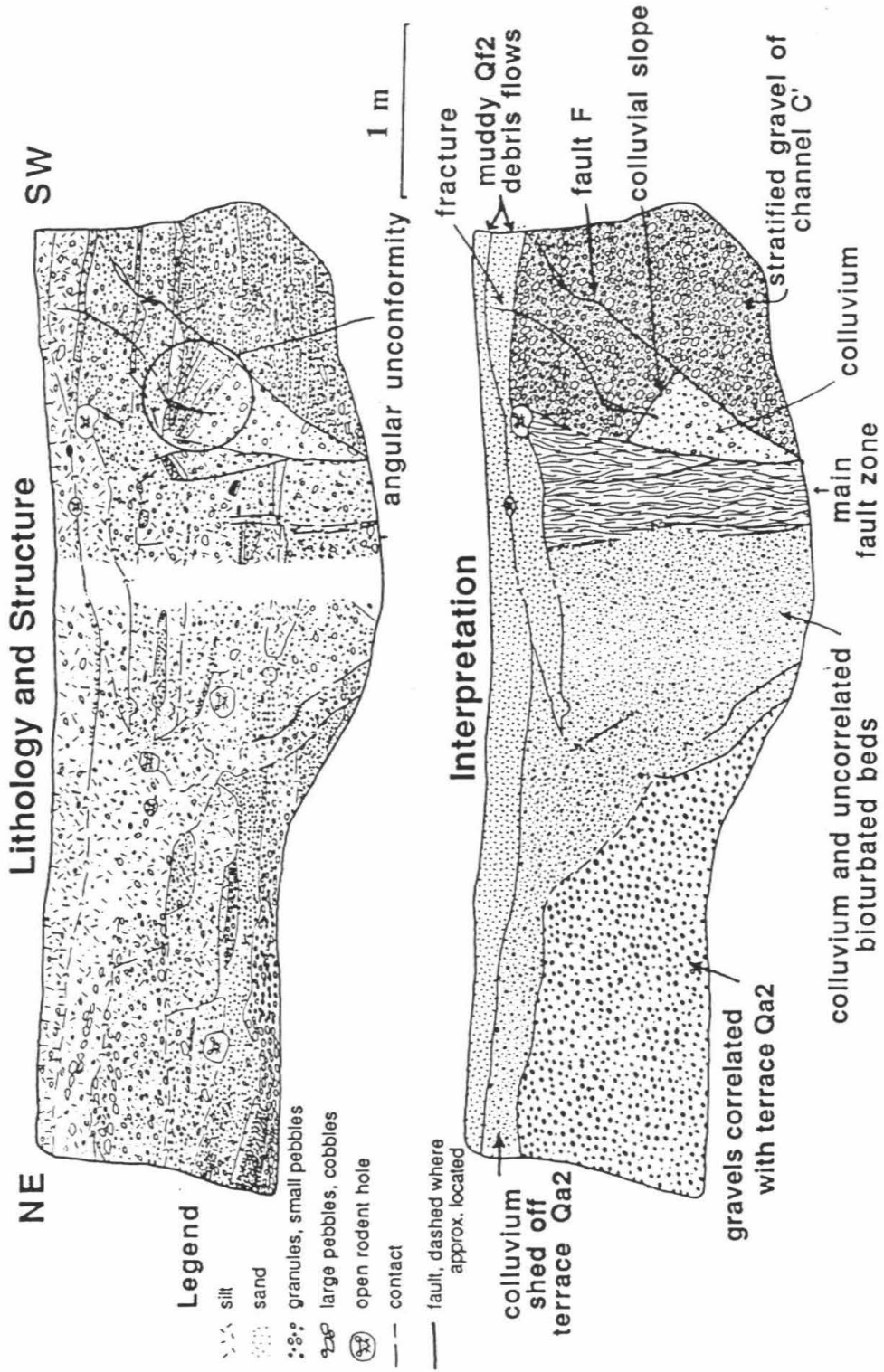
Two left-lateral faults on the northeastern side of the fault zone have rotated a block containing part of the piercing line clockwise. If slip is restored on these small faults, the piercing line intersects the main fault zone at X'. The piercing line can also be projected to the main fault from the closest unfaulted region, to intersect at point X. If we project from beyond trench 4, to account for any faults destroyed by trench 4, the intersection point is Y.

The offsets measured from these points vary between 5.85 m and 7.15 m. To determine the most plausible value, we restore the slip on the major and minor faults and examine the match in trends of the lines on either side of the fault. The best fits (Figure 2-7b) are at points W-X' and Z-X'. In both restorations, the trends of the channel bank on either side of the main fault zone match well. The possibility that additional dextral slip is hidden as warping within the aperture of our excavation is impossible to evaluate conclusively. The arcuate nature of the piercing line suggests the possibility of additional dextral warp, but the coarse nature of the sediments precluded paleomagnetic sampling such as that utilized by Salyards and others (1992) and Nagy and Sieh (in press). Alternatively, the bend in the channel could be non-tectonic. The paucity of secondary faults within the excavations suggests the bend is not tectonic (see photo C-4, appendix C). Therefore, we conclude that the piercing line was offset 6.6 to 6.9 m by the San Andreas fault.

Number of Faulting Events

Trenches 2 and 5 lie approximately perpendicular to the San Andreas fault (Figure 2-4) and display clear evidence of recent faulting. In trench 2, the faults extend through colluvium to within centimeters of the surface, where details are obscured by bioturbation (data not shown). In trench 5, the main

Figure 2-8: Lithologic (upper) and interpretive (lower) logs of Trench 5. The trench was approximately perpendicular to the fault zone. Legend shows meaning of symbols in the upper log. A circle encloses the angular unconformity on the upper log. Units and important structures in the interpretive log are marked with labels and generalized symbols. Observer is facing southeast.



fault zone juxtaposes colluvium, bioturbated beds and beds correlated with terrace Qa2, against the gravels that fill and overtop channel C' (Figure 2-8). A veneer of alluvial fan debris flows covers the faulted units. The highest faults in trench 5 extend upward to the same stratigraphic level as the faults observed in the uppermost channel C' gravels of trench 3. Thus, the sediments of channel C' were dextrally faulted away from their source and juxtaposed against terrace and colluvial deposits.

One of the near-surface debris flows which covers the fault zone in Trench 5 contains a fracture extending upward from one of the fault traces (Figure 2-8). No displacement is observed across the fracture, and it terminates before reaching the top of the bed. Therefore, we interpret that it formed as a result of a small amount of aftercreep, settling or dessication, rather than by seismic faulting. There are no faults in the same debris flow along the wall of trench 3, or in the debris flow above it.

Several faults within the colluvium terminate below the ground surface and could be from older events. However, the colluvium is heavily bioturbated and thus the upward terminations of the fault traces are unreliable indicators of the stratigraphic level of faulting.

Evidence for the number of faulting events which offset channel C' from channel C is ambiguous. Facies changes across one of the faults, and an angular unconformity suggest multiple events. In trench 5, southwest of the main shear zone, a sequence of apparently dipping beds is capped by nearly horizontal beds (Figure 2-8, circle). This sequence can be interpreted as an angular unconformity caused by faulting. If so, it would suggest that channel C-C' was offset by at least two earthquakes. However, the same sequence of beds on the other wall of trench 5 does not show an angular unconformity (see photo C-6, appendix C). Below the angular unconformity, a wedge of

unstratified sand and gravel, interpreted as colluvium, is faulted against stratified gravels of channel C', forming an apparent facies change across the lower reach of fault F (Figure 2-8). The sequence of beds on either side of the upper reach of fault F is similar. One interpretation is that the lower reach of fault F slipped in multiple earthquakes, and the upper part formed and slipped only during the last earthquake, resulting in less offset along the upper reach of the fault.

A single earthquake interpretation is that slip on fault F during the most recent earthquake juxtaposed different facies of channel C-C'. In this interpretation, the dipping beds (Figure 2-8, circle) were deposited on a sloping wedge of colluvium. At the ground surface (Figure 2-4), the deposits of fan Qf2 lap against the southwest-sloping edge of terrace Qa2. The edge of terrace Qa2 is shedding colluvium. Colluvium is also shed off the southwest slope of the Qpf scarp (Figure 2-4). The beds in the angular unconformity (Figure 2-8) appear to dip to the southwest. The dipping beds in Trench 5 were probably deposited against a colluvial slope at the margins of channel C-C', and then faulted into contact with stratified gravels from inner channel C'. We favor this interpretation because it is consistent with the geomorphology at the site. Thus, although we cannot rule out the existence of more than one event, our favored interpretation is that a single, large earthquake offset channel C' 6.6-6.9 m from channel C.

Dating of Units and Faulting

Abundant tiny fragments of detrital charcoal were embedded in debris flows, sandy gravels, colluvium, and in the lithified sediments of unit Qpf. A small percentage of the samples were large enough (> 10 mg of carbon) to be

TABLE 2-1
Radiocarbon Analyses

Sample ID Caltech/Lab	$\delta^{13}C$	Unit	Conventional Radiocarbon Age (years BP, at 1 σ)	Dendro-corrected Age (calendar years AD) 1 σ	Age (calendar years AD) 2 σ
PS2-3/AA5075*	-2.5**	Qpf trench 2	13,860 \pm 100	-----	-----
PS3-1/AA5072*	-12**	colluvium	476 \pm 60	1332-1472	1305-1623
	-2.5**		370 \pm 60	1450-1630	1440-1640
PS3-11/AA5073*	-1.1	debris flow	138 \pm 32	1681-1936	1670-1947
PS3-16/AA5074*	-2.1	gravel	535 \pm 40	1320-1430	1300-1440
PS4-101/QL-4470#	-13.3	fire scar	1016 \pm 19	987-1023	901-1151
PS4-101t/TO-2564##	not reported	fire scar	600 \pm 50	1298-1406	1263-1438

*The samples were dated at the NSF Accelerator Facility at the Univ. of Arizona and were partially funded by NSF grant EAR85-12761. Results are quoted from D. Donahue and T. Jull, and includes an unspecified error multiplier.

**Assumed value. Not measured due to insufficient sample size. Calendar age from method B of Stuiver and Reimer (1986), with no additional error multiplier.

#Measurements quoted from M. Stuiver at Univ. of Washington, Quaternary Isotope Lab. Calendar age from method B of Stuiver and Reimer (1986), with 1.6 error multiplier.

##Measurement from R. P. Beukens, IsoTrace Radiocarbon Lab, Univ. of Toronto. Calendar age from method B of Stuiver and Reimer (1986) with 1.6 error multiplier.

dated by accelerator mass spectrometry (AMS). Some of the samples were too small to measure the $\delta^{13}\text{C}$ ratio, complicating the interpretation of their radiocarbon ages.

A further complication results from the detrital nature of the samples and from the presence of long-lived plant species in the area. These problems, and our interpretations of the radiocarbon dates, are discussed below and summarized in Table 2-1. Dendro-calibrated calendric age ranges are discussed at the 2σ rather than 1σ level because it reduces the likelihood of error in our interpretations.

Charcoal sample PS3-11 was collected from the highest faulted bed above channels C' and B' (Figure 2-6). The reported 2σ calendar age range of sample PS3-11 is A.D. 1670-1947. Hence, offset of C' and B' postdates A.D. 1670-1947. Because A.D. 1857 falls within the age range A.D. 1640-1947, the stratigraphy indicates that the immediately subjacent channel sediments were offset by the most recent large earthquake, and history records that the most recent large earthquake on the San Andreas fault in the Carrizo Plain occurred in 1857 (Wood, 1955; Agnew and Sieh, 1978), we conclude that the channel sediments were offset 6.6-6.9 m during the 1857 earthquake.

The time of channel incision is more difficult to determine. On the southwest side of the fault, the channels cut colluvium containing charcoal sample PS3-1. This sample was too small to permit measurement of its $\delta^{13}\text{C}$, so the lab assumed a $\delta^{13}\text{C}$ of -25 to calculate a radiocarbon age of 370 ± 60 years and a 2σ calendric range of A.D. 1440-1640. Of twelve charcoal samples with measureable $\delta^{13}\text{C}$ collected by the authors at the Phelan fan and Bidart fan sites for this study and other studies (Grant and Sieh, 1991, 1992), eight are C-4 plants with an averaged $\delta^{13}\text{C}$ value of approximately -12. Thus C-4 charcoal samples are more common than C-3 samples in this area. If we assume that

sample PS3-1 has a $\delta^{13}\text{C}$ value of -12, the radiocarbon age is increased by 106 years (T. Jull, NSF AMS Lab, Univ. of Ariz., Tucson, AZ., written communication, 1992) to 476 ± 60 years B.P., and the 2σ calendar range changes to A.D. 1305-1623 (Stuiver and Reimer, 1986). This suggests that the channels cut the colluvium sometime after a date within the age range 1305-1623 A.D., and filled prior to faulting, in 1857.

A piece of charcoal (PS3-16) from a gravel layer that may overlie channel C just above the colluvium in trench 3 yields a radiocarbon date corresponding to a calendar age range of A.D. 1300-1440. This date range overlaps the date of sample PS3-1 below it by 135 years, suggesting that the channel began filling between A.D. 1305 and 1440. However, because the charcoal samples are detrital, it is difficult to place upper limits on the times of channel cutting and filling. The sample dates may be older than the beds which contain them, and therefore we favor the broader time range of A.D. 1305-1623.

An aggregate charcoal sample, PS4-101, was collected directly from the burned horizon in the upper channel C sediments, on the east side of the fault (Figure 2-6). This sample's age is 1016 ± 19 radiocarbon years B.P., corresponding to a 2σ calendar range of A.D. 901-1151 (Stuiver and Reimer, 1986). This date is several centuries older than the age of the charcoal from the colluvium into which the channel was incised. Thus, the age of sample PS4-101 probably reflects either the age of a long-lived plant, a long period of time between plant death and sample deposition, or both, rather than the dates of channel filling. Blong and Gillespie (1978) report up to 1500 years difference between the true age of twentieth century river sediments in Australia, and the charcoal contained within them. They attribute the age

difference to detrital wood storage in the drainage basin prior to deposition, and a 200-300 year life expectancy of local trees.

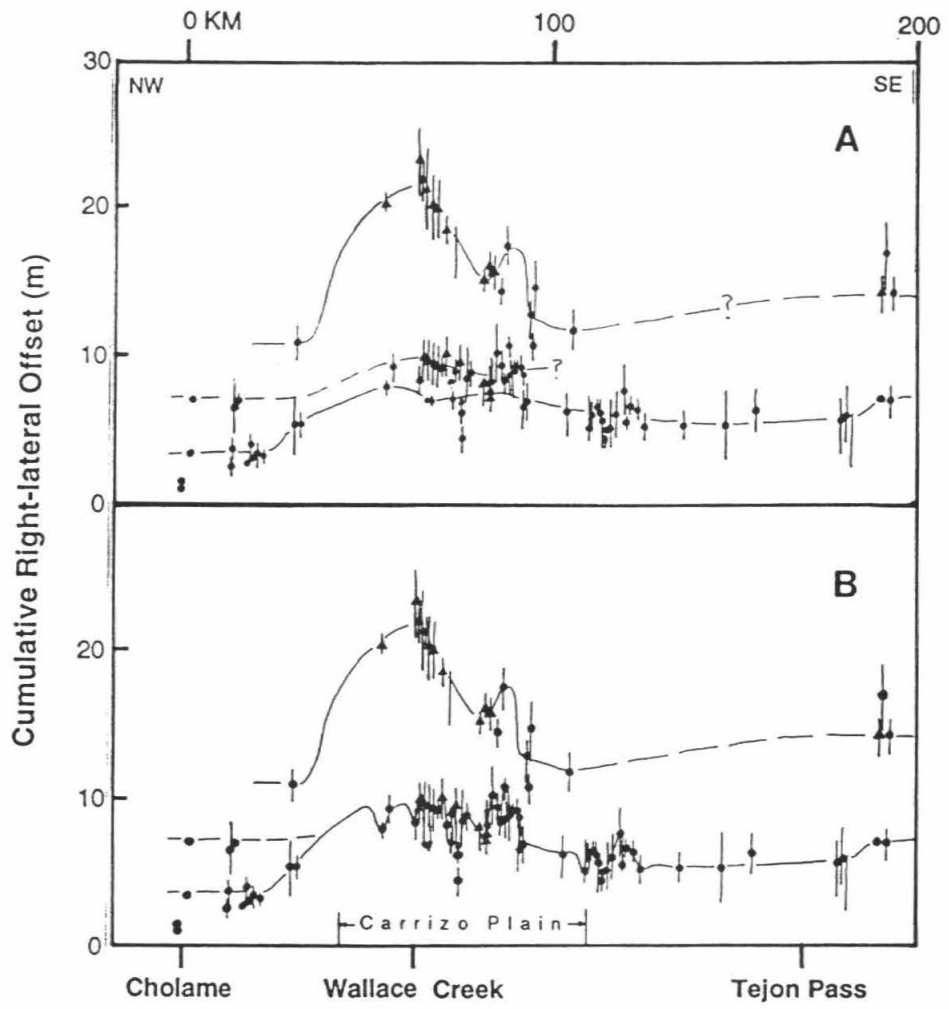
A single piece of charcoal resembling a twig was selected from the aggregate PS4-101 sample for a second date because we judged the twig would likely be younger than heartwood which might 'contaminate' the aggregate sample. The age of the twig, sample PS4-101t, was younger (600 ± 50 radiocarbon years B.P.) than sample PS4-101. This corresponds to a 2σ calendar range of A.D. 1263-1438, one to several centuries younger than the bulk sample. The $\delta^{13}\text{C}$ of the aggregate sample PS4-101 indicates that it came from C-4 plant material. The woody texture and high $\delta^{13}\text{C}$ value of the charcoal suggests that the plant might be *Atriplex polycarpa*, or Common saltbush (Smith and Epstein, 1971; L. Toolin, AMS Lab, Univ. of Ariz., personal communication, 1992; see appendix A for more information). *A. polycarpa* is common in the subshrub plant community of the Carrizo Plain, and was more common prior to the introduction of grazing (Hubert and Kakiba-Russell, 1991). It is difficult to estimate the life expectancy of *A. polycarpa* in the Carrizo Plain. It resprouts after fires (Eben McMillan, personal communication, 1992) and is listed by Barbour and Major (1988) as an 'important long-lived species', along with creosote. Thus, it is possible that the difference in ages of samples PS4-101 and PS4-101t represents the approximate lifespan of a saltbush transported to the excavation site by flood waters, burned in situ as detrital wood by a wildfire, and then buried by sediments. If so, the younger date better represents the time of deposition, although it could still be older than the surrounding sediments. Another possibility is that PS4-101 and PS4-101t are from entirely different plants. In that case, the younger date (A.D. 1263-1438) still gives a better estimate of the time of deposition than the older date.

From the radiocarbon dates and stratigraphic evidence, we conclude that the channel piercing line was offset 6.6-6.9 m by the 1857 earthquake. The offset channel C-C' was cut sometime after a date within the range A.D. 1305-1623. The pre-1857 earthquake occurred prior to the channel incision, prior to a date within the range A.D. 1305-1623. It occurred prior to deposition of channel fill containing pieces of *detrital* charcoal dated at A.D. 1300-1440, 1263-1438, and 901-1151.

Discussion

One interpretation of our observations is that the larger 9 to 10 m geomorphic offsets observed near Wallace Creek by Sieh and Jahns (1984) represent slip from two events; 6 to 7 m in 1857 and 2 to 3 m in a previous event (Figure 2-9). Similar distributions of geomorphic offsets along the Garlock fault have been interpreted as evidence for multiple events (McGill and Sieh, 1991). There is evidence to support a hypothesis of 6-7 m of slip over most of the 1857 rupture length. Lienkaemper and Sturm (1989) argue for 5.7 m of slip from the 1857 earthquake near Cholame, northwest of Wallace Creek, although they have no stratigraphic evidence to prove that all of the offset occurred in a single event rather than two 3 m slip events, as argued by Sieh and Jahns (1984). Approximately 6 m of slip is reported by Sieh (1978) and Sieh and Jahns (1984) along the southern half of the Carrizo segment of the San Andreas fault. Salyards and others (1992) measured approximately 6 m of slip at Pallett Creek (Figure 2-1), where slip was previously thought to be much less (Sieh 1978, 1984). Thus, 6 to 7 m of slip in 1857 has been reported at sites along nearly the entire length of the 1857 rupture, including the Wallace Creek section. If the maximum slip section of the San Andreas fault reported by Sieh (1978) and Sieh and Jahns (1984) near

Figure 2-9: Measurements of offset geomorphic features versus distance along the south-central section of the San Andreas fault, reported by Sieh and Jahns (1984), show peak values along a 35 km stretch of the fault in the Carrizo Plain. Each symbol represents an offset measurement, with error bars. New measurements presented in this paper are included. The lines joining the symbols show two possible interpretations of earthquake rupture patterns. Box A indicates 6 to 7 m of slip near Wallace Creek in 1857, and 2 to 3 m of rupture in the previous earthquake. Box B shows highly variable (6 to 10 m) slip in 1857. Modified from Sieh and Jahns (1984).



Wallace Creek actually sustained 6 to 7 m of slip in 1857, then the peak slip section may have ruptured with 2 to 3 m of peak slip in a previous event (Figure 2-9). Data from other strike-slip earthquakes show that 2 to 3 m of peak slip is plausible for a 35-km rupture, corresponding to a M_S 7.2-7.3 earthquake (Bonilla and others, 1984).

Another plausible hypothesis to explain our observations is that the slip varied by several meters over a distance of about 2 km along strike. Such variation in offsets is not unusual. Dextral offsets from the 1992 Landers earthquake varied several meters in less than a kilometer (Rubin and McGill, 1992). Similar variation has been reported from other strike-slip earthquakes. Slip in the 1940 Imperial Valley earthquake increased from 2 m to a peak of 6 m over a distance of approximately 6.5 km, with a 2-m increase occurring over a 2 to 3 km stretch (Sharp, 1982). Reported slip from the 1968 Dasht-E-Bayaz earthquake in Iran decreased from 3.0 to 1.5 m within approximately 100 m along the fault (Ambraseys and Tchalenko, 1969).

It should also be recognized that slip may vary from earthquake to earthquake at a given site. For example, at Phelan Ranch, we report geomorphic offsets of approximately 7 and 21 m (Figure 2-3). At nearby Phelan Creeks (Figure 2-1), Sims and others (1989) report an offset of $15.8 \pm .6$ m. If 7 m of slip occurred in 1857 at Phelan Creeks, the remaining 8 to 9 m of offset at Phelan Creeks may be from the prior event. Thus, at Phelan Ranch the last 3 earthquakes may have produced approximately 7, 8-9, and 5-6 m of slip respectively, forming offsets of 7m, 15-16m, and 21m. At Wallace Creek, offsets of approximately 9.5, 22 and 33 m have previously been interpreted as the result of 9.5, 12.5 and 11 m of slip respectively, from the last 3 earthquakes. If the gully that is offset 22m was formed by 3 earthquakes rather than by 2 earthquakes (as hypothesized by Sieh and Jahns (1984)), then the slip at

Wallace Creek might have been a more modest 9.5, 6-7, and 6-7 m during the last 3 earthquakes. From the geomorphic data alone, there is no reason to favor one interpretation over another because there is no constraint on the number of events which formed each offset.

Slip variation in 1857 along the section of San Andreas fault we have investigated could be related to long-term variation in the amount of slip on the main fault strand. However, if a slip deficit repeatedly occurs at the same place over several earthquake cycles, complementary structures or multiple traces would be expected to form, unless deformation was distributed over a very broad area.

The most important implication, and perhaps the only conclusion, that can be drawn from the data presented herein is that, due to substantial uncertainties in their measurement and interpretation, the smallest geomorphic offsets in the Carrizo Plain currently provide only rough constraints on the amount of slip per earthquake. An important consequence is that slip-based hypotheses about earthquake recurrence, the location of fault-segment boundaries, and seismic hazard should not ignore these uncertainties. Conditional earthquake probabilities calculated with the assumption of a time-predictable model of earthquake recurrence must reflect the large uncertainties in interpreting the number of earthquakes attributed to each offset. Preliminary dates of paleoseismic events in the Carrizo Plain suggest irregular recurrence intervals for prehistoric earthquakes on the San Andreas fault (Grant and Sieh, 1992). Therefore, mechanical models of a strong Carrizo fault segment which breaks infrequently and with at least 9 m of peak slip may be incorrect and should be reconsidered.

Acknowledgments: We greatly appreciate the support and access given by land owners Arthur Phelan and Leonard Bidart. We also thank S. Grant, G. Holk, K. Hudnut, L. Maepa, S. McGill, E. Nagy, C. Prentice, J. Ritchie, M. Slates, A. Thomas, T. Wachholz, K. Wiese and D. Wood for assistance with the field work. J. Mayne helped draft the figures. Most radiocarbon samples were dated at the NSF Accelerator Facility at the Univ. of Ariz. and were partially funded by NSF grant EAR85-12761. We thank M. Stuiver at the Univ. of Wash. Quaternary Isotope Lab for a high precision radiocarbon date. The Univ. of Toronto IsoTrace lab dated one radiocarbon sample. R. Weldon, S. Wesnousky, S. Grant and an anonymous reviewer greatly improved the manuscript. Financial support was provided by USGS grant # 14-08-001-G1789. This is California Institute of Technology, Division of Geological and Planetary Sciences contribution #5179.

References

- Agnew, D. C. and K. E. Sieh (1978). A documentary study of the felt effects of the great California earthquake of 1857, *Bull. Seism. Soc. Am.* **68**, 1717-1730.
- Ambraseys, N. N. and J. S. Tchalenko (1969). The Dasht-e-Bayaz (Iran) earthquake of August 31, 1968: A field report, *Bull. Seism. Soc. Am.* **59**, 1751-1792.
- Bakun, W. H. and T. V. McEvilly (1984). Recurrence models and Parkfield, California, earthquake, *J. Geophys. Res.* **89**, 3051-8.
- Bakun, W. H. and A. G. Lindh (1985). The Parkfield, California, earthquake prediction experiment, *Science* **229**, 619-624.
- Barbour, M. G. and J. Major, eds. (1988). *Terrestrial Vegetation of California*, California Native Plant Society, Special Publ. 9, Univ. of Calif. Davis.
- Blong, R.J. and R. Gillespie (1978). Fluvially transported charcoal gives erroneous ^{14}C ages for recent deposits, *Nature*, **271**, 739-741.
- Bonilla, M. G., R. K. Mark and J.J. Lienkaemper (1984). Statistical relations among earthquake magnitude, surface rupture length, and surface fault displacement, *Bull. Seism. Soc. Am.* **74**, 2379-2411.
- Grant, L. B. and K. E. Sieh (1992). Irregular recurrence times and increased seismic hazard from earthquakes on the Carrizo segment of the San Andreas fault, southern California, *Proc. of the 35th Ann. Meeting of the Assoc. of Engineering Geologists*, Los Angeles, Oct. 2-9, 567-568.
- Grant, L. B. and K. E. Sieh (1991). New data on the timing and slip per event of earthquakes on the San Andreas fault, southern California, *Trans. Amer. Geophys. Union*, **72**, no.44, 351.

- Huang, J. and D. L. Turcotte (1990). Evidence for chaotic fault interactions in the seismicity of the San Andreas fault and Nankai trough, *Nature*, **348**, 234-236.
- Hubert, E. and K. Kakiba-Russell (1991). Carrizo Plain Natural Area: A checklist of vascular plants, California Energy Commission.
- Lienkaemper, J. J. and T. A. Sturm (1989). Reconstruction of a channel offset in 1857(?) by the San Andreas fault near Cholame, California, *Bull. Seism. Soc. Am.* **79**, 901-909.
- McGill, S. F. and K. E. Sieh (1991). Surficial offsets on the central and eastern Garlock fault associated with prehistoric earthquakes, *J. Geophys. Res.* **96**, 21597-21621.
- Nagy, E. A. and K. E. Sieh (in press). The use of paleomagnetic analysis to assess non-brittle deformation within the San Andreas fault zone, *J. Geophys. Res.*
- Rubin, C. R. and S. F. McGill (1992). The June 28, 1992 Landers earthquake: slip distribution and variability along a portion of the Emerson fault, *Trans. Amer. Geophys. Union*, **73** no. 43, 362.
- Rundle, J. B. (1988). A physical model for earthquakes 2. Application to Southern California, *J. Geophys. Res.* **93**, 6255-6274.
- Salyards, S. L., K. E. Sieh and J. L. Kirschvink (1992). Paleomagnetic measurement of non-brittle coseismic deformation across the San Andreas fault at Pallett Creek, southern California, *J. Geophys. Res.* **97**, 12457-12470..
- Scholz, C. H. (1990). Earthquakes as chaos, *Nature*, **348**, 197-198.
- Schwartz, D. P. and K. J. Coppersmith (1984). Fault behavior and characteristic earthquakes: Examples from the Wasatch and San Andreas fault zones, *J. Geophys. Res.* **89**, 5681-5698.

- Sharp, R. V. (1982) Comparison of 1979 surface faulting with earlier displacements in the Imperial Valley, in *The Imperial Valley, California Earthquake of October 15, 1979*, U.S. Geol. Surv. Prof. Paper 1254, 213-221.
- Sieh, K. E. (1978). Slip along the San Andreas fault associated with the great 1857 earthquake, *Bull. Seism. Soc. Am.*, 68, 1421-1448.
- Sieh, K. E. (1984). Lateral offsets and revised dates of large prehistoric earthquakes at Pallett Creek, Southern California, *J. Geophys. Res.* 89, 7641-7670.
- Sieh, K. E. and R. H. Jahns (1984). Holocene activity of the San Andreas fault at Wallace Creek, California, *Geol. Soc. Am. Bull.* 95, 883-896.
- Sieh, K. E., M. Stuiver and D. Brillinger (1989). A more precise chronology of earthquakes produced by the San Andreas fault in Southern California, *J. Geophys. Res.* 94, 603-623.
- Sims, J. D., T. Ito, J. C. Hamilton, and D. B. Meier (1989). Late Holocene record of earthquakes and slip on the San Andreas fault in excavations on the Carrizo Plain, California, *EOS Trans. Am. Geophys. Union*, 70, 1349.
- Smith, B. N. and S. Epstein (1971). Two categories of $^{13}\text{C}/^{12}\text{C}$ ratios for higher plants, *Plant Physiol.*, 47, 380-384.
- Stuart, W. D. (1986) Forecast model for large and great earthquakes in Southern California, *J. Geophys. Res.* 91, 13771-13786.
- Stuiver, M. and P.J. Reimer (1986). Computer program CALIB, *Radiocarbon*, 28, 1022-1033.
- Sykes, L. R. and S. P. Nishenko (1984). Probabilities of occurrence of large plate rupturing earthquakes for the San Andreas, San Jacinto, and Imperial faults, California, *J. Geophys. Res.* 89, 5905-5927.

Wesnousky, S. G. (1986). Earthquakes, Quaternary faults, and seismic hazard in California, *J. Geophys. Res.* **91**, 12587-12631.

Wood, H. O. (1955). The 1857 earthquake in California, *Bull. Seism. Soc. Am.* **45**, 47-67.

Working Group on California Earthquake Probabilities (1988). Probabilities of large earthquakes occurring in California on the San Andreas fault, *U. S. Geolog. Surv. Open File Report* 88-398.

Chapter 3

1855 and 1991 Surveys of the San Andreas Fault: Implications for Fault Mechanics

Lisa B. Grant
Seismological Lab 252-21
California Institute of Technology
Pasadena, CA. 91125

Andrea Donnellan
Space Geodesy and Geodynamics
238-600 Jet Propulsion Laboratory
Pasadena, CA 91109
Formerly at: Geodynamics Branch
NASA Goddard Space Flight Center
Greenbelt, MD 20771

To be submitted to Bulletin of the Seismological Society of America

Abstract

Two monuments from an 1855 survey which spans the San Andreas fault in the Carrizo Plain have been displaced 11.0 ± 2.5 m right-laterally by the great earthquake of 1857. This magnitude of offset is consistent with geomorphic indications that slip across the fault during the 1857 earthquake and associated foreshocks and aftershocks varied from 6.6 to 10 m over 2.6 km along this section. Comparison of recent geodetic measurements with the late Holocene slip rate at Wallace Creek shows that fault slip rates determined from short-term wide aperture measurements are indistinguishable from rates determined from long-term narrow aperture measurements. Using radiocarbon dates of the penultimate large earthquake and measurements of slip in 1857, we calculate an average slip rate for the last complete earthquake cycle that is at least 25% lower than the late Holocene slip rate on the main fault trace. This suggests that variation in fault slip during the 1857 earthquake left a slip deficit in at least the upper 1 km of crust at Wallace Creek. Slip in future earthquakes may compensate this deficit.

Introduction

Models of earthquake recurrence, calculations of earthquake probability, and theories about the behavior and segmentation of strike-slip faults are often based on estimates of fault slip from measurements of offset landforms. Measurements of late Holocene slip rate and small offset stream channels near Wallace Creek (figure 3-1) have led some to argue that the San Andreas fault there has recurrence intervals of 240 to 450 years. These unusually long intervals result from unusually large (9.5 to 12.3 m) offsets, the smallest of these (9.5 m) being ascribed to the latest large earthquake in 1857 (Sieh and Jahns, 1984; Sieh *et al.*, 1989).

Figure 3-1: Location map of the San Andreas fault in southern California. Resurvey of 1855 section lines in the Carrizo Plain enable estimation of coseismic dextral displacement. The 1857 rupture is in bold (Sieh, 1978). Inset map shows Wallace Creek, measured line D-E, and location of small stream channels offset 9-10m and ~7m (Sieh and Jahns, 1984; Grant and Sieh, 1993). Buried channels at the apex of the Phelan fan are offset 6.6-6.9m (Grant and Sieh, 1993). Geodetic measurements suggest about 11m of coseismic offset.

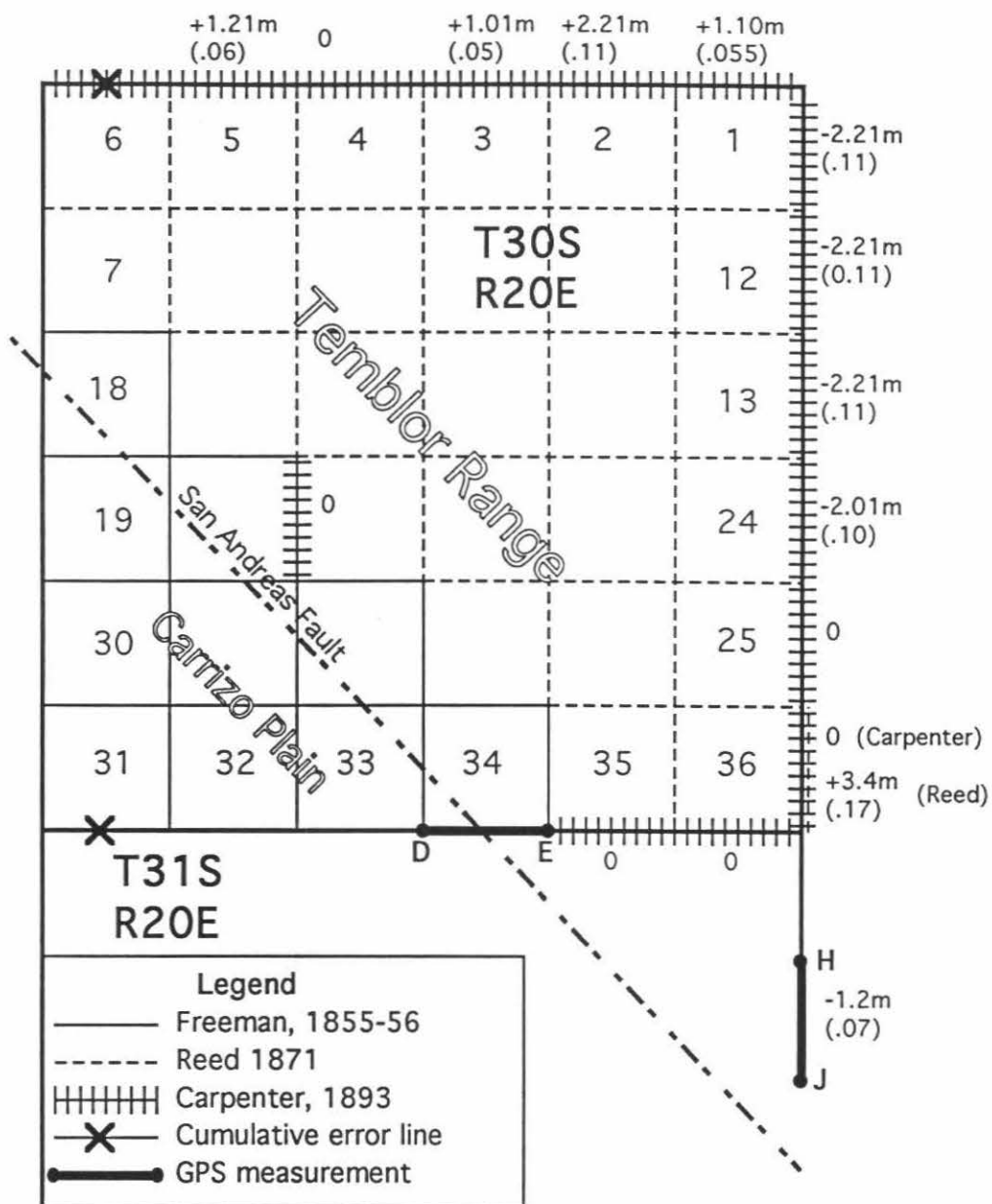
However, it is difficult to prove that each offset corresponds to one earthquake. In fact, several channels 2-5 km southeast of Wallace Creek, which are offset only 6-7 m, suggest that either dextral slip varied from 6 to 10 m within a few kilometers along strike during the 1857 earthquake, or that the individual offsets near Wallace Creek were actually formed by multiple earthquakes. This latter possibility could mean that the time between at least some past earthquakes was less than 240 years and that maximum slip may have been less than 9.5 m (Grant and Sieh, 1993).

To resolve this ambiguity, we undertook to measure directly the amount of slip from the 1857 earthquake. We recovered original monuments from an 1855 survey spanning the San Andreas fault near Wallace Creek and resurveyed them with the Global Positioning System (GPS). From these measurements and other observations we have inferred characteristics of the fault over one earthquake cycle and discuss them in relation to long-term properties of the fault.

The Rectangular Survey System

The rectangular survey system was established by the United States in 1785 to facilitate settling land in the western territories (White, 1983). Land was divided into townships 6 miles square by lines oriented east-west (township lines) and north-south (range lines) with corrections for magnetic declination (White, 1983). Townships were subdivided into 36 sections, each 1 mile square. In the mid- to late-1800's the land in the Carrizo Plain and Temblor Range was divided into townships and subdivided into sections. James E. Freeman sectioned and surveyed the land near Wallace Creek in 1855 and 1856. Freeman also surveyed township boundaries in the Temblor Range in 1855 (Figure 3-2). These townships were later subdivided by other

Figure 3-2: Map of surveyed section lines and land-survey grid, Township 30 south, Range 20 east (T30S R20E) and part of Township 31 south, Range 20 east (T31S R20E), referenced to the Mount Diablo Meridian and Baseline, California. Exterior sections are numbered. Each section is approximately one mile square. Line types indicate areas surveyed by Freeman, resurveyed by Carpenter, Reed, and us. Differences in horizontal distance between Freeman's survey and resurveys are shown in meters and chains next to the resurveyed lines. The endpoints of lines D-E and H-J are marked with corresponding letters.



surveyors.

During the 1800s surveyors used chains to measure horizontal distances. The chains were kept level and under tension during the surveys. The method of chaining is of low but sufficient accuracy to estimate line length changes of a few meters for a mile section line. Distances were measured by a chain 66 feet (20.12m) long with 100 links. 80 chains make up one mile (1609.26m). In establishing the township and range lines the distance along each section was measured twice, and the lines were remeasured when the land was subdivided (White, 1983). Six section lines were measured out consecutively. The first five lines were as close as possible to 80 chains in length. The sixth line was adjusted to intersect the township boundary, and its deviation from 80 chains was recorded (White, 1983). The corners of each section were generally marked by a post in a mound of earth or stones. In some cases stones, approximately 35 X 30 X 8 cm, were used in lieu of posts.

Survey and Error Analysis

We searched microfiche copies of original field notes and plats (maps) of early surveys spanning the San Andreas fault in the Carrizo Plain. Then we examined recent (1950s) USGS topographic quadrangle maps of townships surveyed prior to 1857 to identify potential remaining section markers. We recovered fifteen candidate section markers, and checked Freeman's field notes and plats for authenticity. We conclude that Freeman accurately recorded natural landmarks and performed the survey.

Most section markers did not match Freeman's original description and had obviously been reset since the original survey. We searched records of resurveys and remonumentation filed with the Bureau of Land

Management (BLM) and the San Luis Obispo County Surveyor to find the history of each recovered marker. Because the Carrizo Plain is sparsely populated, few resurveys have been made, and several remonumentations are not on record with the county. U. S. Geological Survey topographic maps indicate that by the 1950's nearly all of the monuments in the Carrizo Plain had been obliterated or lost.

We found and surveyed a total of 8 potential monuments. Four of the monuments were reset by twentieth century surveyors. One of the monuments is a replacement of a lost marker, and therefore is not in its original location. Two of the remaining three were reset without record, or the records were destroyed in a fire in San Luis Obispo, California, in 1981. Our measurements suggest that surveyors reset these monuments outside their original locations and attempted to correct for previous slip on the San Andreas fault. We eliminated from our study monuments that were reset without record because they may have been moved from their original locations. Of the remaining 4 sites, two are the degraded, original monuments, and two appear to be in the locations of the original monuments (Grant, 1993). The original monuments (D and E) form a line spanning the fault. The other monuments (H and J) are on a range line that does not cross the fault. We were unable to find any other original pre-1857 monuments in the Carrizo Plain region to resurvey with GPS.

In 1991 we remeasured both lines. To minimize errors, we used GPS dual frequency receivers to remeasure horizontal distance between the monuments. GPS does not require line of site so it was only necessary to observe at the end points. Conventional surveying techniques would have required traverses between the monuments, thus increasing measurement error. We collected data simultaneously for each of the lines measured, for a

period of 1-3 hours. By simultaneously sampling data we eliminate the possibility of errors due to adjustment of a network. We used precise orbits obtained from Scripps Institution of Oceanography to process the data.

Results are shown in Table 3-1. Formal errors in the GPS survey are 1-4 cm.

Errors in the original survey are much larger than the GPS errors. In the following discussion we mix units of meters and miles because the original survey was measured in miles and we are measuring deviations from one mile. The total measurement error is dominated by errors in the original chained survey and errors in recognizing the center of degraded original monuments. Historical resurveys of Freeman's 1855 survey (Figure 3-2) of T30S, R20E indicate that Freeman's average chaining error was less than 1:950 for a 1-mile line. One interior section line established in 1856 was remeasured by John Reed in 1871, and 14 additional lines in the Temblor Range were remeasured by Howard Carpenter in 1893. Although we are unable to establish the absolute accuracy of the method of chaining we can use the repeated line measurements to estimate the precision of the method. Comparison of the repeat measurements with the originals, including our measurement of distance H-J, yields a root-mean-square (rms) error of 1.6 m for a 1 mile section line. All of the repeated measurements except line H-J were conducted in mountainous terrain. The largest deviation from one mile (3.4 m) is probably larger than Freeman's error because it was measured along a "random" line while Reed was setting his compass. The largest deviation measured by Carpenter in "mountainous" terrain was 2.2 m. The terrain across line D-E is flat to rolling, so we assume that the average error of 1.6 m applies to our measurement line across the San Andreas.

There is additional uncertainty in determining the center of the monuments. For monuments D, H and J, the uncertainty is less than half a

TABLE 3-1: Line lengths, formal errors, total displacement, post seismic accumulation and fault parallel displacement.

Line	Horizontal Distance (m)	Δ Mile (1609.265m)	Formal Error (m)	Fault Slip (right-lateral)	Post-Seismic Accumulation	Fault Parallel Displacement
D-E	1616.713	+7.448	0.009	11.1 m	0.1 m	11.0 m
H-J	1608.064	-1.201	0.040	N/A	N/A	N/A

TABLE 3-1

meter. Site E is marked by a diffuse mound of stones approximately 0.6m in radius. Uncertainty in surveying to the same position as Freeman increases the overall line-length error to 1.7m. The San Andreas strikes 48 degrees from measurement line D-E, so the fault parallel error is 2.5m (1σ).

Results

The length change of line D-E corresponds to 11.1m of dextral displacement parallel to the fault, if one does a simple trigonometric correction, assuming purely dextral slip between two blocks. Assuming a constant strain rate during the 136 years since the 1857 earthquake, and velocities estimated from recent surveys (Lisowski *et al.*, 1991), we calculate that line D-E has increased 0.1m elastically since the 1857 earthquake. This amount of post-seismic displacement is small compared to the errors associated with the survey. Time-dependent effects such as visco-elastic relaxation following the earthquake are negligible. Subtracting 0.1m of post-seismic deformation, we calculate that markers D and E were displaced 11.0 ± 2.5 m relative to each other by the 1857 earthquake and associated foreshocks, aftershocks and afterslip.

Implications

The large displacement value provides a strong argument that the 9.5m offsets near Wallace Creek, as well as the smaller offsets to the southeast were produced entirely by the 1857 earthquake, rather than by multiple smaller earthquakes. Furthermore, this measurement shows that the geomorphic evidence for ~7 to 9.5 m of slip over a distance of a mere 2.6 km must mean that slip across the fault trace varied at least this much in 1857.

Similar slip variation was reported after the M_s 7.4 1992 Landers earthquake (Rubin and McGill, 1992).

Within the (1σ) measurement error, the maximum ($9.5\pm 0.5\text{m}$) geomorphic offsets at the fault are indistinguishable from the $11.0\pm 2.5\text{ m}$ off-fault dextral offset of D and E. Similarly, the difference between the smallest (6 to 7m) and largest (9 to 10 m) offsets along the fault trace is barely discernible within measurement error. Yet the total difference between the amount of strain released by 6 to 7m or $11\pm 2.5\text{m}$ of slip may be as much as 50%. This is an important observation for geologists who try to characterize prehistoric earthquakes by measuring offset landforms. The magnitude of spatial variations in strain release along a fault may not be recognizable from measurements of offset landforms.

Short-wavelength variations in slip during a large earthquake may reflect uneven release of accumulated strain, or deformation on secondary structures. The former hypothesis implies that complementary slip will fill-in the areas of low slip in future large earthquakes, or during smaller events. Alternatively, movement on secondary faults and folds can be hypothesized to explain lower values of slip along the main fault. Repetition of slip patterns should result in the growth of complementary structures along the fault. Several late Quaternary folds and minor fault scarps that strike parallel to the San Andreas are found in the Carrizo Plain. Between Wallace Creek and the Bidart fan, however, the wavelength of slip variations during the 1857 earthquake (from Grant and Sieh, 1993) appears to be different than the wavelengths of visible structures.

Co-seismic deformation away from the main fault zone may cause local variations in slip rate along the main fault trace. Given that the geomorphic offsets were produced by one earthquake, we can use them to

estimate the average slip rate over one earthquake cycle. The most recent large earthquake prior to 1857 occurred in A.D. 1405-1510 (Grant, 1993; Grant and Sieh, 1992). Thus, the time span of the last complete earthquake cycle is 400 ± 53 years, and the average slip rate during this cycle at Wallace Creek is 24 ± 4 mm/yr. At the Phelan and Bidart fans the average slip rate over the cycle is only 16 ± 2 and 18 ± 3 mm/yr, respectively. These rates are lower than the late Holocene average slip rate of 33 ± 3 mm/yr (recalculated from Sieh and Jahns, 1984) at Wallace Creek by about 25-50%. Stated differently, 13 ± 2 m of slip should have accumulated during the last earthquake cycle, yet <10 m of slip were released along the section of fault studied. (All errors reported here are 2σ .) Therefore, either a slip deficit resulted from the 1857 earthquake, or the slip rate of the fault is lower than far-field deformation rates.

Despite the discrepancy between pre-1857 strain accumulation and strain relief in 1857, we do not believe that the current rate of elastic strain accumulation differs from the late Holocene slip rate. The magnitude of the single cycle slip rate deficit is well outside the errors in measurement of the geodetic and geologic slip rates. Geodetically determined accumulation rates from networks spanning several tens of kilometers across the Carrizo Plain are indistinguishable from millennial strain relief rates measured geologically across the ~ 20 -m-wide main fault zone at Wallace Creek (Sieh and Jahns, 1984; Lisowski *et al.*, 1991; Feigl *et al.*, 1992). Dislocation models that fit trilateration data and recent GPS results indicate that 31-35 mm/yr of elastic accumulation is occurring over a 175-km-wide zone spanning the fault. These rates are similar to the 32 ± 2 mm/yr rates of fault slip measured across the creeping section of the San Andreas fault (Lisowski and Prescott, 1981) and the late Holocene rate of strain relief.

This similarity between the slip rates averaged over many earthquake

cycles at the fault trace and the short-term wide aperture accumulation rate means that slip deficits must average out over time. Theoretical and laboratory models of faults exhibit similar behavior (Rundle, 1989; King, 1991). Block-and-spring models of faults indicate that the total stress is rarely relieved in one event, but the long-term average slip rate is stable because it must keep up with the far-field displacement rate (Rundle, 1989). Unless the slip deficit resulted from dynamic slip "overshoot" during the A.D. 1405-1510 earthquake, or anelastic deformation, the surface slip in the next large earthquake should compensate the deficit.

Assuming the slip deficit hypothesis, it is interesting to estimate how deeply the 1857 slip deficit may have extended. Assuming isotropic homogeneous elastic properties, we have calculated the predicted displacement of marks D and E for different fault slip distributions. In the absence of subsurface geologic data, we chose a simple 2-part fault slip model in which constant slip occurs in the lower part and horizontally varying but vertically constant slip occurs in the upper part (figure 3-3). Note that this is a quasi-one-dimensional model since we do not specify the 2-dimensional details of slip in either the upper or lower part. We varied the thickness of the upper part, and the amount of slip at depth. The lower part extends 15 km to the base of the seismogenic zone. The results (figure 3-4) indicate that the upper part of variable slip is thin and probably does not extend much deeper than about 1 or 2 km because there is a steep gradient in the curve at 1 to 2 km. The upper part could be even thicker, however, suggesting more than 11m of slip at depth. Therefore, if the behavior is elastic, the surface slip during the 1857 earthquake, as represented by geomorphic offsets, probably does not reflect the total average slip on the fault at depth.

Figure 3-3: Dimensions of the two-part model used in the elastic dislocation model. The figure shows a section along the San Andreas fault with the locations of monuments D and E projected onto the fault. Vertically constant right-lateral displacement is imposed on each part. Displacement of the upper part varies horizontally with 9.5 m of slip imposed from Wallace Creek northward, 7 m of slip imposed from the Phelan fan southward, and a linear interpolation of slip between.

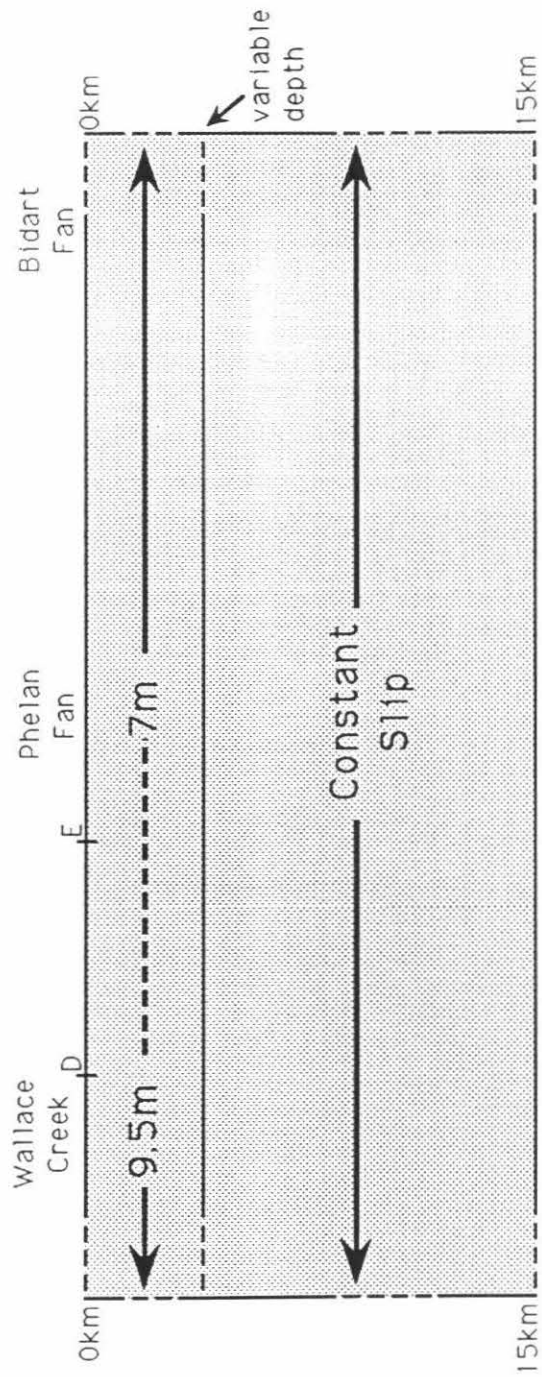
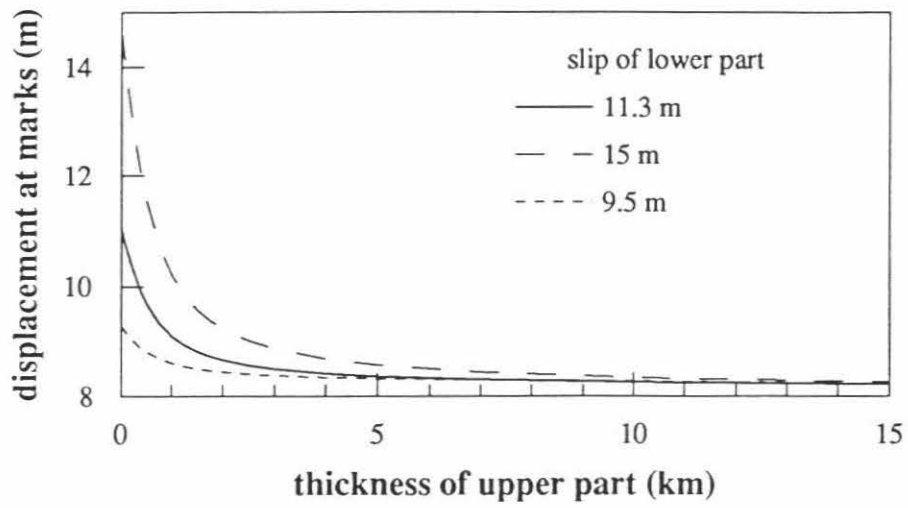


Figure 3-4: Displacement of monuments D and E calculated from the elastic dislocation model for varying thicknesses of the upper part, and slip of 9.5, 11.3 or 15 m on the fault in the lower part. Properties of lower part are constant horizontally and vertically to a depth of 15 km. Results suggest that the upper, variable-slip part of the fault is at least 1 kilometer thick.



There are several implications of the 1857 slip deficit and surficial slip variation for earthquake forecasting and fault mechanics. If the surficial slip during an earthquake is not equivalent to the amount of strain accumulated since the last earthquake, then the size of past or future events and the "characteristic" properties of fault segments are difficult to estimate accurately. Even if the date of an earthquake could be predicted, elastic strain accumulation models may inaccurately predict the amount of slip at the surface trace of a fault during the earthquake by up to 25% or more. In the design of critical structures that cross active faults, it would be prudent to anticipate greater amounts of co-seismic slip than the amount estimated from elastic strain accumulation models.

Acknowledgments

Supported by USGS grant #14-08-001-G-1789, Caltech ERA and fellowships from NRC and F. Beach. Leighton. L. Vredenburg of BLM Cadastral Survey Office, Bakersfield brought the early surveys to our attention. We thank K. Sieh, S. Bryant, P. Dunham, J. Satalich, Caltrans and reviewers for assistance. Caltech Division of Geological and Planetary Sciences contribution #5249.

REFERENCES

- Grant, L. B., and K. Sieh (1993). Stratigraphic evidence for seven meters of dextral slip on the San Andreas fault during the 1857 earthquake in the Carrizo Plain, *Bull. Seism. Soc. Am.*, in press.
- Grant, L. B. (1993). Characterization of large earthquakes on the San Andreas fault in the Carrizo Plain: Implications for fault mechanics and seismic hazard. Ph.D. Thesis, California Institute of Technology, Pasadena.
- Grant, L. B., and K. Sieh (1992). Irregular recurrence times and increased seismic hazard from earthquakes on the Carrizo segment of the San Andreas fault, southern California, *Proceedings of the 35th Ann. Meeting of Association of Engineering Geologists*, Long Beach, CA., 567, Oct. 1992.
- Feigl, K. L., D. C. Agnew, Y. Bock, D. Dong, A. Donnellan, B. H. Hager, T. A. Herring, D. D. Jackson, T. H. Jordan, R. W. King, S. Larsen, K. M. Larson, M. H. Murray, Z. Sheng and F. H. Webb (submitted). Measurement of the velocity field of central and southern California, 1984-1992, *J. Geophys. Res.*
- King, C-Y. (1991). Multicycle slip distribution along a laboratory fault *J. Geophys. Res.* **96**, 14377.
- Lisowski, M., J. C. Savage, W. H. Prescott (1991). The velocity field along the San Andreas fault in central and southern California *J. Geophys. Res.* **96**, 8369.
- Lisowski, M. and W. H. Prescott (1981). Short-range distance measurements along the San Andreas fault system in Central California, 1975-1979, *Bull. Seism. Soc. Am.* **71**, 1607.
- Okada, Y. (1985). Surface deformation due to shear and tensile faults in a half-space *Bull. Seism. Soc. Am.* **75**, 1135.

- Rubin, C. R., and S. F. McGill (1992). The June 28, 1992 Landers earthquake: slip distribution and variability along a portion of the Emerson fault, *EOS, Trans. Amer. Geophys. U* , **73** no. 43, 362.
- Rundle, J. B. (1989). A physical model for earthquakes 2. Application to Southern California *J. Geophys. Res.* **93**, 6255.
- Sieh, K. E., M. Stuiver, D. Brillinger (1989). A more precise chronology of earthquakes produced by the San Andreas fault in Southern California, *J. Geophys. Res.* **94**, 603.
- Sieh, K. E. and R. H. Jahns (1984). Holocene activity of the San Andreas fault at Wallace Creek, California, *Geol. Soc. Am. Bull.* **95**, 883.
- Sieh, K. E. (1978). Slip along the San Andreas fault associated with the great 1857 earthquake, *Bull. Seism. Soc. Am.* **68**, 1421.
- White, C. A. (1983). *A History of the Rectangular Survey System*, Bureau of Land Management, U.S. Dept. of Interior.

Chapter 4

Paleoseismic Evidence of Clustered Earthquakes on the San Andreas Fault in the Carrizo Plain, CA.

by

Lisa B. Grant and Kerry Sieh

Seismological Lab 252-21
California Institute of Technology
Pasadena, CA. 91125

To be submitted to *Journal of Geophysical Research*

Abstract

Exposures we have excavated across the San Andreas fault disprove the hypothesis that part of the fault in the Carrizo Plain is unusually strong and experiences relatively infrequent rupture. The exposures record evidence of at least 7 surface rupturing earthquakes which have been approximately dated by AMS radiocarbon analysis of detrital charcoal and buried in-situ herbaceous plants. Five large earthquakes have occurred since approximately 1218 A.D.. The most recent earthquake, Event A, was the 1857 Fort Tejon earthquake, which we have associated with 6.6 m to 10 m of dextral slip along the main fault trace. The penultimate earthquake, Event B, occurred within the period A.D. 1405-1510. Slip from either events B and C combined, or from event B alone, totals 7 to 11m. Three earthquakes, events C, D, and E, occurred in a temporal cluster prior to event B and after approximately A.D. 1218. The average recurrence interval within this cluster is no more than 116 and no less than 73 years, depending on assumptions. Events F and G occurred after 200 years B.C. A depositional hiatus between events F and E may hide evidence of additional earthquakes. Two of the four earthquakes within the Carrizo cluster of A.D. 1218 to 1510 may correlate with events T (A.D. 1329-1363) and V (A.D. 1465-1495) at Pallett Creek. This would imply two fault ruptures similar in length to that of 1857. The remaining earthquakes in the cluster do not correlate with dated prehistoric earthquakes in southern California, which suggests that the Carrizo segment has ruptured independently or in combination with segments to the north. This pattern of earthquakes suggests that clusters of earthquakes occur at the end of seismic "supercycles".

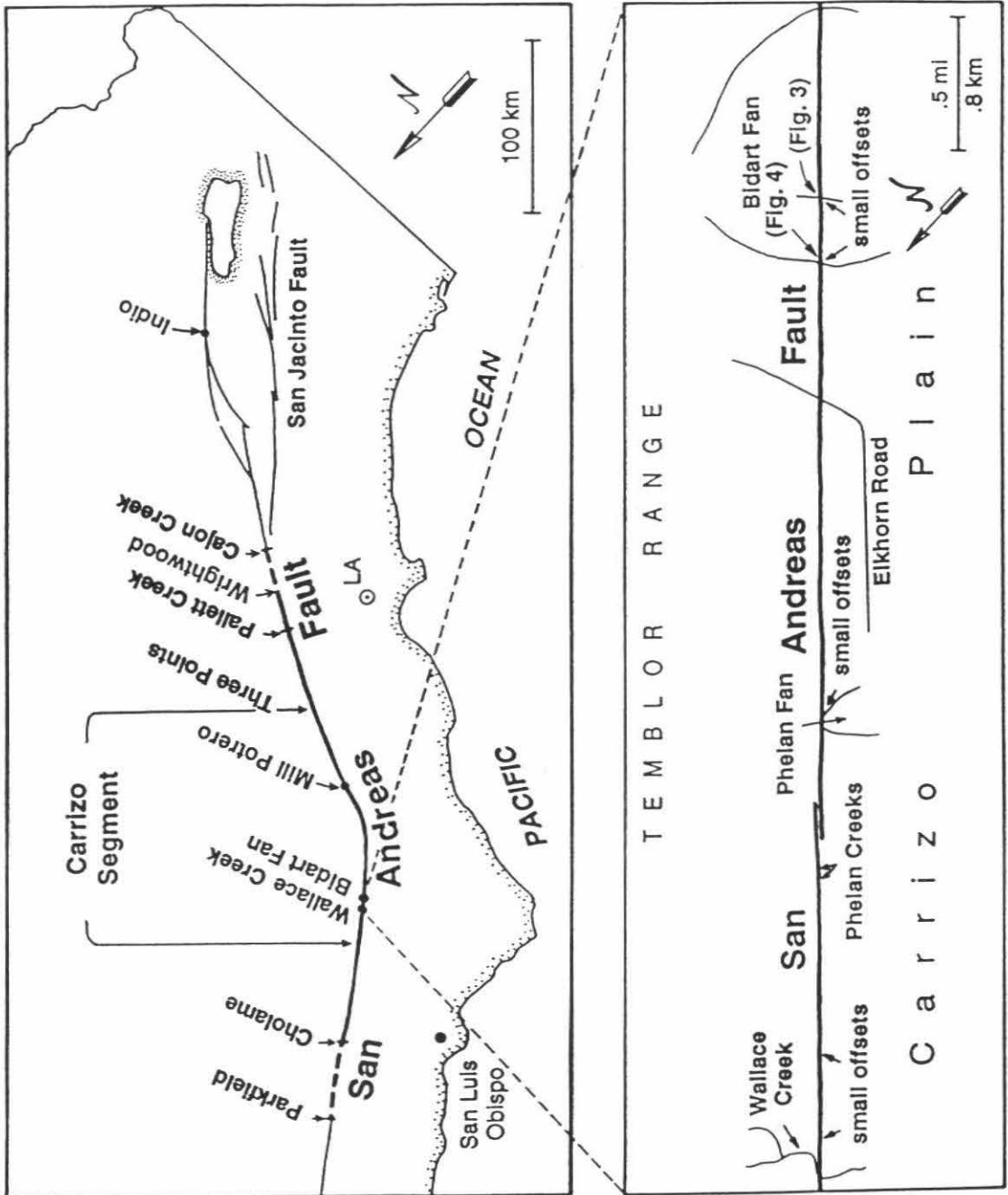
Introduction

Within the past two decades, geologists and seismologists looking at ancient and modern patterns of large earthquakes have concluded that active faults typically do not generate regular patterns of earthquake recurrence (Sieh *et al.*, 1989; Jacoby *et al.*, 1988; Thatcher, 1989; Matsuda *et al.*, 1978). These discoveries have inspired theoretical work that suggests that even deterministic physical systems may produce complex temporal and spatial patterns of fault rupture (Rundle, 1988; Stuart, 1986; Ward, 1991). The timing and rupture extent of large earthquakes may even be chaotic, rather than time-predictable or characteristic (Huang and Turcotte, 1990; Scholz, 1990).

Nevertheless, several observations and models suggest that the strongest segments of faults may control the timing of the largest earthquakes along a fault and may have histories that most closely approximate uniform recurrence (Thatcher, 1989; Sieh *et al.*, 1989; Ward, 1991). In this paper we report data that enable a test of this idea.

The Carrizo segment of the San Andreas fault (figure 4-1) has been interpreted as an unusually strong fault segment (Sieh and Jahns, 1984; Schwartz and Coppersmith, 1984; Sykes and Seeber, 1985; Stuart, 1986) which ruptures relatively infrequently during large earthquakes. The basis for this hypothesis is geomorphic. This segment experienced the largest offsets during the latest large earthquake - in 1857. Previous measurements of stream channels offset 9.5, 21.8 and 33 m near Wallace Creek (figure 4-1) suggest that 9.5, 12.3 and 11 m of dextral slip occurred during the past three large earthquakes. If strain accumulates uniformly at the average Holocene slip rate of 34 ± 3 mm/yr, and if it is relieved according to a time-predictable model, then the time intervals following these 3 earthquakes should be 250 to

Figure 4-1: Map of the southern San Andreas fault, with 1857 rupture in bold, dashed where uncertain. The study site is located on the Carrizo segment of the fault, the segment which contains the largest offsets associated with the great 1857 earthquake (Sieh, 1978; WGCEP, 1988). Inset map shows local features mentioned in the text.



450 years (Sieh and Jahns, 1984).

Recent geomorphic and geodetic measurements, respectively, confirm that 6.6 to 9.5 meters of dextral slip occurred on the main trace, and 11.0 ± 2.5 m of displacement occurred across the San Andreas fault zone in the Carrizo Plain during the 1857 earthquake (Grant and Sieh, 1993; Grant and Donnellan, submitted). Recent geologic work has confirmed that the previous large earthquake occurred several centuries prior to 1857 (Grant and Sieh, 1993). More precise dates and offsets of this penultimate event, and its predecessors have, until now, been unavailable. Without such data, the abovementioned earthquake recurrence hypotheses are highly speculative.

Relatively complete paleoseismic records of earthquake dates spanning more than a few earthquake cycles have previously been available at only two sites along the Mojave segment: the Pallett Creek and Wrightwood sites (figure 4-1; Sieh *et al.*, 1989; Fumal *et al.*, 1993). More complete sets of dates and slip in pre-historic earthquakes elsewhere along the fault is needed to formulate better models of fault behavior and seismic hazard. This paper presents and interprets additional evidence of past large earthquakes on the Carrizo segment of the San Andreas fault.

Site Selection

To determine the dates and offsets associated with the past several large earthquakes, we sought a site where sediment has been accumulating across the fault over the past millenium. To allow discrimination of individual events, the sedimentation must have occurred more frequently than surface rupturing earthquakes. For optimum use of radiocarbon dating methods, the

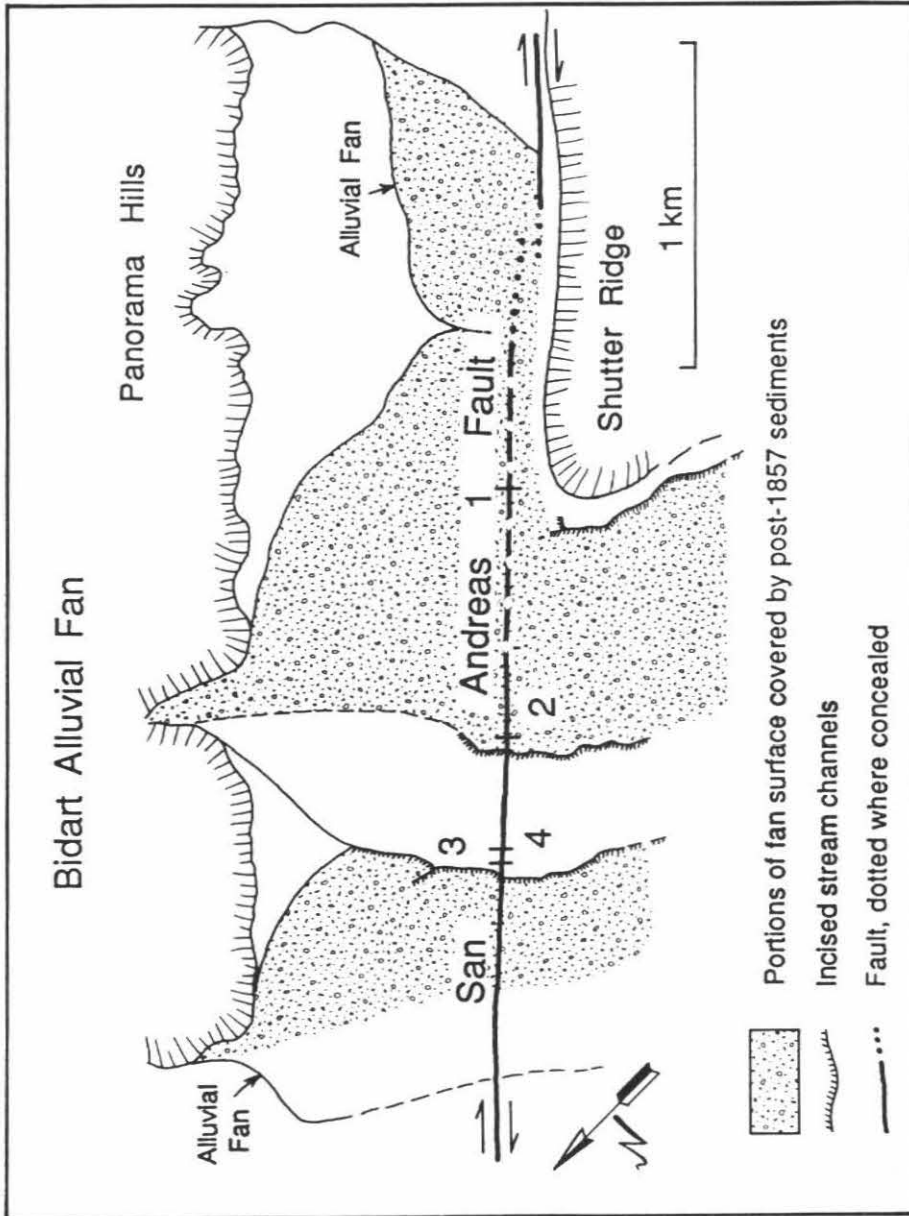
time interval between depositional events should be less than the error bars on radiocarbon analyses, that is, less than a few decades.

In the semi-arid Carrizo Plain, sediment is deposited primarily as debris flows on alluvial fans during the wetter winter months. Inspection of twentieth-century aerial photos indicates that storm runoff deposits sediments on the fans every decade or two. However, the locus of deposition migrates across the fans on a time scale that is much longer than the interval between storms. Therefore areas on the fans experience long hiatuses in deposition interspersed with periods of frequent sedimentation. Hence, for this study we sought an aggrading alluvial fan, traversed by the San Andreas fault and with a discernible pattern of pre-historic sedimentation. On the Bidart Ranch 5 to 6 km southeast of Wallace Creek the fault traverses an alluvial fan that appeared on geomorphic grounds to meet this requirement.

The Bidart Fan

The Bidart fan is fed by ephemeral streams that drain the western flank of the Temblor Range and the northern Panorama Hills (Figures 4-1, 4-2). It is heavily grazed and sparsely vegetated with drought-tolerant shrubs and annual grasses. Photographs taken in 1966 and 1978 show recent sediments covering the southwestern part of the fan. Floods in 1991 buried an even larger area with fresh sediment, but negligible deposition occurred on the northwestern part of the fan.

Figure 4-2: Map of the Bidart alluvial fan and nearby fans, showing locations of trenches, entrenched and offset stream channels. Stippled pattern marks recent deposition, mapped from 1966 and 1978 air photos and from ground inspection in 1991. Base: from 1:6000 and 1:35000-scale aerial photographs taken in 1966 and 1978.



Bidart Alluvial Fan

Panorama Hills

Alluvial Fan

Andreas Fault

Shutter Ridge

1 km

San

Alluvial Fan



The surficial pattern of sedimentation and channel incision on the Bidart fan suggests that the area of active sedimentation has swept across the fan from northwest to southeast over the time period of several earthquake cycles. Northwest of the center of the fan, an incised stream channel is offset approximately 7 m (figure 4-3). We suspected that this offset formed during the 1857 earthquake because the Phelan fan and a channel 3 km to the northwest (figure 4-1) were offset approximately 7 meters during the 1857 earthquake (Grant and Sieh, 1993). Therefore, the adjacent parts of the Bidart fan had probably been actively sedimenting prior to, but not since 1857. At the northwestern edge of the fan, another incised ephemeral channel is offset 14.6 to 18.4 m (figure 4-4). This amount of slip would represent at least the 1857 and one previous prehistoric earthquake. Thus, parts of the fan adjacent to this incised channel probably were active before but not after the last 2 or more earthquakes.

From these geomorphic clues, we anticipated we would be able to piece together a complete recurrence story from several well-placed excavations across the Bidart fan. Trench 1, excavated by Prentice and Sieh (1989) on the southeastern lobe of the fan revealed frequent sedimentation from about A.D. 1500 to the present. The 1857 earthquake was clearly expressed within this 1-meter-thick section. Deeper in the section, three depositional hiatuses of several hundred to a thousand years duration led Prentice and Sieh (1989) to conclude that their record of 7 earthquakes in 3000 years BP was a minimum. From this partial record, they calculated a maximum average recurrence interval of 500 years.

We expected to find a better record of the penultimate event near the 7-meter offset because we hypothesized that sediment was deposited on the central portion of the fan prior to incision of the channel, which occurred

between the penultimate event and 1857. We placed trench 2 next to this offset to search for evidence of the penultimate earthquake (figure 4-3).

Because the incised channel offset 14.6 to 18.4 m at the northwestern edge of the Bidart fan was presumably formed by more than one earthquake (Sieh, 1978), the northwestern part of the fan would have been the depositional lobe of the fan between the penultimate event and one or more previous events. Therefore, we placed trench 3 next to this offset and trench 4 astride a small graben nearby to examine evidence of older earthquakes (figure 4-4).

Methods

After excavating the trenches, we cleaned off, surveyed and mapped the walls in detail at a scale of 1:20. We collected hundreds of samples of organic material and charcoal from the trench walls. Only a few of these samples were large enough for radiocarbon dating by accelerator mass spectrometry (AMS).

We recorded stratigraphic evidence of surficial rupture associated with earthquakes. Several stratigraphic features indicate large prehistoric earthquakes. Events are recognized in the trench walls primarily by broken and tilted beds overlain by unbroken beds, and by upward terminations of fault traces. A single upward termination of a fault trace may be tenuous evidence for an event (Bonilla and Lienkaemper, 1990), especially if the vertical separation across the fault is less than a few centimeters. To be confident of a distinct event, evidence must exist at the same stratigraphic horizon at several locations in the trench, and on both walls. Therefore, all of the events we report were caused by substantial surficial rupture, on the order of a meter or more. Fault zone breccia is distinguished from bioturbated zones

Figure 4-3: Topographic map of the offset stream channel incised near the middle of the Bidart alluvial fan. Contour interval is 10 cm. The channel was cut and the northwestern fan surface became inactive prior to A.D. 1857. Elevations are measured relative to an arbitrary datum. The 7.2 meter offset represents the mismatch of thalwegs outside the fault zone. We assume the bend of the channel downstream from the fault zone is not tectonic. The walls of trench 2 shown in figure 4-5 are solid. Unmapped ends of the trench are dashed. The width of the fault zone, as exposed in the trench, is indicated with brackets. See photo C-11, appendix C.

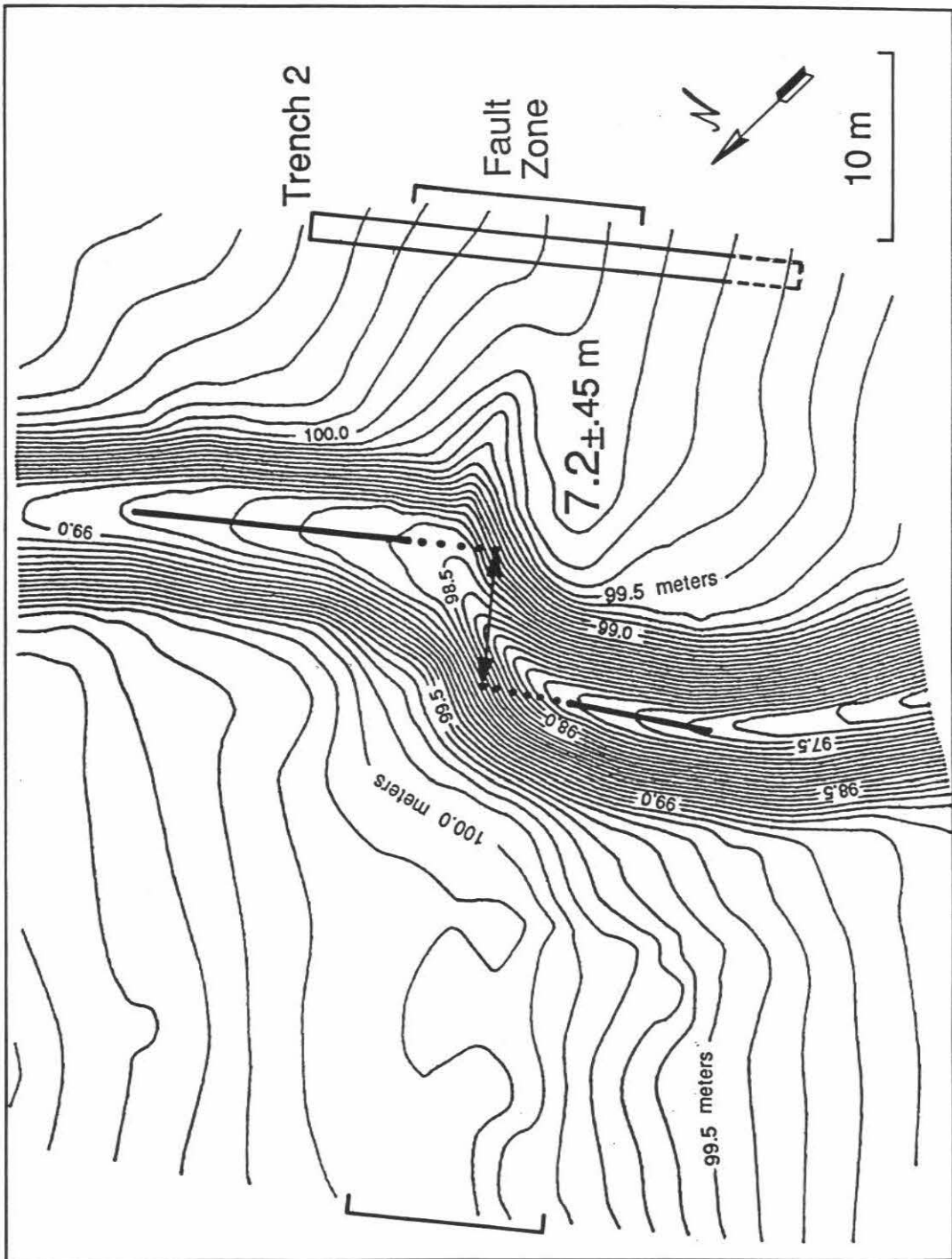
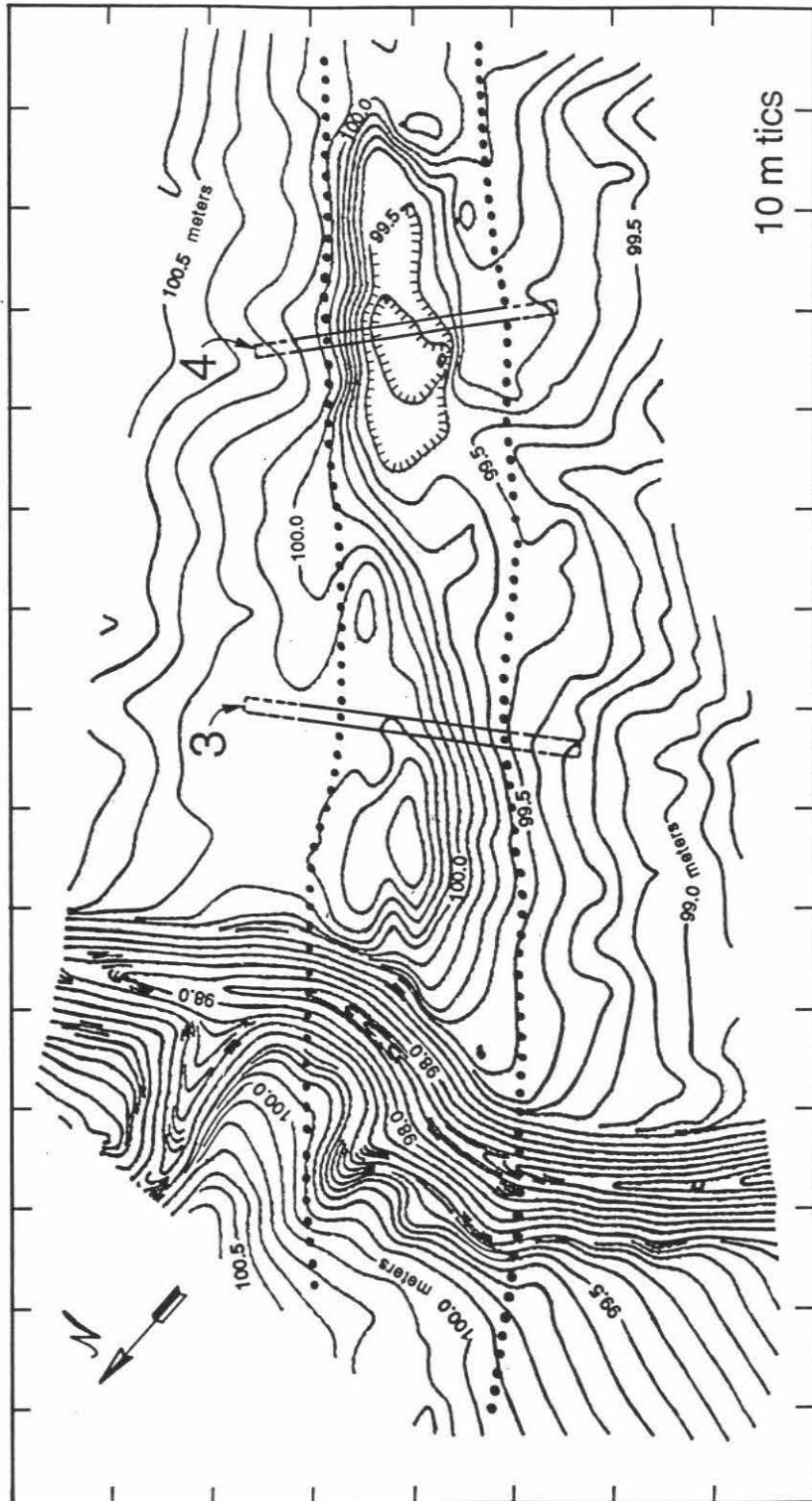


Figure 4-4: Topographic map of the fault zone in vicinity of trenches 3 and 4. Contour interval is 10 cm. Trench 3 cuts a moletrack and trench 4 traverses a tectonic depression. The large (14.6 to 18.4 meter) offset of the channel indicates that this northwestern margin of the Bidart alluvial fan was inactivated prior to at least A.D. 1857 and a prior large slip event. Structural and stratigraphic relations in the trenches constrain the date of abandonment of the surface (see text). The mapped portions of trenches 3 and 4, shown with solid lines, are displayed in cross-section in figures 8 and 9. Approximate width of the fault zone in recent surficial rupture events is delimited with bold dots.



by vertical fabrics and facies changes or differences in beds on opposite sides of the zone. We assign letter names to each event and describe the evidence in each trench.

Trench 2: the Penultimate Earthquake

Structure and Stratigraphy

Trench 2 was cut next to the 7-m offset to search for subsurficial evidence of a large earthquake prior to the 1857 earthquake. Figure 4-5 is a simplified cross-section of the faults and major units in the walls of a portion of trench 2. The stratigraphic position and lithologic description of the beds in this trench is summarized in figure 4-6. The beds are numbered to facilitate discussion. Primary sedimentary structures are preserved in the upper half of the section above unit 20, except for bioturbated unit 1, immediately below the present ground surface. Most beds are hardened debris flows or loose fluvial deposits ranging in texture from finely laminated silts to gravels.

Long and short depositional hiatuses are represented by thick bioturbated layers and thin paleosols. A bioturbated layer (unit 20) with scattered remnants of original sedimentary structure forms the lower half of the section above several debris flow beds at the base of the trench. Unit 20 represents a hiatus in deposition during a time when the rate of bioturbation of the fan surface exceeded the rate of sedimentation. The texture and thickness of the bioturbated layer is similar to several units in trench 1 (Prentice and Sieh, 1989). Radiocarbon dates from trench 1 reveal that these units record periods of time ranging from several hundred to nearly a thousand years (unpublished manuscript, K. Sieh, 1991).

Figure 4-5: Cross-section through sediments in the walls of trench 2 shows fault traces, radiocarbon sample locations, and units 3, 8 and 20. The ground surface ceased being an active fan surface prior to A.D. 1857, so the faults of the latest great earthquake extend to the ground surface. At least two prehistoric disruptions also appear in these trench walls. Boxes outline stratigraphic sections shown in detail in figures 7a,b and c, where stratigraphic levels of the three disruptions are especially clear. View is toward the northwest.

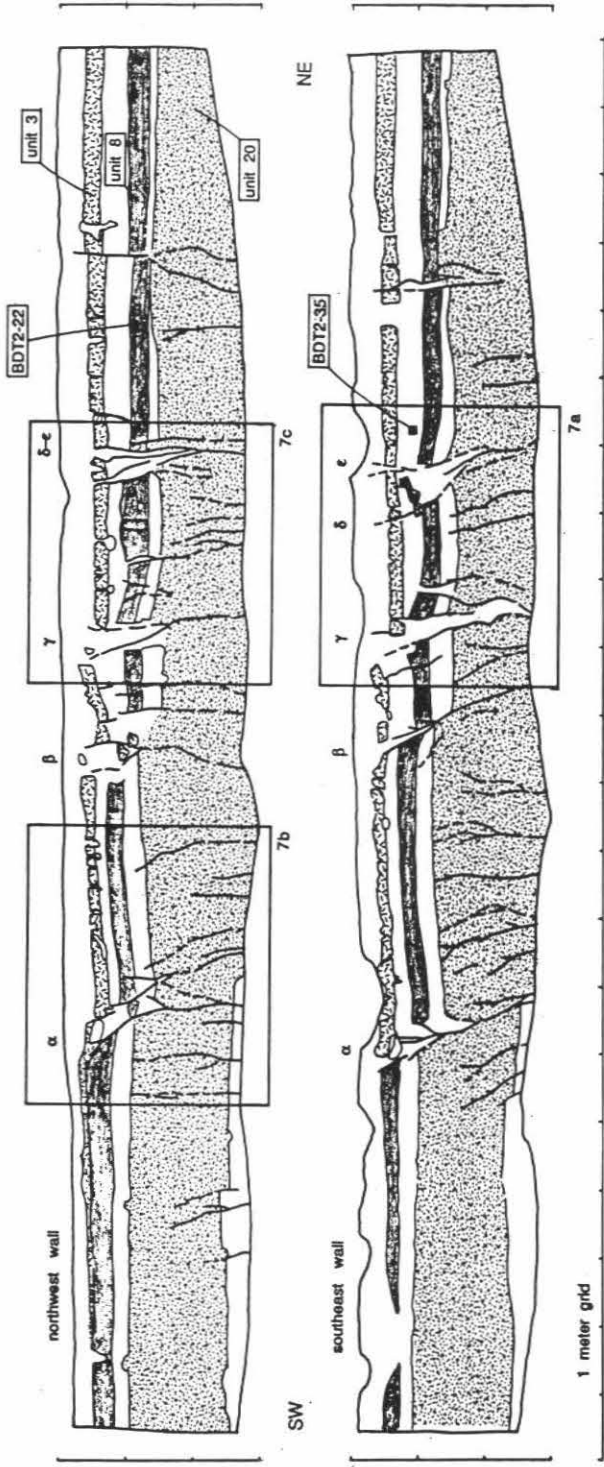
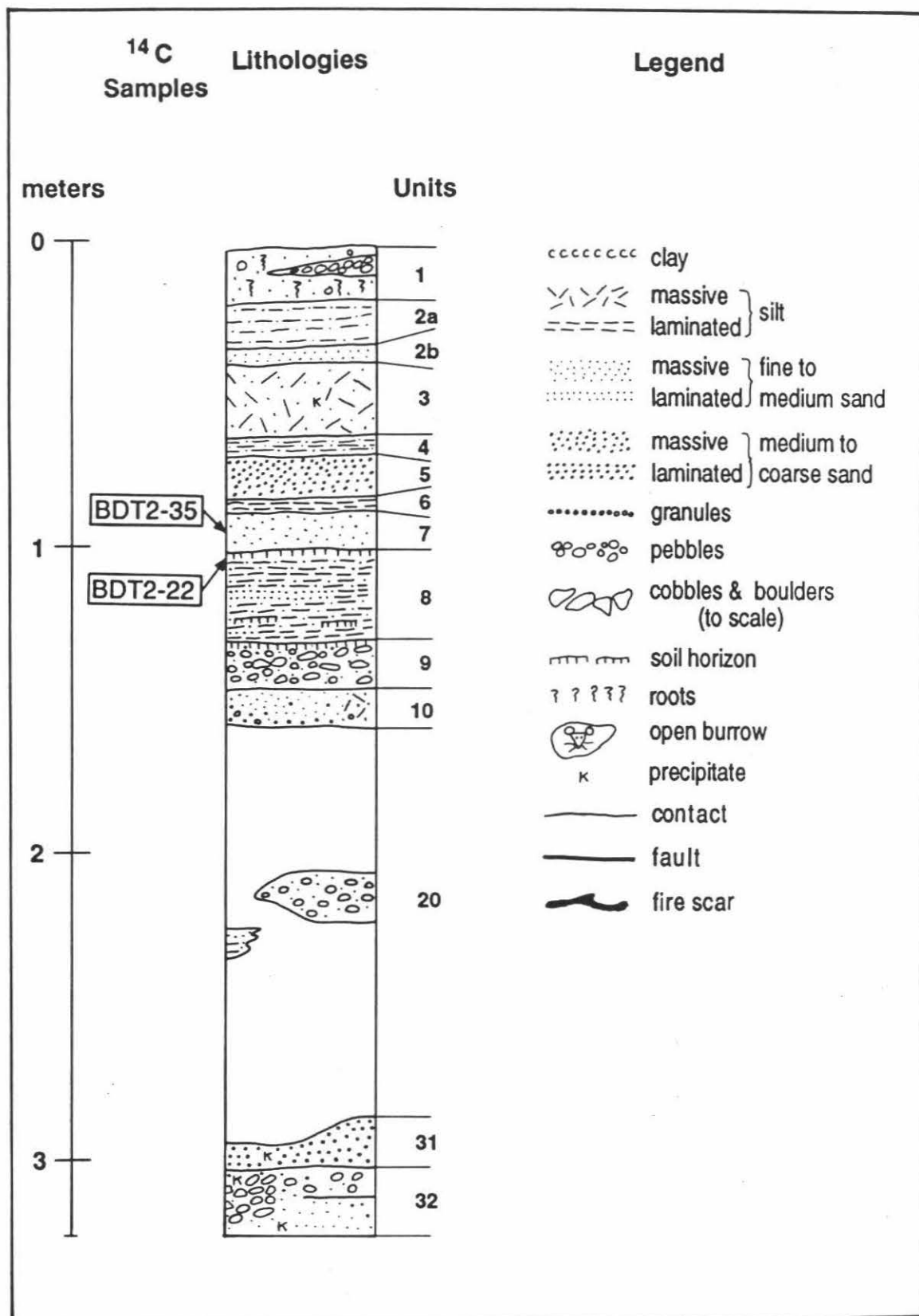


Figure 4-6: Generalized stratigraphic column of sedimentary deposits in trench 2. Distinctive or laterally extensive units and groups of units are numbered to facilitate discussion. The units consist primarily of debris flow deposits, fluvial deposits and bioturbated layers. Sedimentary characteristics are represented by symbols shown in the legend.



Three paleosols form time-stratigraphic markers across much of trench 2. A 1 to 4 cm thick paleosol with root holes, high porosity and random grain orientation is present in the matrix supporting the pebbles at the surface of unit 9 (figure 4-6). A poorly developed, discontinuous soil horizon of similar appearance is present near the base of laminated silt and sand bed 8, indicates that unit 8 was deposited by more than one sedimentary event. The upper 1 to 4 cm of unit 8 is a well-developed, continuous paleosol with root holes of a few millimeters diameter, scattered flakes of carbonized organic matter and an irregular lower boundary (see photo C-12, appendix C).

These thin paleosols are formed by roots and other agents of bioturbation. Field observations after the 1991 storms indicate that growth of grasses and other plants begin forming similar soil horizons a few weeks to months after deposition of fine sediment. We have calibrated the approximate formation time of the thin paleosols by digging pits on surfaces of known age, such as at the site of trench 1. We find that the few-centimeter-thick soils form on time scales of years to decades, but not centuries (unpublished manuscript, K. Sieh, 1991).

Several beds thin to the southwest or pinch out against paleo-fault scarps (figure 4-5). The sense of apparent displacement across several faults is down to the northeast, suggesting that northeast facing scarps may have ponded the thicker beds to the northeast.

Evidence of Earthquakes

Event A: The Fort Tejon Earthquake

The presence of a 3-meter deep gully only 15 m northwest of trench 2 and disrupted fan topography nearby is a clue that very little sedimentation

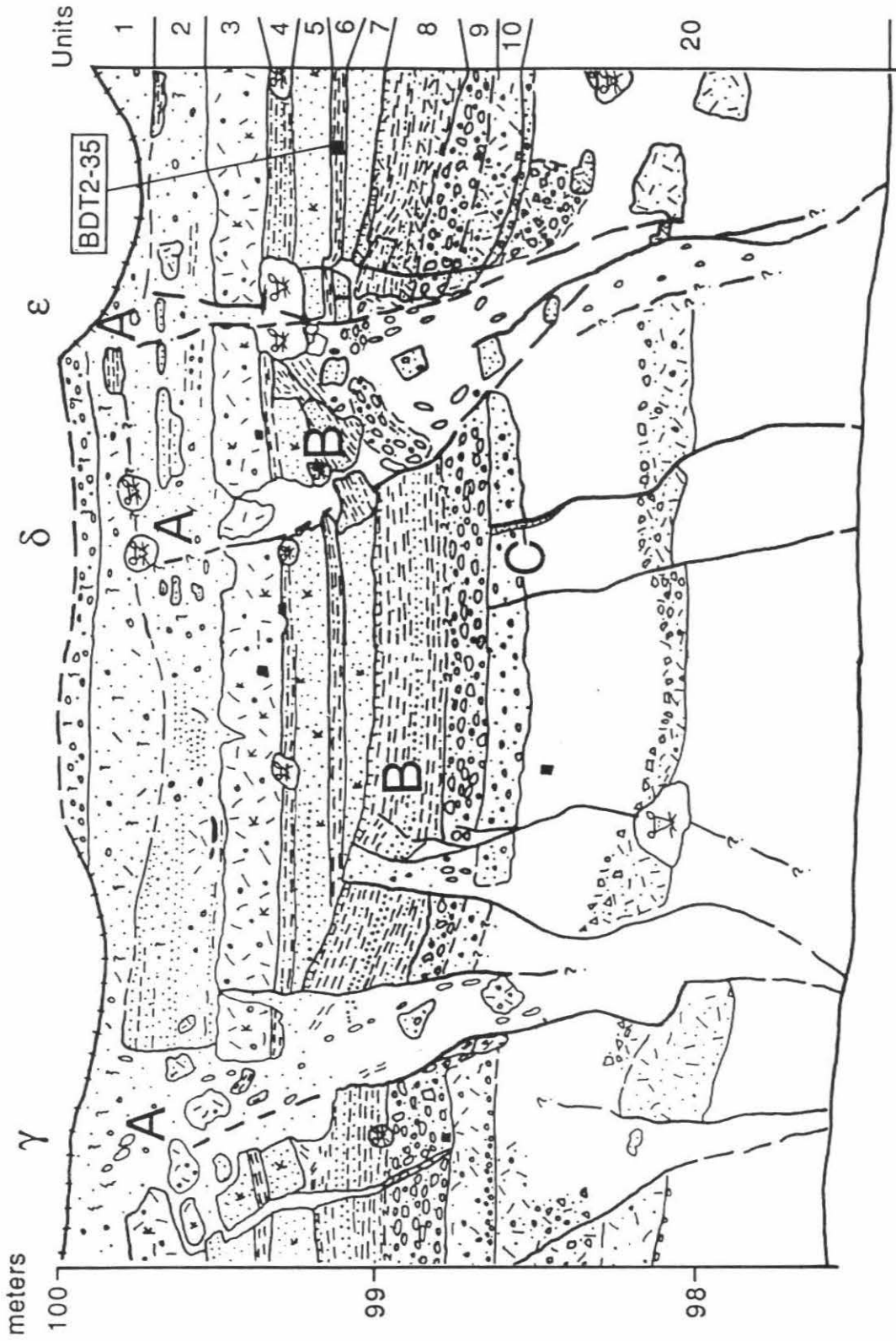
has occurred at the site of trench 2 since the latest major fault rupture (figure 4-3). Indeed the walls of trench 2 display a 13-m-wide zone of faults, many of which extend upward to the bioturbated surficial units 1 and 2 (Figures 4-5 and 4-7). The near-surface fault traces from the most recent rupture are designated 'event A'. Unit 3, a debris flow bed, is the youngest faulted bed which can be correlated across all major faults in the trench. Although units 2a and 2b display evidence of faulting at the northeastern end of the trench, they are absent in two thirds of the trench due to bioturbation. In the southwestern half of trench 2, unit 3 is broken by 3 major faults, labelled α , β and γ (figure 4-5). Beds exhibit facies changes across each of the faults; these changes indicate a strike-slip component of motion. Each fault also has a normal component of motion, northeast side down. Faults δ , ϵ and ϕ at the northeast end of trench 2 also break unit 3 and extend upward into unit 2 on the southeastern wall.

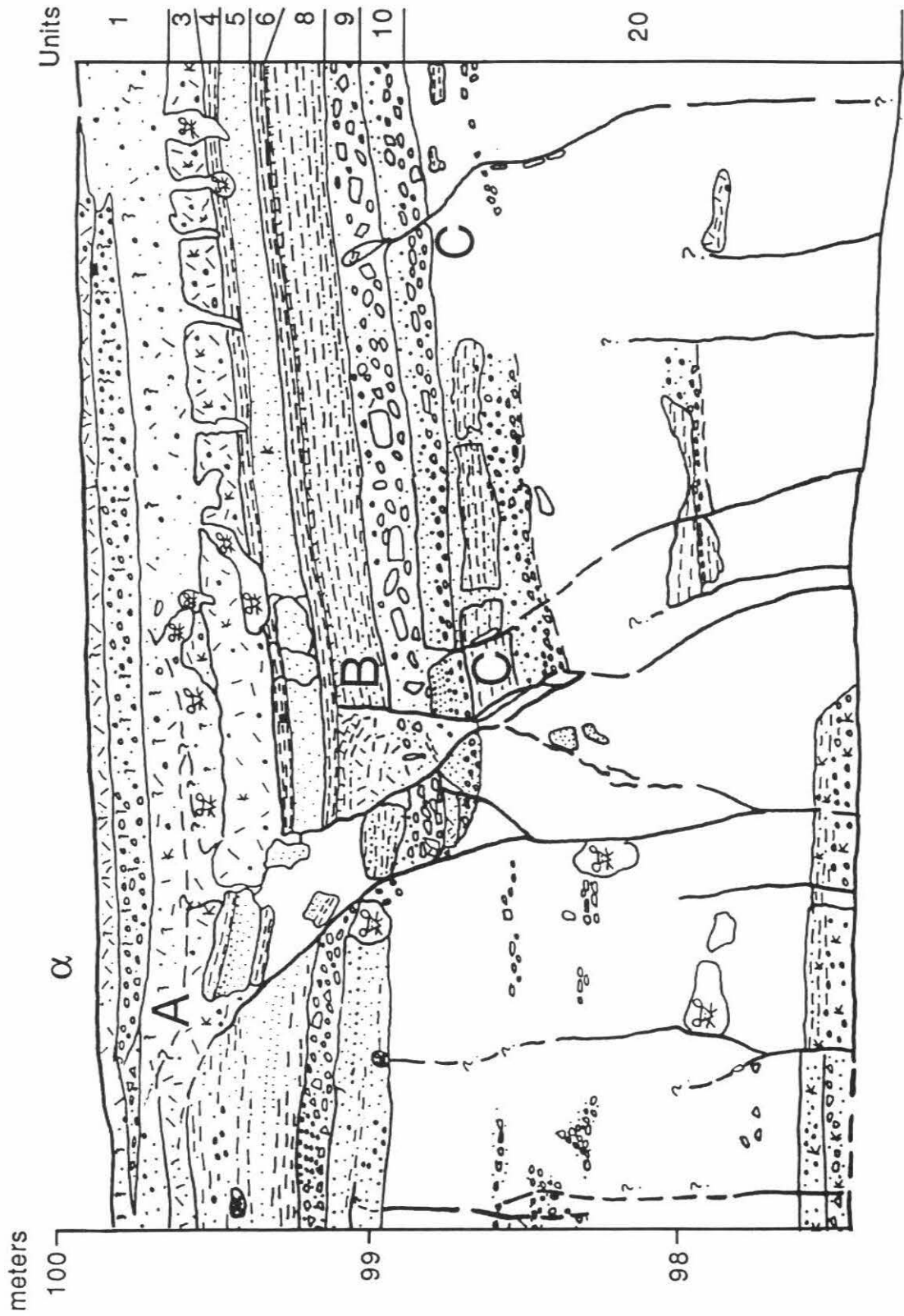
Because the 1857 earthquake generated at least 6.6 to 6.9 m of slip along the main fault trace at the Phelan fan 3 km northwest of trench 2 (Grant and Sieh, 1993), and 11.0 ± 2.5 m of dextral offset away from the fault (Grant and Donnellan, submitted), it is virtually certain that the approximately 7-m offset next to trench 2 represents surficial rupture in 1857. Therefore the youngest event, A, which breaks units 2 and 3 in the walls of trench 2 is the 1857 Fort Tejon earthquake and its associated foreshocks, aftershocks and afterslip. In trench 2, event A (1857) ruptured a 13-m-wide zone with $7.2 \pm .45$ m of net dextral slip.

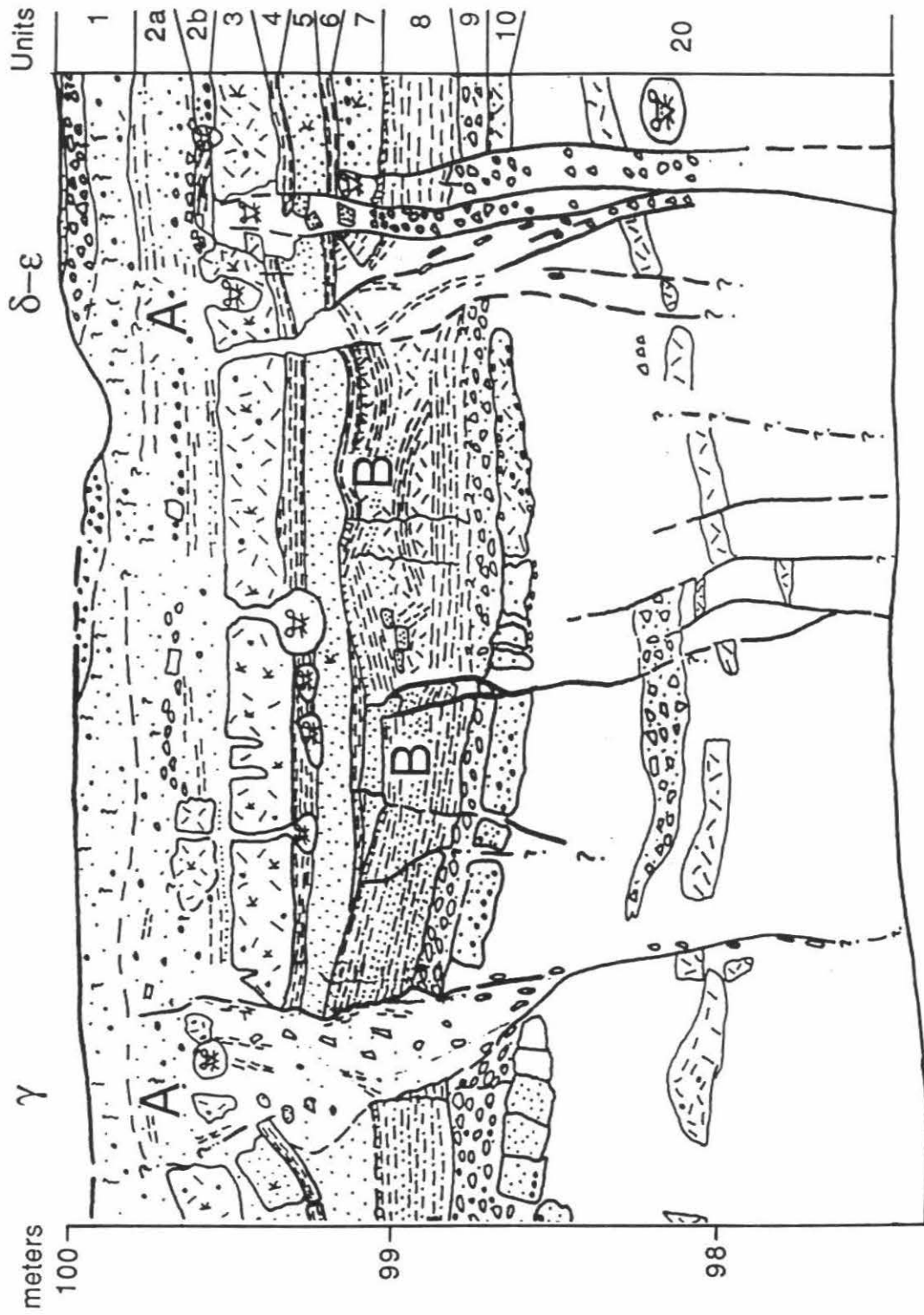
Event B: the Penultimate Earthquake

The youngest deformation event prior to event A occurred when unit 8 was at the surface (figure 4-5). At the time of the penultimate earthquake, a thin paleosol had developed on the surface of the laminated silt and sand of

Figure 4-7a, b, c: Portions of the walls of trench 2 that display particularly clear evidence for earthquake disruption A(1857), B and C. Greek letters indicate fault zones mentioned in text. Letters A, B and C mark the approximate locations of stratigraphic evidence for these events. View is toward the northwest. See figure 4-6 or appendix D for symbol legend. Blank areas are fault-zone breccia or bioturbated zones. See figure 4-5 for locations.







unit 8 (figure 4-7). The soil horizon has a maximum thickness of 5 cm in the northeastern part of the trench. Units 7, 6 and 5 overlie the faulted paleosol surface of unit 8.

Several angular unconformities are clear evidence of deformation between the time of deposition of units 7 and 8 (Figures 4-5, 4-7a and 4-7c). Just northeast of fault zone γ , on both walls, flat-lying units 6 and 7 pinch out against tilted unit 8. Similarly, unit 7 pinches out against upturned unit 8 northeast of fault zone δ - ϵ on the southeast wall of the trench (figure 4-7c). Another angular unconformity exists between faults δ and ϵ on the southeast wall (figure 4-7a). A strand of fault zone α also terminates at the top of unit 8 and is overlain by unfaulted unit 6 on both walls of the trench (figure 4-7b).

On the northwest wall of trench 2 between fault zones γ and δ , there is an anticlinal fold composed of comminuted upper unit 8 (figure 4-7c). The fold appears to rest above a basal detachment within a sandy lamination of unit 8. The anticline and basal shear plane probably resulted from compression between fault zones γ and δ during event B. A fissure cuts unit 8 on the southwest flank of the anticline. Sands and silts of units 6 and 7 above the fold and fissure are not deformed. Hence, the event occurred when the top of unit 8 was the ground surface. The anticlinal folding of unit 8 suggests that it may have been wet enough during the earthquake to deform semi-ductily. Opposite the fold on the southeast wall between fault zones γ and δ , a 10-cm-wide zone of fault breccia from event B extends to the surface of unit 8 and is covered by unfaulted units 7 and 6 (figure 4-7a).

Fault zones α , β , γ and δ - ϵ ruptured in both events A and B. All of the angular unconformities noted above are next to faults that also broke in event A. Fault zone β also shows evidence of movement during both events: the apparent offset of unit 8 is greater than the offset of unit 3 across the fault

(figure 4-5). The total width of the fault zones exposed in trench 2 is approximately the same for events A and B, suggesting that event B might have been as large as event A. Beds 2a thru 7 were deposited between events A and B, suggesting that at least a century, and possibly several centuries separated the earthquakes.

Event C

In trench 2, event C occurred at the end of a depositional hiatus that could hide evidence of additional events. Numerous fault traces terminate at the top of bioturbated unit 20, and in units 9 and 10. These traces represent at least one ground rupturing earthquake, and possibly several. Because bioturbation has destroyed the original stratigraphy in unit 20, it is difficult to correlate beds and faulting events in the lower half of the trench. There are up to three apparent events with fault terminations in unit 9 or 10, at the top of unit 20, and in the middle of unit 20 (figure 4-5, 7a and 7b). However, bioturbation in unit 20 may have obliterated the upper part of some traces and not others, leaving the appearance of 2 or more separate events. The best evidence in support of a multiple event hypothesis is southwest of fault zone α , on both walls, where at least one fault trace terminates below a remnant, unbroken bed in the central part of unit 20. This suggests that more than one rupture event terminates within the thick bioturbated layer.

Additional evidence that event C is more than one earthquake is between fault zones α and β . There several faults terminate at the top of bioturbated unit 20, on the southeast wall of trench 2 (figure 4-5). On the northwest wall two traces from the same set of faults appear to extend upward into units 9 and 10 (figure 4-7b). Beds 9 and 10 are broken, but no displacement is apparent on either side of the traces suggesting that the

amount of offset, if any, is small. These upward terminations may have formed during an earthquake which ruptured above unit 20, or the upper part of these traces may be misidentified rodent holes or settling of units deposited above fault traces formed during event C.

Thus, at least one, and probably several earthquakes ruptured to the surface of unit 20. We define the earthquake as event C and recognize that in trench 2 event C could represent up to 3 earthquakes which cannot be stratigraphically separated because of bioturbation during a depositional hiatus preceding event C. The width of the fault zone which ruptured during event C is approximately the same as for events A and B, and is located slightly further to the southwest.

Radiocarbon dating of Event B

Numerous fragments of detrital charcoal and organic material were embedded in the walls of all three trenches, but very few of the samples were large enough to be dated with AMS (Table 4-1). Some of the dated samples from trenches 3 and 4 were too small to measure the $\delta^{13}\text{C}$ ratio, which complicates the interpretation of their ages. A more serious complication is the detrital nature of most samples. The radiocarbon age of detrital wood can be considerably greater than the depositional age of a bed which contains it (Blong and Gillespie, 1978; Nelson, 1992). In the Carrizo Plain, radiocarbon dates on samples from the same stratum can differ by several hundred years (Grant and Sieh, 1993). Thus, the radiocarbon ages of samples must be evaluated with other information to determine the age of the events.

The date of event B is constrained by analysis of two radiocarbon samples from trench 2. The uppermost part of the paleosol at the surface of

Table 4-1) Radiocarbon dates, isotopic ratios and calibrated calendric dates of samples analyzed by the NSF AMS Facility at the University of Arizona, partially funded by NSF grant EAR85-12761. Sample number BDT2-22 is the 22nd sample collected from Bidart trench 2. Other samples are named similarly.

Table 4-1
Radiocarbon Samples

Sample#	$\delta^{13}\text{C}$	Radiocarbon Yrs, BP	Calendar Yrs, (1 σ), (2 σ)	Description
BDT2-22	-11.3	445 \pm 40	A.D. 1425-1465 A.D.1405-1510	grass fragments
BDT2-35	-12.0	580 \pm 40	A.D. 1310-1405 A.D. 1290-1415	charred twig
BDT3-17	-21.6	2750 \pm 70	BC 993-828 BC 1060-800	charcoal
BDT3-30	-9.4	2545 \pm 50	BC 800-603 BC 812-530	shell, genus Helminthoglypta
BDT3-46	-25*	1965 \pm 99	A.D. 98-126 BC 200 - A.D 250	charred plant (grasses?)
BDT4-39	-25*	815 \pm 45	A.D. 1180-1263 A.D. 1063-1274	charcoal
BDT4-40	-12.9	995 \pm 45	A.D. 998-1035 A.D. 970-1159	charcoal
BDT4-53	-25.9	1720 \pm 55	A.D. 241-395 A.D. 144-430	charred woody plant material
BDT4-57	-10.8	595 \pm 50	A.D. 1291-1405 A.D. 1280-1430	charred plant material
BDT4-64	-23.7	775 \pm 30	A.D. 1235-1269 A.D. 1218-1276	charred plant fragments
BDT4-66	-11.35	940 \pm 50	A.D. 1020-1162 A.D. 1000-1220	charcoal
BDT4-76	-10.4	795 \pm 58	A.D. 1195-1271 A.D. 1054-1280	charcoal
BDT4-84	-11.0	650 \pm 30	A.D. 1283-1379 A.D. 1277-1392	charcoal
BDT4-89	-25*	820 \pm 80	A.D. 1159-1270 A.D. 1029-1290	charred plant (grass?)

* $\delta^{13}\text{C}$ is assumed to be -25 because sample was too small to permit measurement.

unit 8 contained non-woody flakes of organic material resembling blades of grass which we collected for AMS dating (sample BDT2-22). The radiocarbon age of sample BDT2-22 yields a 2σ calendric age range of 1405-1510 A.D. The measured $\delta^{13}\text{C}$ is consistent with values reported elsewhere for C-4 plants (Smith and Epstein, 1971). Woody sample BDT2-35 was collected from overlying unit 6. It yields an overlapping but older 2σ calendric age range of A.D. 1290-1415. This sample is almost certainly detrital and, thus, may be older than the bed which contained it. However, the grassy fragments of sample BDT2-22 were preserved in-situ, could not have been detrital, and probably had a short lifespan. Since the paleosol is broken by event B, the earthquake occurred after the paleosol had formed. The estimated time of formation of the soil is a few decades or less, considerably less than the calendric date range from the radiocarbon date. Therefore we think that the age range of sample BDT2-22 includes the date of event B. We estimate the date of event B to be between A.D. 1405 and 1510 and favor the latter part of the interval.

Trenches 3 and 4: Older Events

Trenches 3 and 4 were cut next to the 14 to 18 m offset to find evidence of earthquakes prior to event B. Because the stream channel is offset at least twice as much as the channel near trench 2, we assume that the offset formed during slip in earthquakes A and B, at least. It is a reasonable assumption that incision of the channel occurred prior to offset, that is, prior to event B. We hypothesized that this area was the depositional lobe of the Bidart fan during the time of a depositional hiatus in the sections of trenches 1 and 2. We placed trench 3 next to the offset channel to date earthquakes prior to event B

and to try to determine the amount of slip associated with the last few earthquakes. Sediment was deposited in a neighboring graben (figure 4-4) during the 1991 storms, suggesting to us that enough sediment might have been deposited in the graben to preserve evidence of post-incision earthquakes which occurred after the depositional lobe of the fan migrated southeast. Therefore, we excavated trench 4 across the graben to relate the stratigraphic section of trench 3 to the number of earthquakes which occurred after incision of the offset channel.

Structure and Stratigraphy

The sediments and structures in trenches 3 and 4 reflect the depositional environment and structural evolution of a graben. Trench 3 straddles a topographic high, or moletrack, within the fault zone (figure 4-4). Thick beds in the central blocks of trench 3 suggest that they were deposited in a graben and subsequently uplifted. Thicker, down-dropped beds below the topographic graben in trench 4 indicate that the structural depression has persisted over several earthquake cycles.

Major fault zones separate stratigraphically coherent blocks within each trench (Figures 4-8 and 4-9). A 4-m-wide shear zone underlies the northeastern flank of the moletrack in trench 3. There are major faults at the edges of the graben in trench 4, and paleo-graben in trench 3.

We correlated beds across faults and between trenches using stratigraphic position, texture and appearance. Stratigraphic columns in Figure 4-10 show correlation of individual beds between trenches 3 and 4 and across major faults within the trenches. None of the beds were correlated with beds in trench 2. Most of the ground surface (unit 10) is bioturbated in

Figure 4-8: Cross-section through sediments in the walls of trench 3 shows fault traces, radiocarbon sample locations, and gravel units 80 and 220/230. This section shows moletrack at ground surface, which formed with 14 to 18 meters of dextral slip since the area ceased being an active depositional surface. At least 2 large-slip events ruptured thru to the ground surface. Thick gravels indicate filling of an older graben produced during earlier slip events. Fault-bounded stratigraphic blocks marked with Roman numerals are discussed in text. Boxes outline stratigraphic areas shown in detail in figures 12a,b, c and d to accompany discussions of evidence of various disruptions. Clear evidence of earthquakes is marked with capital letters. Selected carbon sample locations are marked. View is toward the southeast.

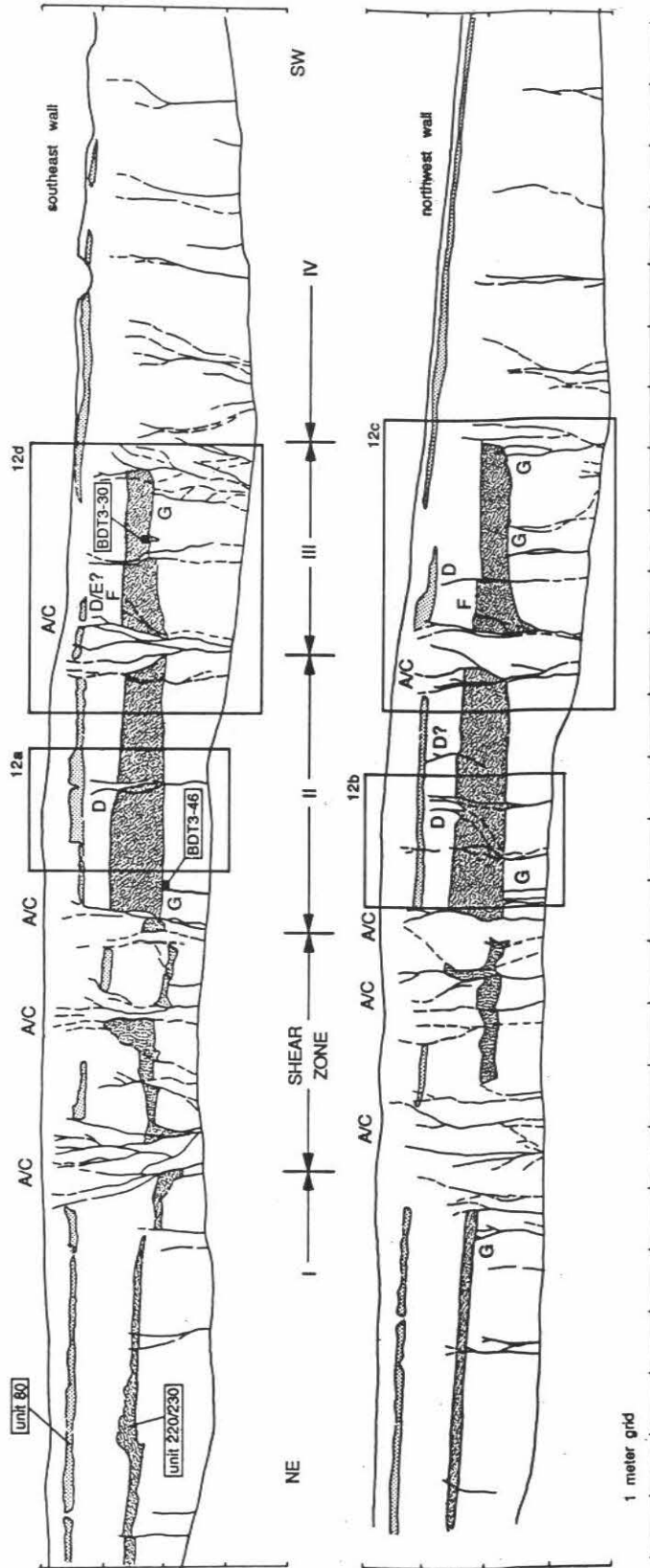


Figure 4-9: Cross-section through sediments in the walls of trench 4 shows fault traces, radiocarbon sample locations, and units 80, 150 and 220/230. The section shows a tectonic depression, or graben, in which sediments have accumulated. Evidence of several earthquakes is preserved in the sediments. Individual earthquakes are marked with capital letters. Fault-bounded stratigraphic blocks are numbered with Roman numerals keyed to the text. Boxes outline stratigraphic sections shown in detail in figures 11a-f. Selected carbon sample locations are marked. View is toward the southeast.

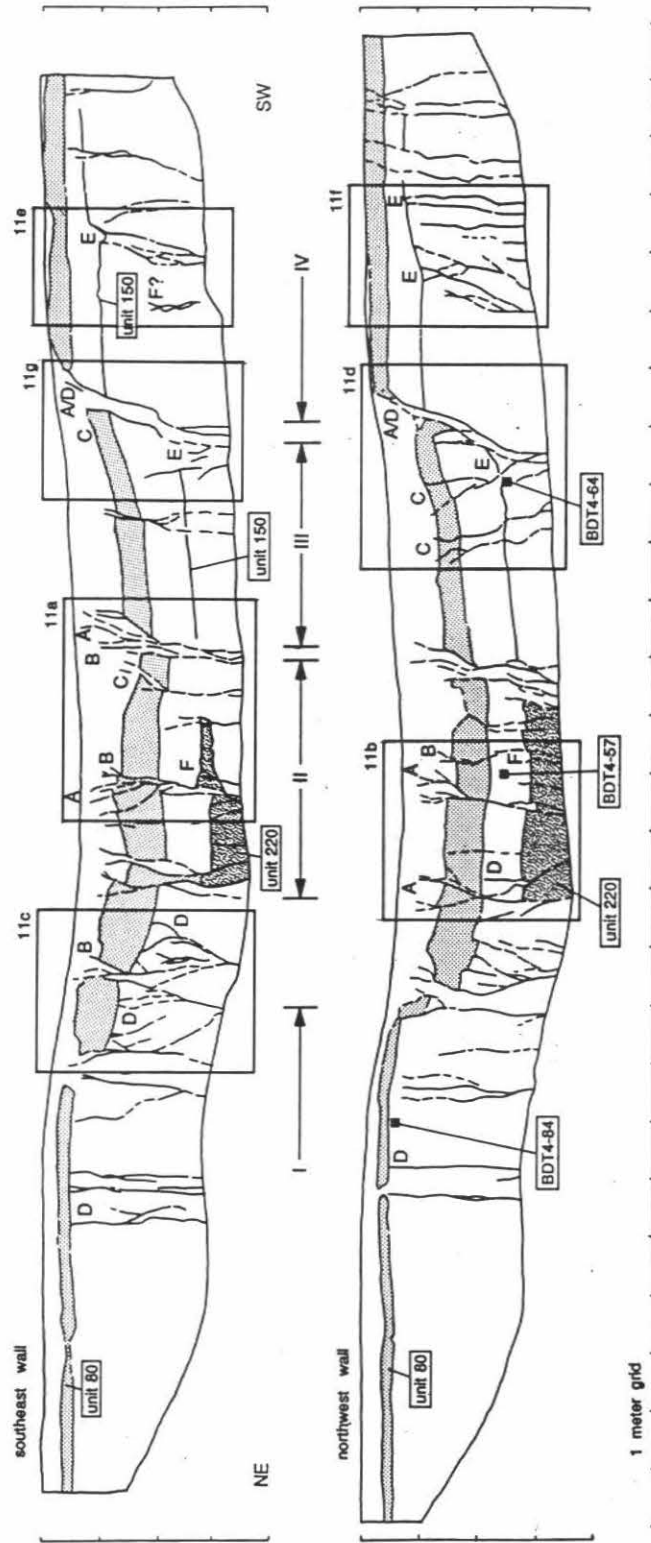
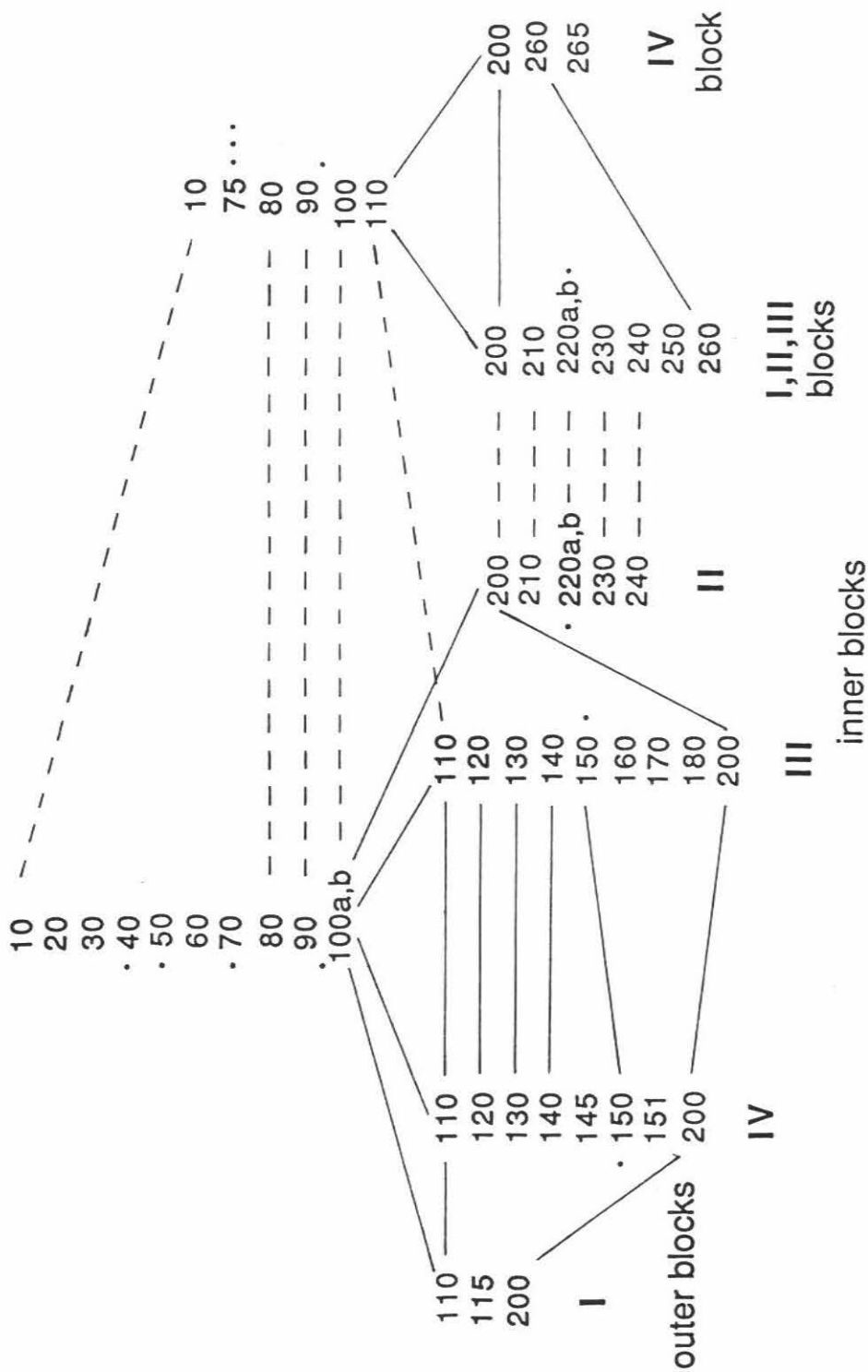


Figure 4-10: Stratigraphic sequences in trenches 3 and 4. The numbers correspond to units discussed in text and shown in greater detail in figures 4-11 and 4-12. Solid lines join units correlated across faults in each trench. Dashed lines connect units correlated between the trenches. Stratigraphic blocks are labelled with Roman numerals, as in figures 4-8 and 4-9.

TRENCH 3

TRENCH 4



both trenches. Units 20-70 in the graben near the top of trench 4 are not found in trench 3. Units 20-70 were probably deposited in the graben of trench 4 after the trench 3 graben was filled in and uplifted.

At the northeastern ends of trenches 3 and 4, outside the graben and paleogaben, the uppermost meter of section has an identical sequence of beds. Bioturbated unit 200 and overlying beds 80, 100 and 110 can be traced across all major faults in both trenches. Below bioturbated layer 200 is a thick, cobble gravel (unit 220) capped with a locally preserved laminated silt and fine sand bed. The cobble gravel is thickest in the central part of trenches 3 and 4, indicating that it was deposited in a previous longer graben along the fault.

At the base of the southwesternmost exposures of unit 220 is a laminated coarse sand and granule bed (unit 230) in both trenches. Units 220 and 230 rest on silty clay unit 240 which is well exposed in trench 3, and partially exposed in trench 4.

In the outer blocks of both trenches, a sequence of beds below unit 200 was not correlateable between or across the trenches. Beds in blocks I and IV have been offset from each other by multiple earthquakes, making correlation difficult. Additionally, both trenches are at the northwestern edge of the Bidart fan. Prior to incision of the channel which currently forms the boundary between the Bidart fan and a fan to the northwest (figure 4-2), sediments from the two fans may have interfingered, complicating correlation of the older sediments.

Evidence of Earthquakes*Event A*

The proximity of trenches 3 and 4 to the 14 to 18 m offset channel led us to expect that little deposition would have occurred there since at least 2 large slip events ago. We expected only very thin and bioturbated beds above the event A horizon and we expected 1857 and event B to be difficult to distinguish in trenches 3 and 4, except in the topographic graben of trench 4. Indeed, numerous fault traces extend to within a few centimeters of the surface in trenches 3 and 4, but the number of earthquakes represented by each of them is difficult to determine outside the graben of trench 4. Recent deposition in the graben, however, has preserved evidence of event A.

Unit 40 ruptured during event A (Figures 4-11 a,b) within the graben. Unit 30 pinches out against fault scarps from event A on the southeast wall, and covers faulted unit 40 on the northwest wall of trench 4, which indicates that unit 30 was deposited after the earthquake. The fresh appearance and relatively steep slopes of the graben boundaries suggest that the graben boundary faults also moved during event A (figure 4-4).

The incised stream channel northwest of trench 3 is offset 14.6 to 18.4 m (figure 4-4). Nearly 7m of slip occurred on the main trace of the San Andreas during the 1857 earthquake at the Phelan fan, approximately 3 km to the northwest (Grant and Sieh, 1993; figure 4-1). The 7.2 m offset at trench 2 indicates that approximately 7 m of slip was associated with event A on the Bidart fan. Although slip can vary by several meters over short distances along a fault (Rubin and McGill, 1992; Grant and Donnellan, submitted) the amount of slip at trench 3 is probably about the same as the slip at trench 2.

Figure 4-11a: Portion of the southeast wall of trench 4. Capital letters mark the approximate locations of stratigraphic evidence for the events. Units are numbered. View is toward the southeast. See figure 4-6 or appendix D for symbol legend. Blank areas are fault zone breccia or bioturbated zones.

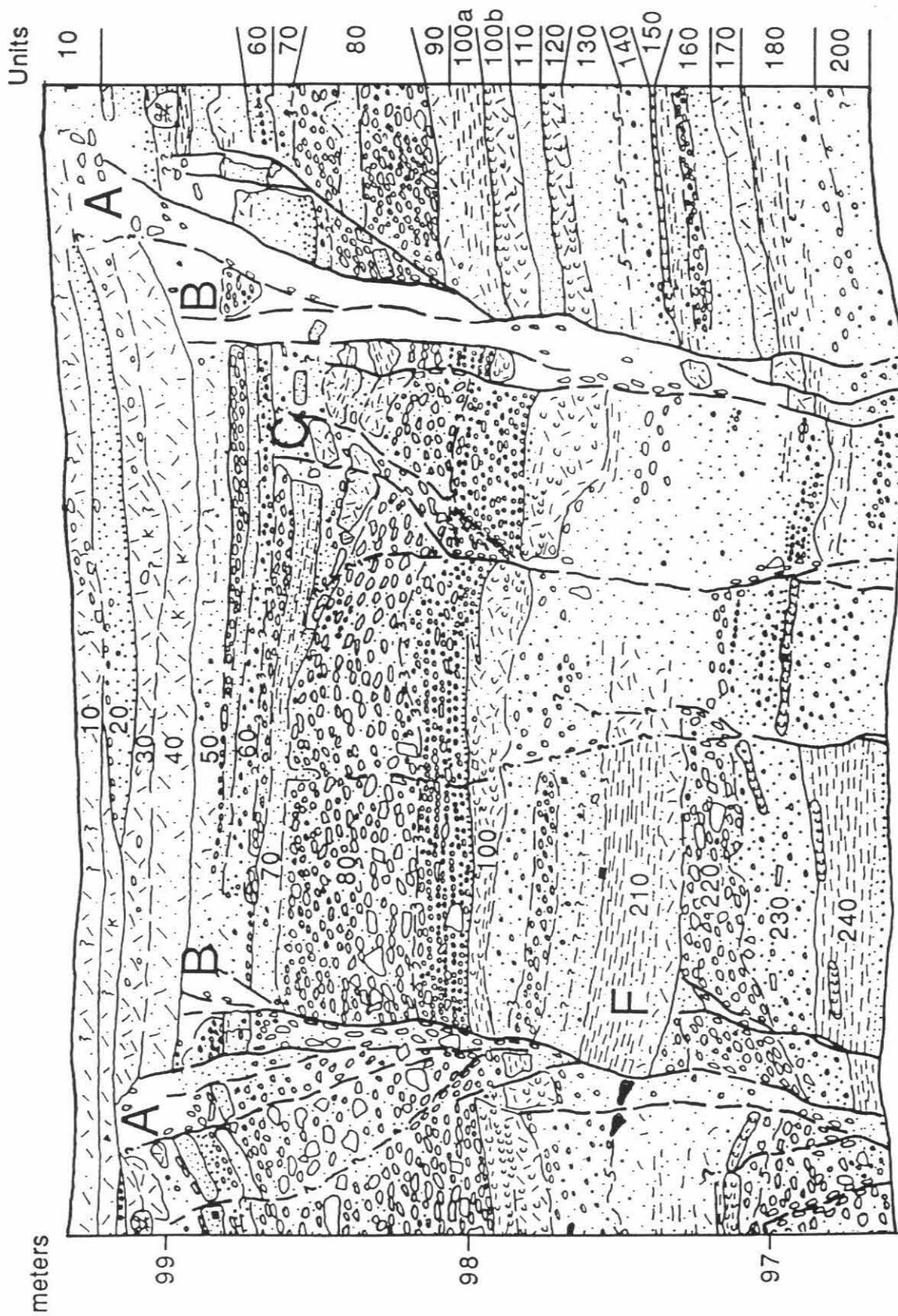


Figure 4-11b: Portion of the northwest wall of trench 4. Capital letters mark the approximate locations of stratigraphic evidence for the events. Units are numbered. View is toward the southeast. See figure 4-6 or appendix D for symbol legend. Blank areas are fault zone breccia or bioturbated zones.



Figure 4-11c: Portion of the southeast wall of trench 4. Capital letters mark the approximate locations of stratigraphic evidence for the events. Units are numbered. View is toward the southeast. See figure 4-6 or appendix D for symbol legend. Blank areas are fault zone breccia or bioturbated zones.

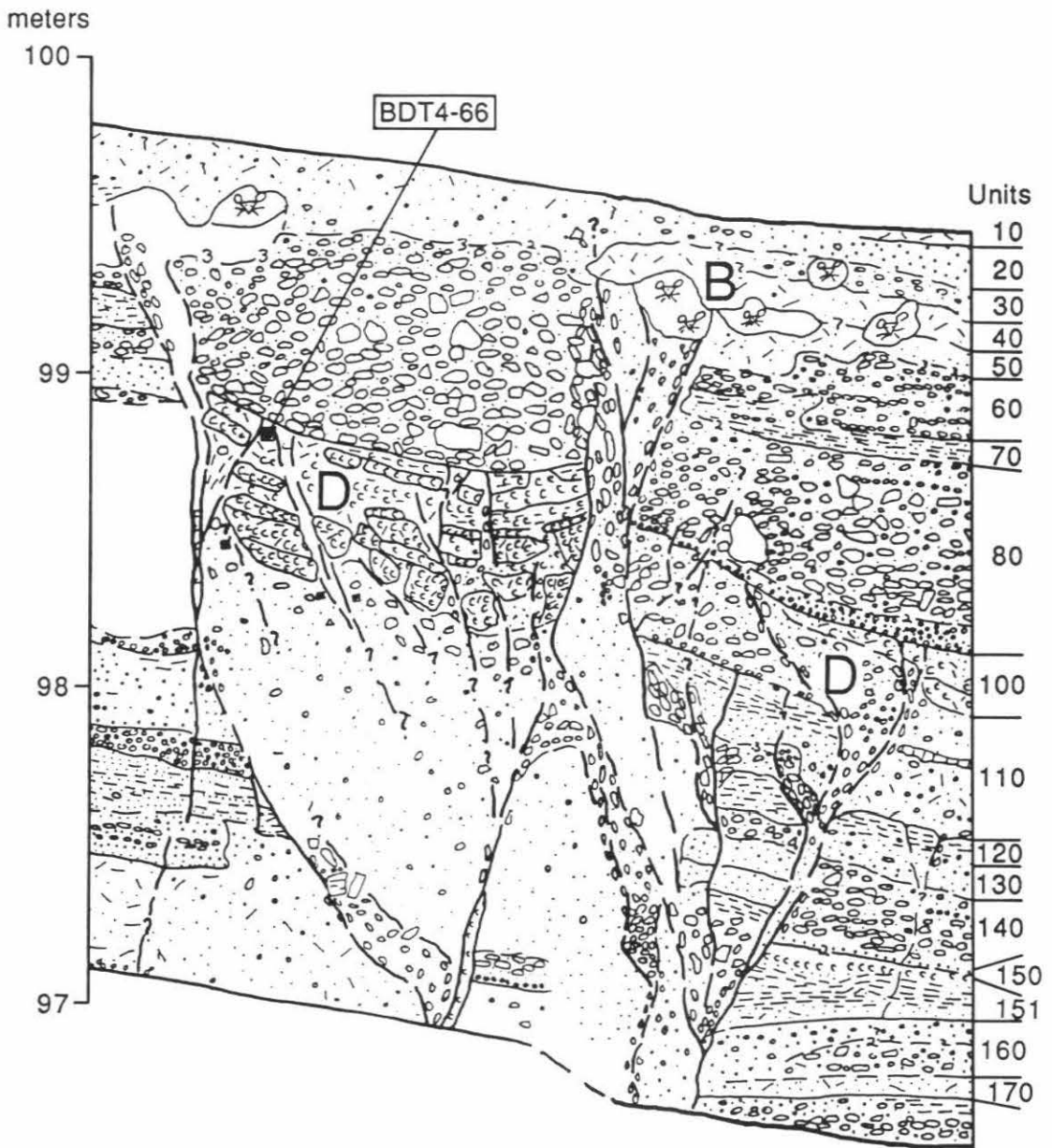


Figure 4-11d: Portion of the northwest wall of trench 4. Capital letters mark the approximate locations of stratigraphic evidence for the events. Units are numbered. View is toward the southeast. See figure 4-6 or appendix D for symbol legend. Blank areas are fault zone breccia or bioturbated zones.

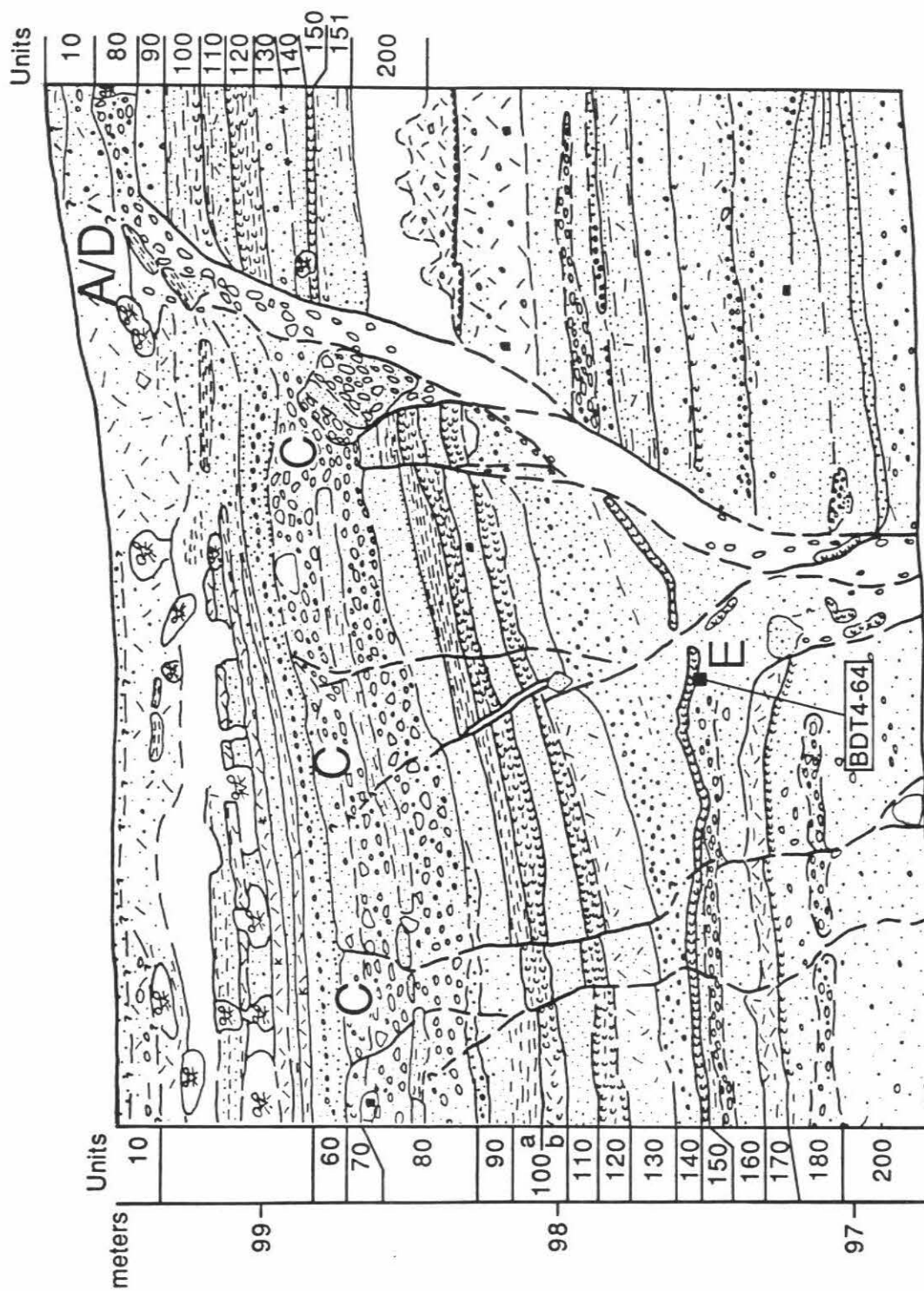


Figure 4-11e: Portion of the southeast wall of trench 4. Capital letters mark the approximate locations of stratigraphic evidence for the events. Units are numbered. View is toward the southeast. See figure 4-6 or appendix D for symbol legend. Blank areas are fault zone breccia or bioturbated zones.

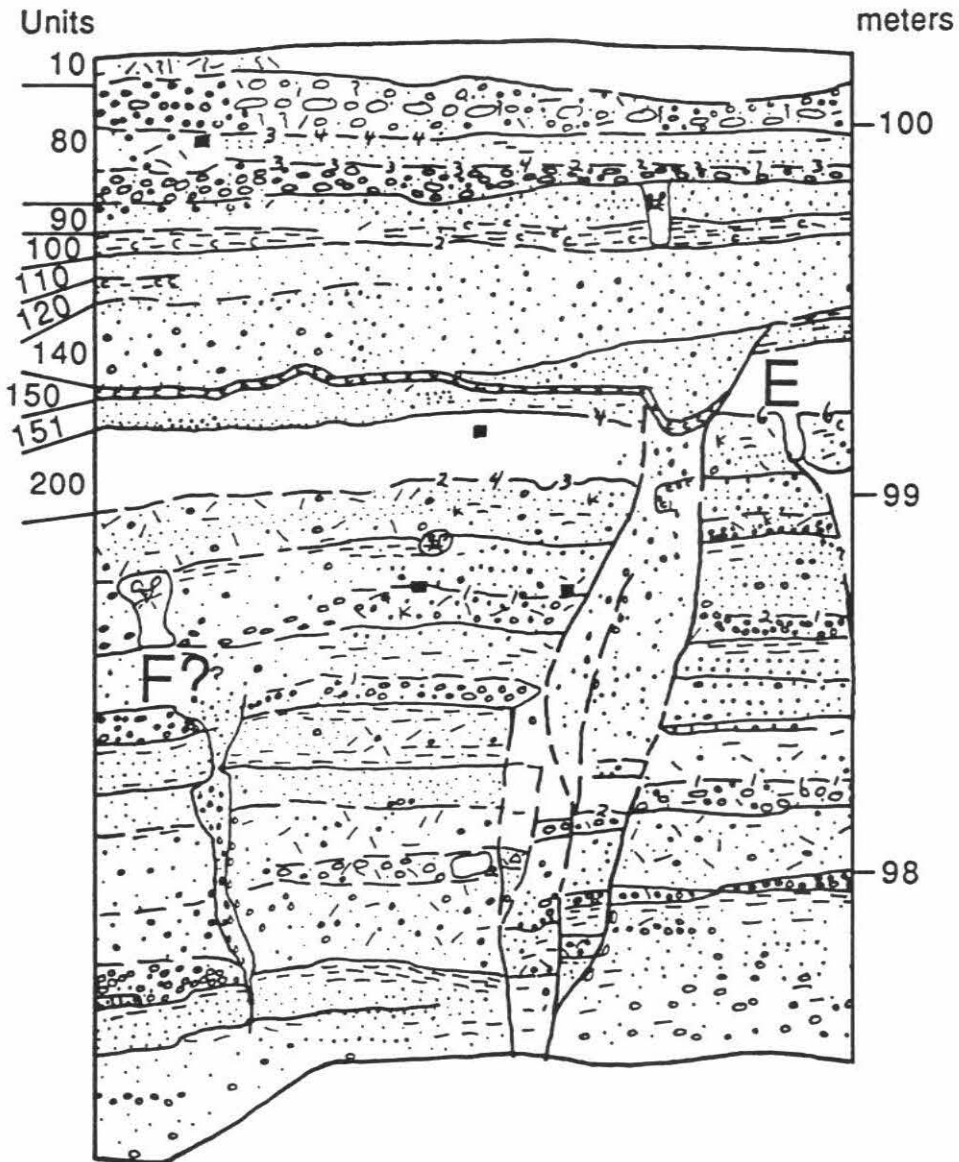


Figure 4-11f: Portion of the northwest wall of trench 4. Capital letters mark the approximate locations of stratigraphic evidence for the events. Units are numbered. View is toward the southeast. See figure 4-6 or appendix D for symbol legend. Blank areas are fault zone breccia or bioturbated zones.

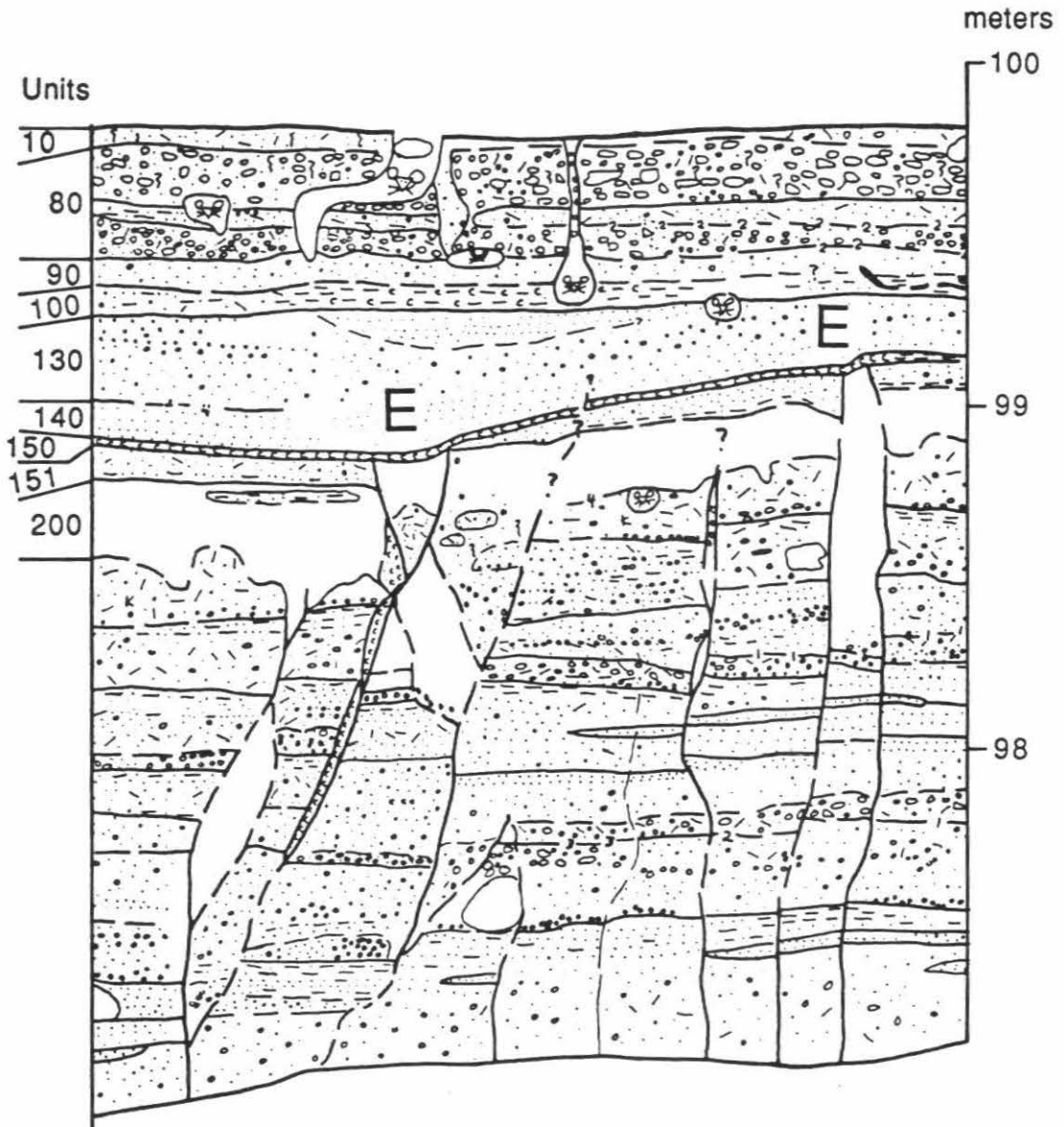
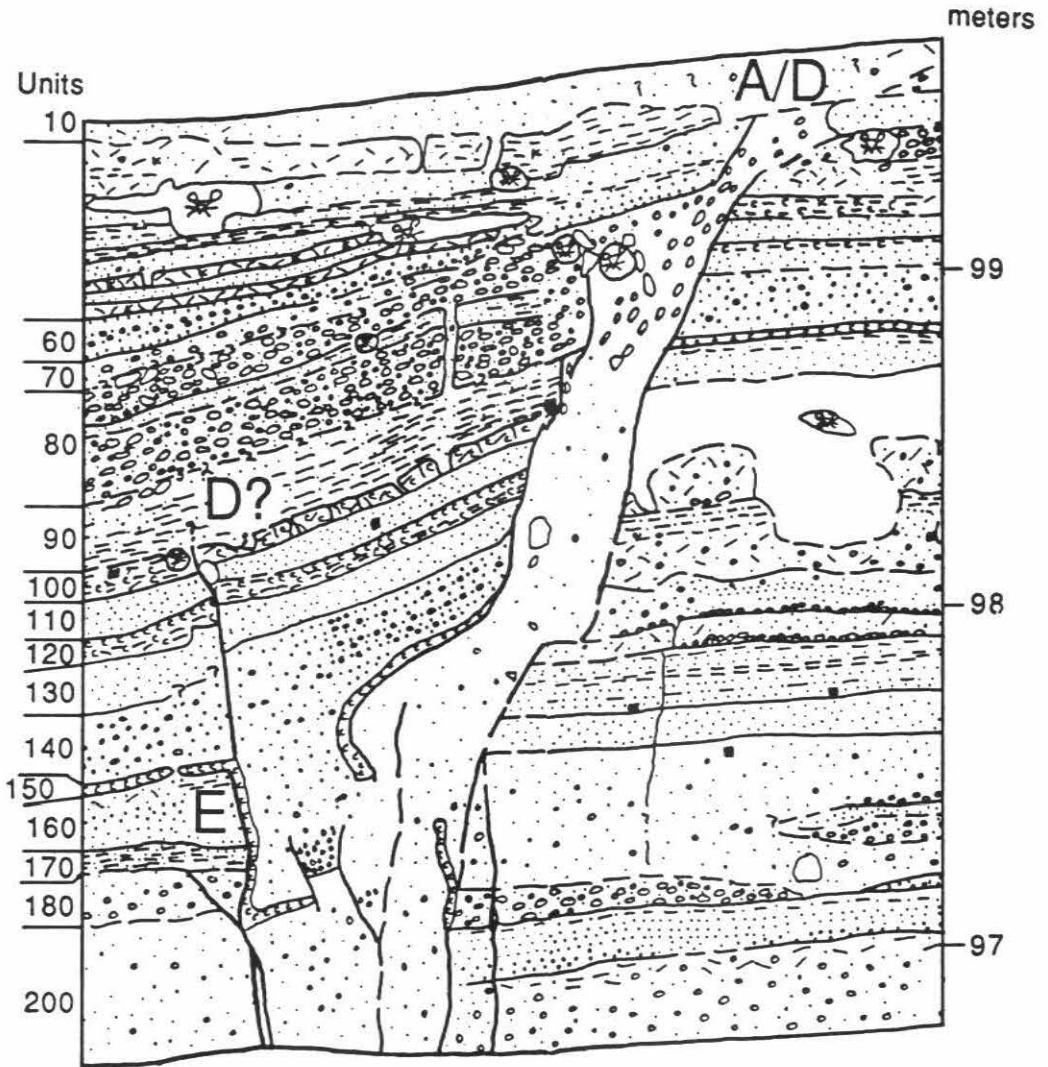


Figure 4-11g: Portion of the southeast wall of trench 4. Capital letters mark the approximate locations of stratigraphic evidence for the events. Units are numbered. View is toward the southeast. See figure 4-6 or appendix D for symbol legend. Blank areas are fault zone breccia or bioturbated zones.



Therefore, event A probably generated approximately half of the channel offset at trench 3.

Event B

Stratigraphic evidence of event B is also preserved in the uppermost beds of the graben in trench 4, and in places can be distinguished from event A. Because most of the fault traces which broke in event B were reactivated in event A, and because so little sediment was deposited between the two earthquakes, events A and B are difficult to distinguish from each other except in a few places.

Event B broke beds below unit 40. The best expression of event B is on the northwest wall of trench 4 (figure 4-11b), where it is expressed as a single trace that terminates below unit 40. Elsewhere, faults from event B appear to splay outward from fault zones associated with event A (figure 4-11a,b). These "splays" consistently terminate below unit 40. The existence of major facies changes across fault zones that appear to have moved in both events A and B suggest substantial strike-slip motion (figure 4-11a). Substantial facies changes are present across the graben boundary faults as well (Figures 4-11d,e), suggesting that they have been active for more than one event, including event B.

The dearth of sedimentation after deposition of unit 80 in trench 3 prevents determination of the number of earthquakes represented by the near-surface ruptures exposed in the walls of trench 3. The geomorphology of the site, however, yields indirect evidence for event B. The incised stream channel next to trench 3 is offset approximately twice as much as the channel near trench 2, less than a kilometer away. Thus, the larger offset was caused

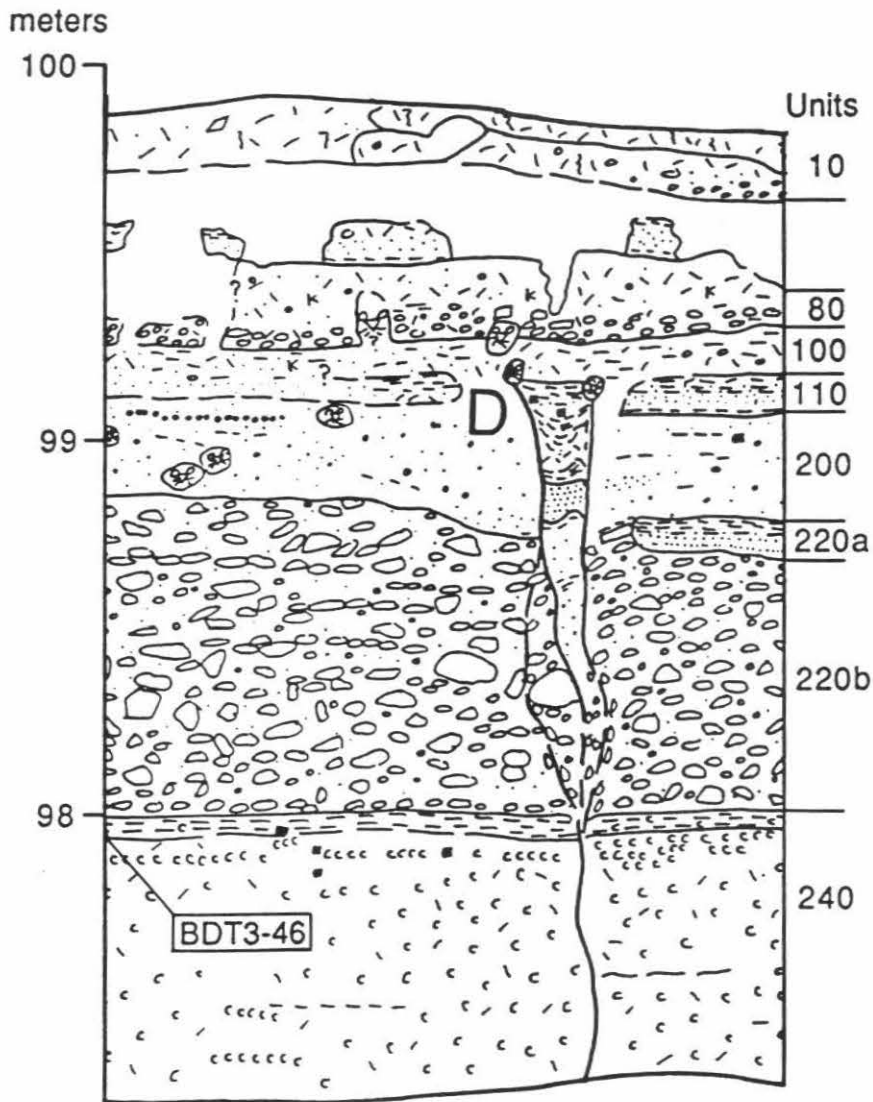
by at least two earthquakes. This is indirect evidence for surficial rupture at trench 3 during event B.

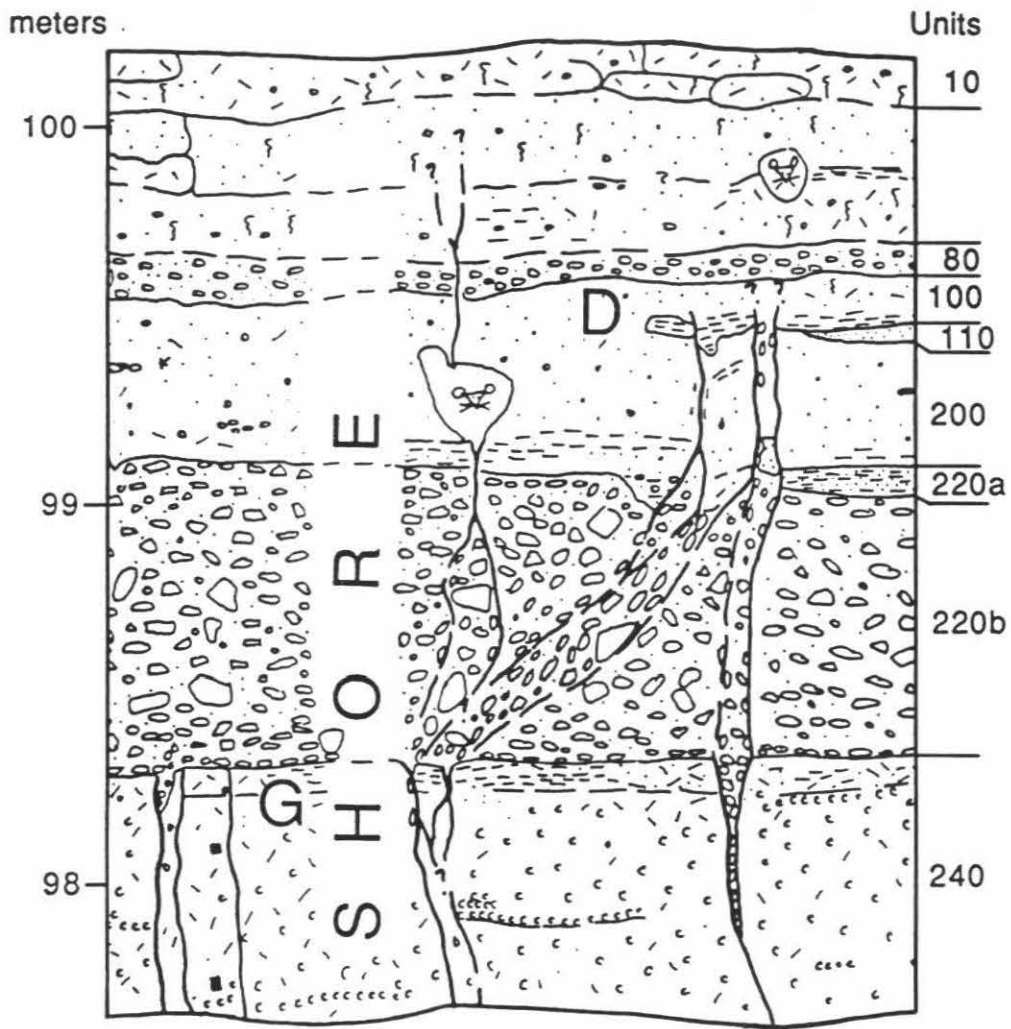
Event C

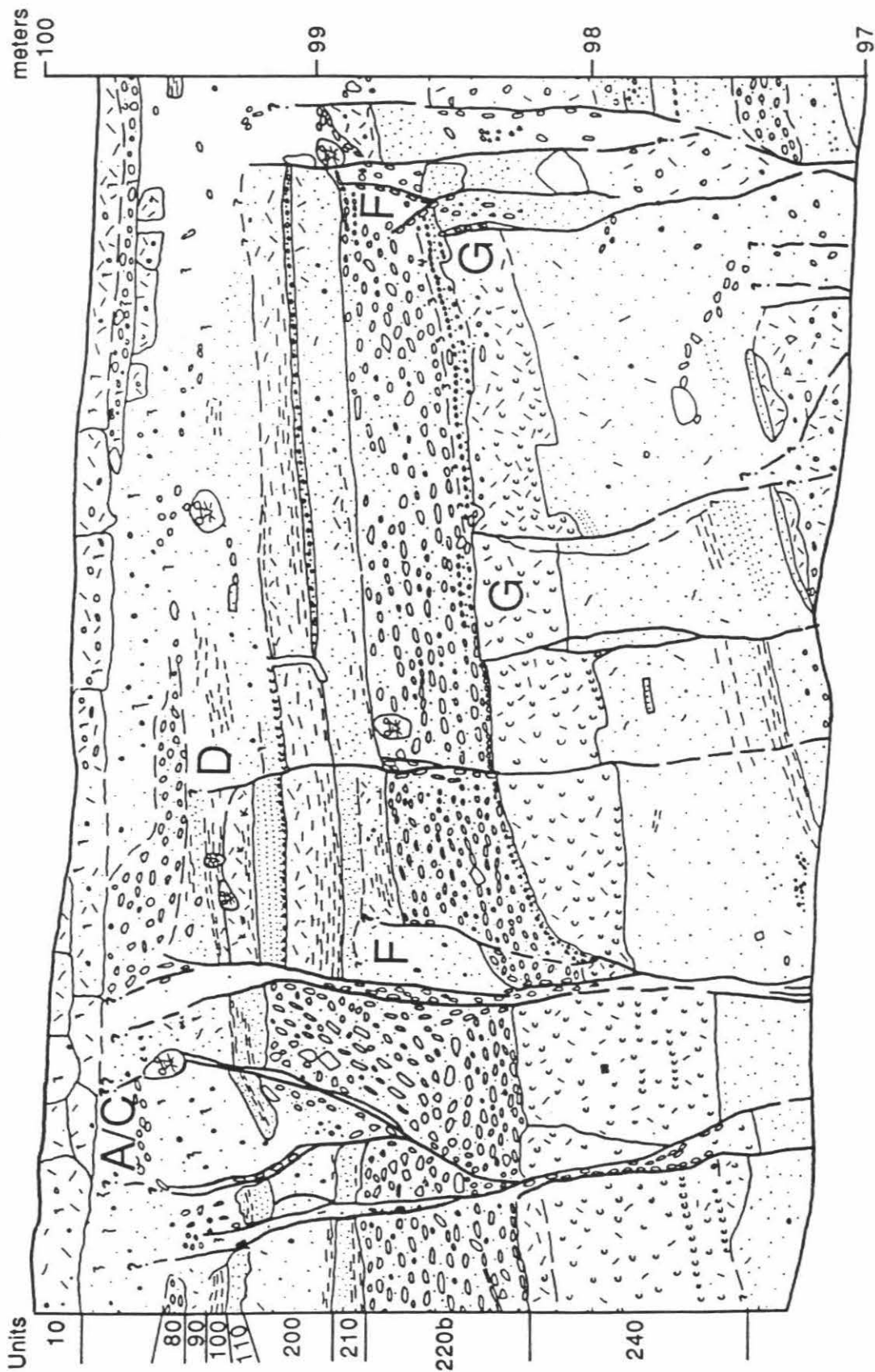
Event C is distinguishable from event A and B only in the graben sediments of trench 4. It is not discretely separable from A and B in the stratigraphy of trench 3. Where event C ruptured up to the surface of unit 70, faulted unit 70 is covered by undeformed unit 60. This is most pronounced in figure 4-11a. There units 70, 80 and 100 are broken and tilted. Several of the fault zones which separate structural blocks with very different stratigraphy may have moved during event C. Unit 60 overlies these beds without disruption. Several minor faults which terminate at the upper surface of unit 70 provide additional examples of event C in trench 4 (figure 4-11d). Units 70 and 80 are tilted by faulting during event C. Finally, the main graben boundary fault in figure 4-11g displays evidence of event C. Unit 80 is planar-bedded but tilted. Overlying unit 70 thins toward the fault, which indicates deposition against a scarp that formed in event C.

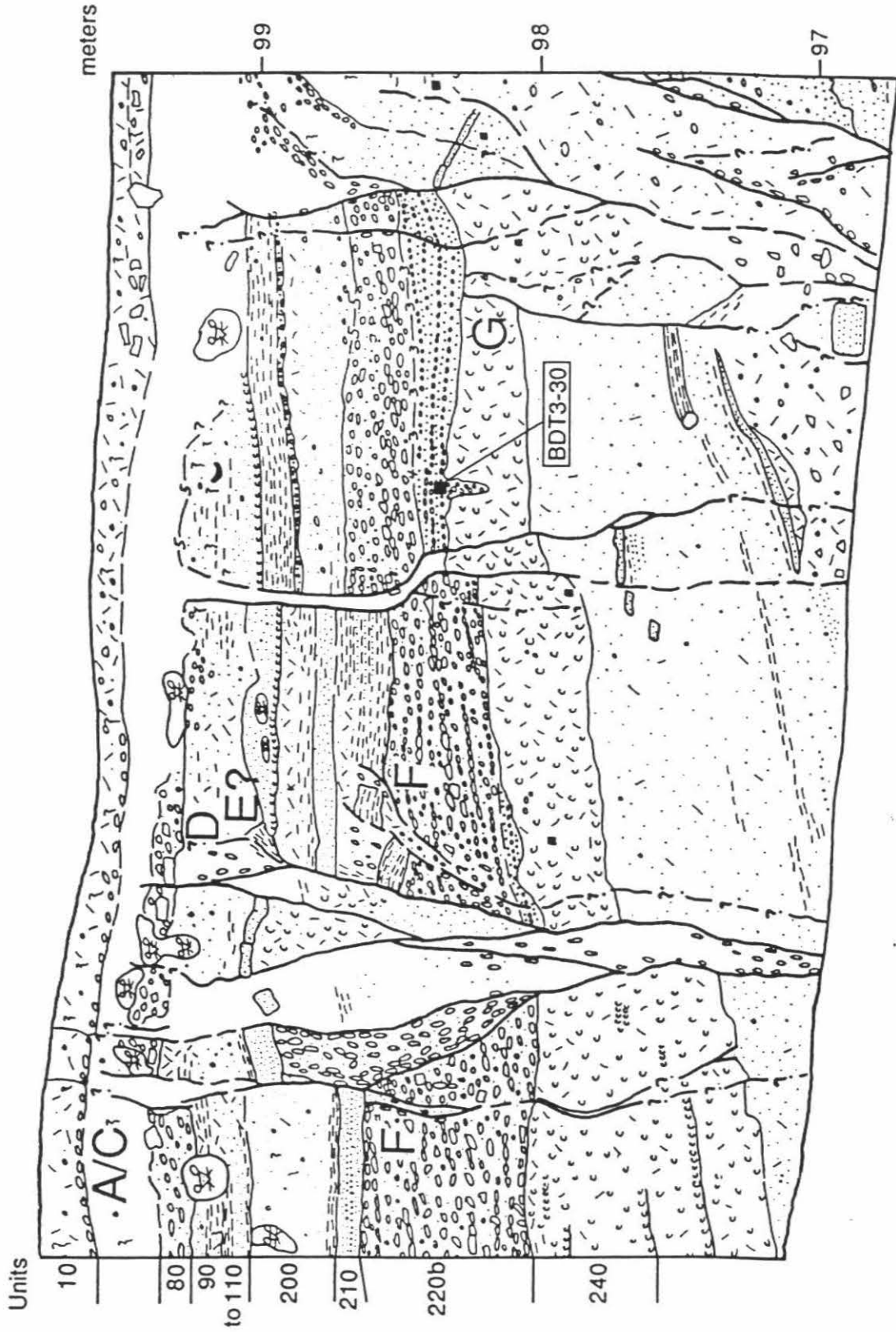
There is no direct evidence of event C in trench 3. Presumably some of the fault traces that ruptured through unit 80 to terminate near the ground surface broke during event C. The dearth of sedimentation after deposition of unit 80 at trench 3 prevents discrimination of individual events younger than unit 80. Surficial unit 10 is bioturbated and therefore it cannot be correlated with beds in the graben of trench 4 which record events A, B and C. Because several beds are present (or preserved?) only in the graben in trench 4, they cannot be correlated with the time of channel incision. We can conclude that the stream channel incised after deposition of unit 80. We can

Figure 4-12a,b,c,d: Portions of the southeastern (a, d) and northwestern (b, c) walls of trench 3 that display clear examples of disruption from earthquakes D thru G. Events A(1857), B and C ruptured to the ground surface after the graben filled with sediment and deposition ceased. Capital letters mark the approximate location of stratigraphic evidence of the earthquakes. Units are numbered. View is toward the southeast. See figure 4-6 or appendix D for complete symbol legend. Blank areas are fault zone breccia or bioturbated zones.









even hypothesize that the channel was incised by the same stormwater which deposited the coarse clasts of unit 80, but this is highly speculative.

Assuming that all large earthquakes younger than unit 80 are recorded and recognized in the graben sediments of trench 4, the channel was offset by a maximum of three events (A,B,C) and a minimum of two. Thus, events B and C jointly, or event B alone offset the channel by approximately 7 to 11 m.

Event D

Event D breaks unit 100 in trenches 3 and 4. In Figures 4-12a and 4-12b from the central part of trench 3 below the crest of the moletrack, fault zones on both walls break unit 100 and appear to terminate in the partially bioturbated layer below the gravels of unit 80. Major faults to the southwest (figure 4-12c,d) also display evidence of event D on both trench walls. Facies changes and apparent vertical offsets across these faults suggest multiple episodes of slip within the same fault zone. Several traces splaying out from the larger fault zone break unit 100 and terminate below unit 80.

Trench 4 contains abundant examples of event D. On the northwest wall (figure 4-11b), a 30-cm-wide shear zone terminates in unit 100, below the sharp base of overlying bouldery gravel of unit 80. On the southeast wall (figure 4-11c), unit 100 is extensively disrupted by a 2-m-wide shear zone. The top of the shear zone is the scoured basal contact of unit 80. A similar shear zone is present below unit 80 on the northwest wall, but the upper boundary is not as well defined (figure 4-9). Northeast of the graben in block I, several minor faults break unit 100 and the bioturbated zone above it, but do not extend upward into the gravels of unit 80 (figure 4-9).

Good evidence of event D is present in the northeast and central parts of trench 4, especially at the northeastern boundary of the graben (figure 4-9).

In trench 3, unequivocal evidence of event D is only found in the central portion of the graben exposures (in blocks II and III, figure 4-8). Thus, the northeastern graben-boundary fault zone in trench 4 (between blocks I and II), and faults in trench 3 below the crest and southwest flank of the moletrack moved during the same event. They likely formed a continuous fault trace across the graben. The west-northwest striking flank of the moletrack surface (figure 4-4) suggests uplift on such a 'cross-fault'. The uplift may have initiated during event D.

Event E

Event E is best preserved in the southwestern half of trench 4, a few centimeters above a bioturbated layer (unit 200). Elsewhere in trench 4, and in all of trench 3, the stratigraphic position of event E would place it within a thick bioturbated layer (unit 200).

In trench 4, a thin clay bed (unit 150) preserves evidence of earthquake E in (Figures 4-11e,f). On both walls, several fault traces with measurable offset terminate at unit 150. The clay bed is irregular above the fault terminations. It is not clear whether the bed was at the ground surface at the time of the event, or was deposited shortly after the event. In figure 4-11f, the clay bed is uneven, but unbroken, at the faults. This suggests that fresh fault scarps may have been draped with a coating of mud after event E. Also, unit 151 appears truncated beneath 150. On the opposite wall (figure 4-11e), the clay bed appears to be broken and folded by earthquake E, suggesting that unit 150 was the ground surface at the time of the event. A colluvial wedge shed off the fault scarp buries the clay bed at the fault, indicating that if unit 150 was deposited after event E, it was deposited while the scarp was fairly pristine.

Unit 150 is also irregular in the exposure of figure 4-11d. The clay bed appears folded near the base of the graben boundary fault, suggesting that it was tectonically deformed or deposited on a concave surface. Faults associated with events A,B and C have broken and displaced the clay bed at the edge of the graben. This makes it difficult to determine if 150 was also broken by event E. On the northwest wall near the base of trench 4 (figure 4-11g), however, it appears that a fissure formed during event E or shortly thereafter. The clay bed lines the walls of the fissure. The clay may have fallen into the fissure during event E, or, more probably, the the fissure may have been coated by unit 150 clay shortly after its formation. Similar fissures formed within a few days of the Borrego Mountain earthquake during heavy rains (Clark, 1972). Similar sedimentary features exposed in trenches at Pallett Creek are interpreted as clay-lined sandblows which formed during seismically induced liquefaction of fault zone sediments (Meisling and Sieh, 1979).

Graben growth during events A-E

In trench 4, events C, D and E appear to have ruptured alternating ends of the graben. Clear evidence of event E is limited to the southwestern half of trench 4. The best exposures of event D are in the northeastern half of trench 4 and the central part of thrench 3. Uplift of the graben deposits in trench 3 probably initiated with formation of a cross-graben fault between the northeastern part of trench 4 and the central part of trench 3 during event D. The 'cross-fault' may have formed in response to uneven deformation and stress distribution across the graben. The alternating pattern may have continued during event C, with slip on faults in the central and southwestern half of the graben in trench 4. The width of the fault zone during event B is

uncertain. Deformation occurred across the entire graben at trench 4 during the 1857 earthquake.

Event F

Fault traces from event F break the coarse gravels of unit 220 in both trenches. The best exposures are preserved in trench 3, where the gravels (unit 220b) are capped by a laminated silt and sand bed (unit 220a). On the southeast wall of trench 3 (figure 4-12d), the gravels of unit 220b are disrupted by faults which break and offset unit 220a. Unit 210 covers the faulted beds. The fault zone was reactivated during event D and younger event(s). A smaller fault zone to the northeast breaks gravelly unit 220, but does not disrupt unit 210 which was deposited over the fault after event F.

On the northwest wall of trench 3, faults from event F cut through units 220a and 220b (figure 4-12c). The faults are overlain by unbroken unit 210, at the margins of 2 shear zones with evidence of multiple events. Near the southwestern edge of figure 4-12c, faults splaying off a wide fault zone cut through the gravel of unit 220, but do not extend to the top of the gravel bed. These traces may be splays of faults which were also active during younger events, or they might be near-surface breaks from event F. At the northeast end of trench 3, in block I, several fault traces break the gravels of unit 220 but do not extend upward into the bioturbated zone (unit 200) above (figure 4-8). These faults could be either remnants of event E, with the upper part of the traces obliterated by bioturbation, or they could be from event F.

Event F is visible near the base of trench 4. A sand filled fissure breaking unit 220 (figure 4-11a) is interpreted as event F. A fault trace which breaks up through the surface of unit 220a on the northwestern wall of trench 4 is also attributed to event F.

Event G

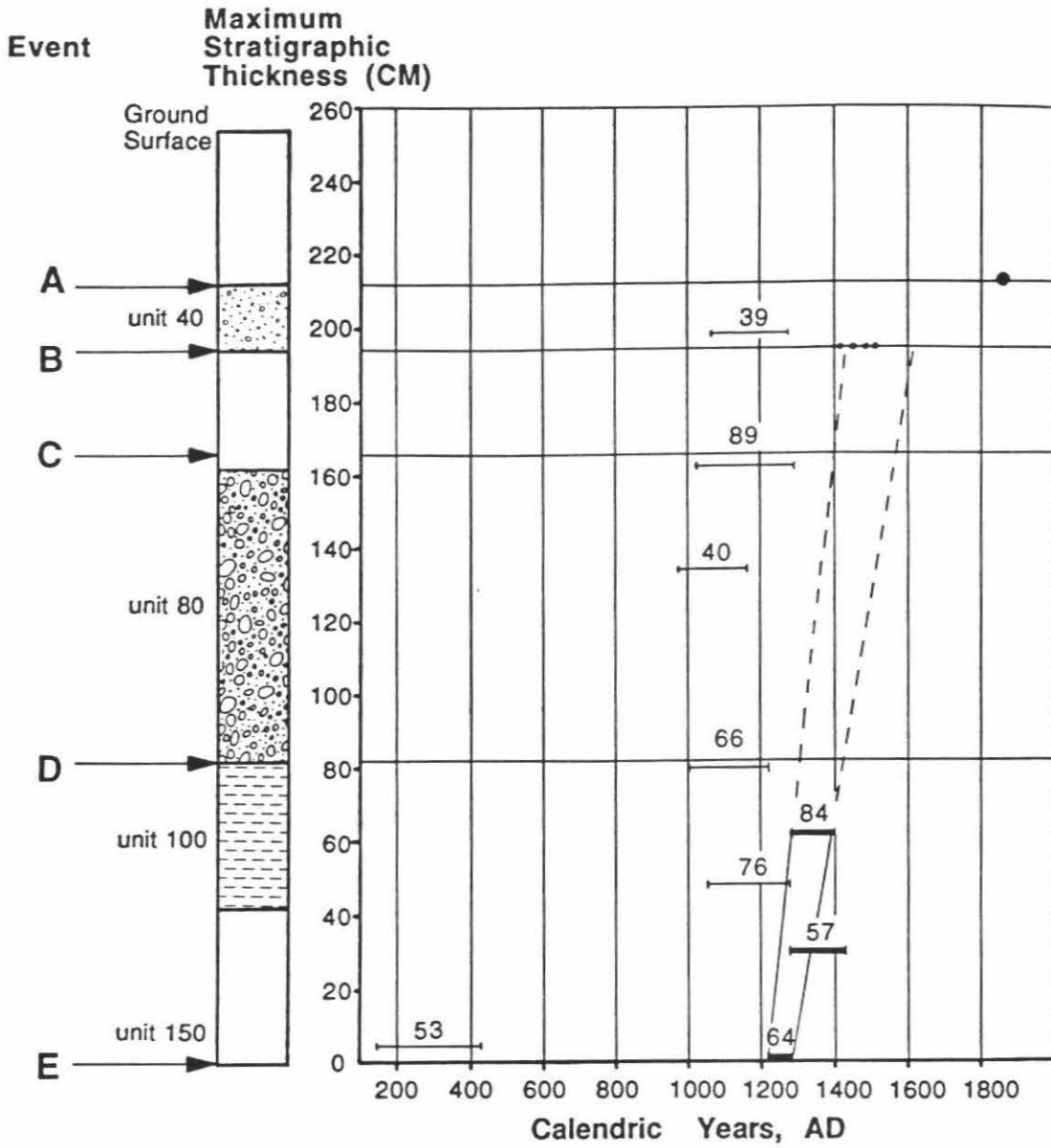
Event G breaks a thick, massive or laminated, silty clay bed (unit 240) near the base of the exposed section. Since unit 240 is barely exposed at the base of trench 4 (figure 4-11a), there are no definitive examples of event G in trench 4. Event G is visible as discrete fault traces a few centimeters wide that terminate at the top of clay-rich unit 240. Fissures at the surface of unit 24 are filled with gravels from overlying unit 220 (figure 4-12b,c). Differences in the thickness of unit 240 across faults (figure 4-12c), and the presence of nearly horizontal slickensides indicate that the discontinuities are faults and not mud cracks.

Radiocarbon Dating of Beds and Earthquakes

Radiocarbon dating of samples from trenches 3 and 4 yields estimates of the dates of events prior to event B. The results of radiocarbon analysis of all dateable samples is summarized in Table 4-1.

In trench 3, two samples place gross constraints on the date of event G. Sample BDT3-46 was embedded in clay at the top of unit 240, which is faulted by event G. Error bars on the radiocarbon age of this sample are unusually large (Table 4-1) and the $\delta^{13}\text{C}$ was not measurable. We collected a snail shell (sample BDT3-30) from the base of gravel unit 230, which overlies faulted unit 240. The shell is at least 300 years older than the plant material beneath it, making the date of event G difficult to determine. We estimate that event G occurred after deposition of the sample BDT3-46, sometime during or after B.C. 200 to A.D. 250. Event F occurred after event G and prior to event E. In both trenches, bioturbated unit 200 is above the units that are faulted by

Figure 4-13: Plot of radiocarbon dates of samples from trench 4. The vertical axis is a generalized stratigraphic column, which uses maximum thicknesses for units above unit 150. Arrows mark the stratigraphic level of events A thru E. The horizontal axis is calendric date, A.D.. The horizontal bars indicate 2σ calibrated calendric dates of radiocarbon ages of 9 samples from trench 4. Sample numbers are above the bars. Thicker bars indicate high-precision dates. Several dates in the upper part of the section are as old or older than the dates near the base of the section, and sample 53 is much older than the others. The apparent stratigraphic age inversion is caused by detrital wood. Detrital contamination prevents determination of the dates of individual events but allows calculation of the average length of intervals between events by using the youngest samples from each stratigraphic level. See Table 4-1 for radiocarbon details.



— High precision 2σ AMS date
 — Standard 2σ AMS date

--- 1405-1510 AD date from Trench 2
 • 1857 Fort Tejon earthquake

events F and G. Thus, a depositional hiatus of at least a few centuries occurred after event F and before event E. Therefore, we suspect that event F occurred closer in time to event G than to the event E.

Dates of younger samples from trench 4 are plotted on figure 4-13. To the best of our knowledge, these samples were collected from intact beds, which were not bioturbated. Several samples in the upper part of the section are as old, or older, than samples near the base of the trench. The lack of appreciable difference in the age of most samples probably is due to their detrital nature. It is possible that a range fire in the Temblor Range, about A.D. 1100, produced charcoal that continued to be carried to the Bidart site for two to three centuries. To minimize dating problems from detrital wood contamination, we assume that the youngest samples represent the closest approximation to the date of a particular stratigraphic level. This allows us to estimate the average length of intervals between events, despite large error bars on the dates of individual events (Table 4-2).

Average Recurrence Intervals

Sample BDT4-64 (Table # 4- 1, figure 4-13) was embedded in the clay (unit 150) bed which was either cut by event E, or draped the fissure from event E shortly after the earthquake. A high-precision 2σ radiocarbon age for this sample is A.D. 1218 to 1276. The texture of the sample and its isotopic composition indicate that it is detrital wood. Thus, although it is younger than several samples above it, it may still be older than bed 150, which entombed it. Since unit 150 was deposited shortly before or after event E, the earthquake most likely occurred between A.D. 1218 to 1276, or later. Thus five

Figure 4-14: Visual representation of average recurrence intervals, assuming evenly spaced events. The average recurrence interval has been 160 years, between 1218 and 1857, but ^{14}C dates provide other constraints that show the actual intervals have varied markedly. The interval between 1857 and its predecessor was 350 to 450 years, whereas earlier intervals averaged closer to 100 years.

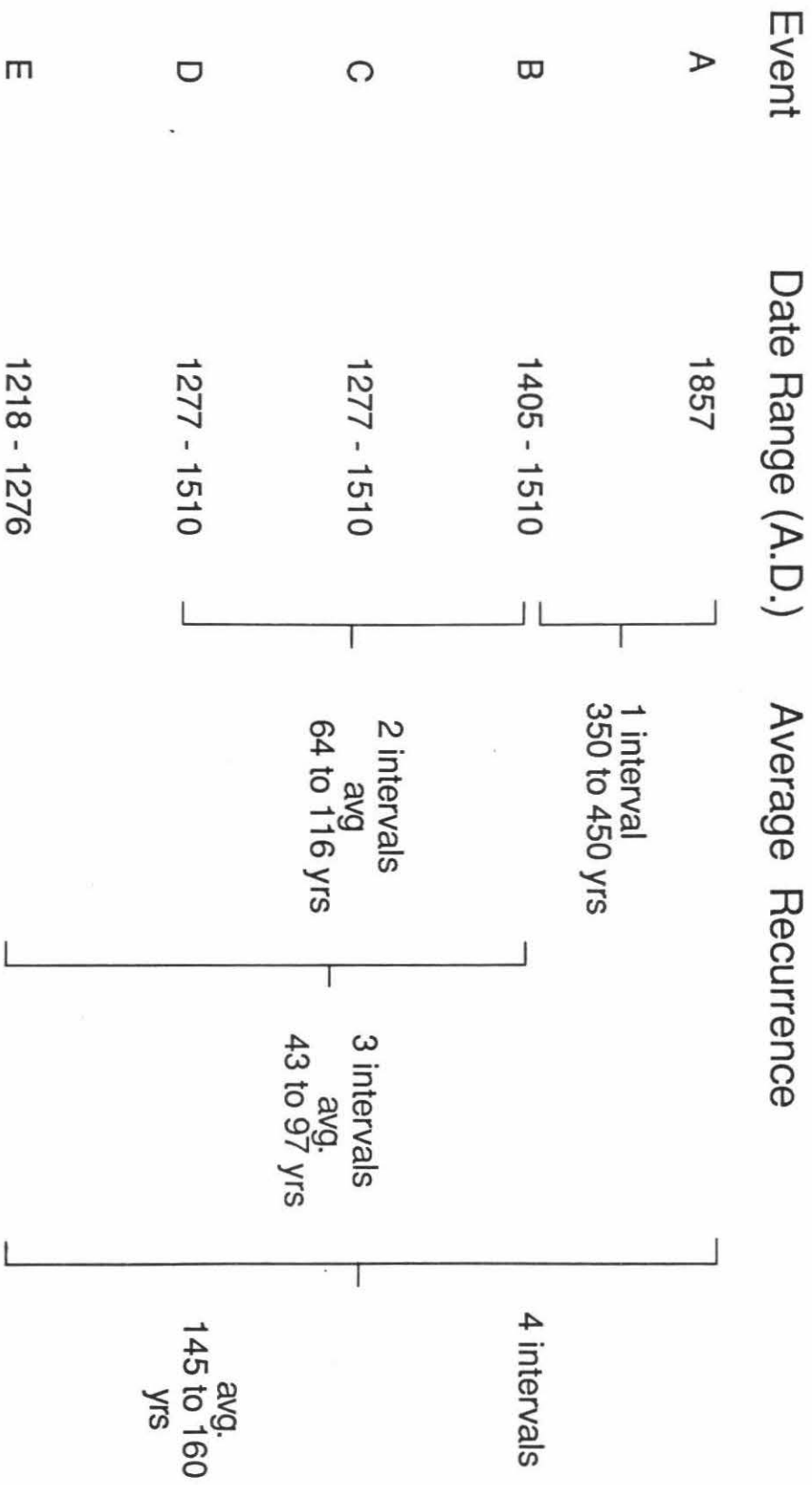


Table 4-2: Summary of dates of earthquakes from radiocarbon analysis.

Table 4-2: Summary of Event Dates

<u>Event</u>	<u>Dates(A.D)</u>
A	1857
B	1405-1510
C	1277-1510
D	1277-1510
E	1218-1276
F	after 200 BC
G	after 200 BC

surface rupturing earthquakes (and four intervals) occurred between A.D. 1218 and 1857.

Sample BDT4-84, of calendar age A.D. 1277 to 1392 (Table 4-1, figure 4-13), was collected from unit 100 which is faulted by event D. Four earthquakes (and three intervals) have occurred since deposition of the bed containing this sample. The same four earthquakes occurred after deposition of sample BDT4-57, of calendric age A.D. 1280-1430.

If events A thru E were evenly spaced in time, with event A in 1857 and event E in 1218, the average recurrence interval would be 160 years. This is very unlikely because event B occurred during the period A.D. 1405-1510. If we assume that event A is the 1857 earthquake, and event B occurred between 1405 and 1510 A.D., then 350 to 450 years of quiescence separates the two most recent events. Therefore, prior to event B, earthquakes C, D and E must have occurred in relatively rapid succession. The maximum average recurrence interval for these earthquakes can be calculated several ways (figure 4-14). If event E occurred in 1218 A.D. and event B in 1510 (the maximum time interval), then the maximum average time between events B, C and E was 97 years. If event B occurred in 1510 and event D in 1277 (the earliest date permitted by samples BDT4-57 and BDT4-84), the average intervals between B, C and D would be 116 years, but then only 59 years would separate events D and E.

Analysis of stratigraphic data can be combined with the radiocarbon dates to further constrain the length of the earthquake intervals. In trench 2, at least one, and possibly three beds were deposited between events B and C. In trench 4, two thin beds were deposited between events B and C, and at least two thicker beds separate events C and D. There are at least nine beds between events D and E. If the beds are deposited at semi-regular intervals,

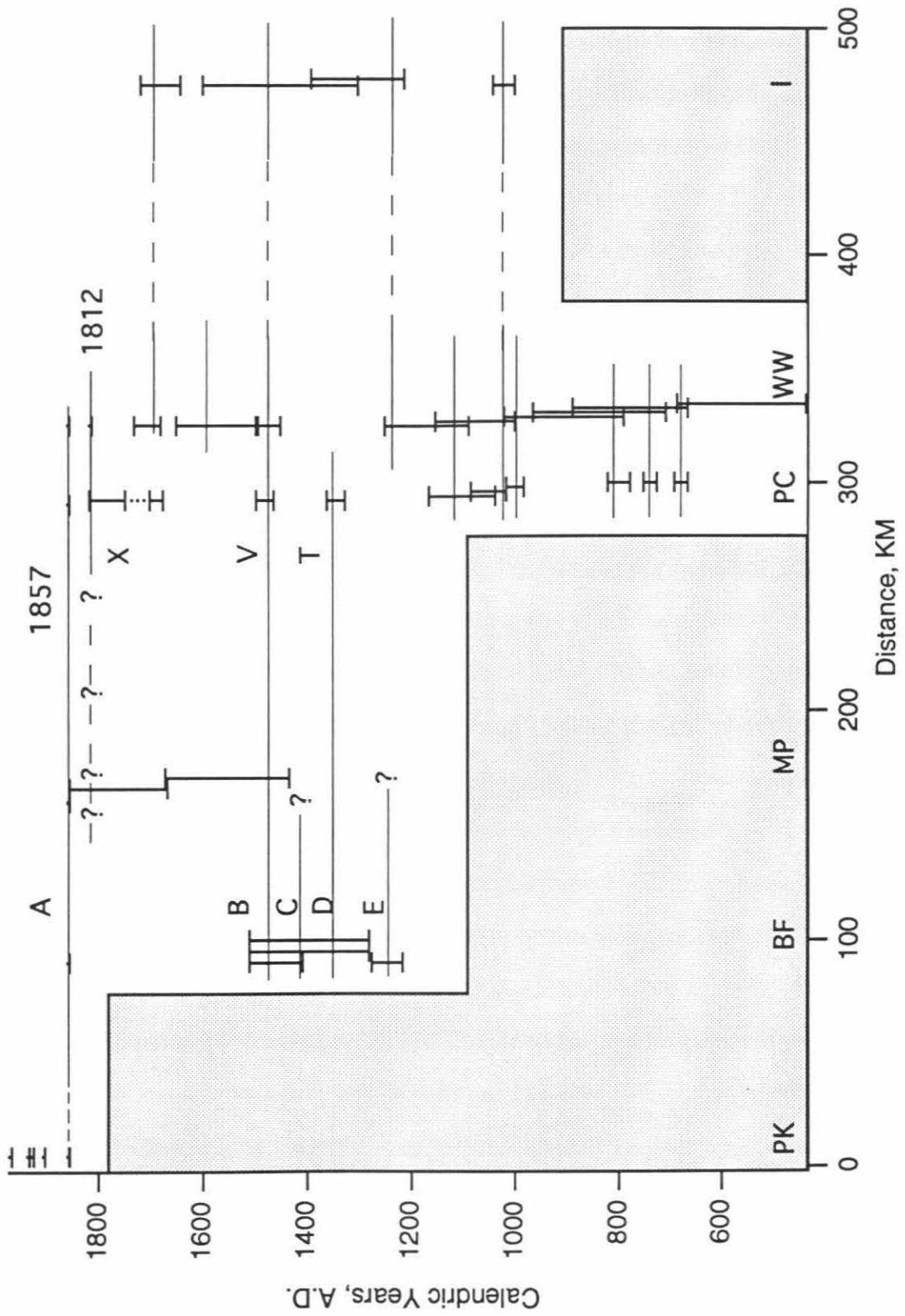
then the time period between earthquakes D and E is two to three times as long as the intervals between B, C and D. Thus, if we assume that event B occurred in A.D. 1510 and event E in A.D. 1218, the most conservative interpretation yields an interval of 73 years between events B, C and D, and 146 years between events D and E. If event E occurred in 1218, and event B occurred in 1480, as suggested below, then the sedimentary record suggests intervals of 65 to 66 years between B, C and D, and 131 years between D and E. Plausible arguments can be made for even shorter intervals.

Correlation of Earthquakes

We can use radiocarbon dates of pre-historic earthquakes and accounts of historical earthquakes to hypothesize the length of past rupture events on the southern half of the San Andreas fault (figure 4-15). Overlapping error bars on the dates of paleoseismic events at different locations suggest the possibility of simultaneous rupture during a large earthquake. This method of correlating earthquakes is biased toward hypothesizing larger events because several smaller ruptures at different sites occurring within a few decades of each other are indistinguishable from a single large earthquake rupturing the same sites. Nonetheless, the potential for great earthquakes on the San Andreas fault was demonstrated by the 1857 and 1906 events, and hypothetical correlation of radiocarbon dates of past events is presently the only way to detect similar large prehistoric earthquakes. With this caveat, we estimate the rupture lengths of past Carrizo earthquakes. Our hypotheses may be tested in the future as more data becomes available.

The rupture length of the historic 1857 earthquake (event A) has been discussed by Sieh (1978) and Sieh *et al.* (1989). Although there is debate about

Figure 4-15: Hypothetical correlation of rupture events along the southern half of the San Andreas fault. Vertical bars are published 95% likelihood errors for dates of earthquakes at paleoseismic sites along the fault. The dates of the historical 1857 and 1812 earthquakes have no errors. Horizontal lines are hypothesized rupture extents of past earthquakes. All lines are conjectural. Dashed and queried lines show a greater degree of uncertainty, respectively, for prehistoric and historical events. Bidart fan events are labelled with capital letters A - E. Events X, V and T are preserved at Pallett Creek. Paleoseismic dates from Wrightwood are from Fumal *et al.* (1993) and Weldon (1991). Other earthquakes are from summaries of published data by the Working Group on California Earthquake Probabilities (1988). Length of the 1812 rupture is interpreted from data in Jacoby *et al.* (1988), Weldon (1991) and Fumal *et al.* (1993). Sites of historic and prehistoric earthquakes are labelled as PK= Parkfield, BF= Bidart fan, MP= Mill Potrero, PC= Pallett Creek, WW= Wrightwood, I= Indio. Stipple marks areas of no data.



the northernmost extent of the 1812 rupture (Jacoby *et al.*, 1988; Weldon, 1991; Fumal *et al.*, 1993) evidence from tree rings near Mill Portrero (Meisling and Sieh, 1980) and evidence presented in this paper indicate that it did not reach the Carrizo Plain. The San Andreas fault did not generate a large earthquake in the Carrizo Plain for nearly four centuries prior to the 1857 earthquake.

At all paleoseismic sites along the southern San Andreas, there is evidence of an event that could correlate with event B (A.D. 1405-1510) in the Carrizo Plain (figure 4-15). At the Pallett Creek and Wrightwood sites, an event occurred A.D. 1480 \pm 15 and 1470 \pm 20 respectively (Sieh *et al.*, 1989; Fumal *et al.*, 1993). At Indio, an earthquake occurred sometime during the period A.D. 1450 \pm 150 (Sieh, 1986). Thus, the event-B rupture may have been even longer than that of the 1857 earthquake. Alternatively, several shorter ruptures may have generated earthquakes along the southern half of the fault in rapid succession within a few decades of A.D. 1480. The error bars on radiocarbon dates of this event are too large to test the hypothesis of simultaneous rupture.

Contrary to hypotheses of infrequent, large magnitude Carrizo earthquakes, closely spaced events in the Carrizo Plain may have been produced by both short and long ruptures of the San Andreas fault. Only two of the last three prehistoric Carrizo events - B and either C or D - can correlate with earthquakes recorded at Pallett Creek to form a large earthquake similar to the 1857 event. We propose that event D was the same earthquake as event T (1329-1363) at Pallett Creek (Sieh *et al.*, 1989), and was probably similar to the 1857 earthquake in size and rupture extent. Our reasoning is based on the estimated date of event D derived from stratigraphic information and radiocarbon dates. If we assume that event E occurred in A.D. 1218 and B in A.D. 1480, then the stratigraphically estimated recurrence intervals suggest

dates of ~A.D. 1349 and ~1415 for events D and C respectively. The estimated date of event D falls within the 2σ calendar date range of event T (1329-1363). Even without stratigraphic data, the error bars on radiocarbon dates of Carrizo event D are large enough to permit simultaneity of events D and T.

Event C does not appear to correlate with earthquakes at either Pallett Creek or Wrightwood. Thus, either event C is missing from the earthquake record at Pallett Creek, which is unlikely because the Pallett Creek record is nearly continuous between ~A.D. 1400 to 1812, or event C involved a more northerly section of the fault. Similarly, event E ruptured the San Andreas in the Carrizo Plain, but is not in the earthquake record at Pallett Creek. Thus, it appears that events C and E were smaller than A, B and D, although all the events reported herein were large enough to generate substantial surficial rupture in the Carrizo Plain.

A large earthquake may have ruptured the southern San Andreas fault between Wrightwood and Indio within a few decades of either event D or E, perhaps in a pattern of alternating rupture similar to the sequence of 1857 and 1906 earthquakes in southcentral and northern California, respectively. Prior to event E, the Bidart paleoseismic record is poor. A depositional hiatus at the sites of Bidart fan trenches 3 and 4 probably hides evidence of additional large earthquakes between events F and E.

Discussion

Dates of earthquakes at the Bidart fan demonstrate convincingly that the San Andreas fault in the Carrizo Plain is not characterized by repeated very large earthquakes separated by unusually long recurrence intervals, as originally proposed by Sieh and Jahns (1984), and built upon by Sykes and

Seeber (1985), Stuart (1986), Sykes and Nishenko (1984), Rundle (1988), Sieh *et al.* (1989) and the Working Group on California Earthquake Probabilities (1988). Rather, the past 8 centuries have been characterized by a cluster of earthquakes and 400 years of quiescence, followed by the 1857 earthquake. This pattern of long and short recurrence intervals is similar to temporal clustering of earthquakes reported at Pallett Creek (Sieh *et al.*, 1989; figure 4-15) and Wrightwood (Fumal *et al.*, 1993), the only other sites along the southern half of the San Andreas where relatively complete paleoseismic data exist.

Temporal clustering of large earthquakes may be characteristic of some active faults and fault systems. In addition to earthquakes reported from the southern San Andreas fault, Scholz (1990b) reviews several examples of historic "compound" earthquakes which could be interpreted as clustered events. A series of 8 large strike-slip earthquakes occurred between 1939 and 1967 on the north Anatolian fault in Turkey. These earthquakes ruptured nearly the entire fault in succession (Scholz, 1990b, p.214-216). In south Iceland, 4 large strike-slip earthquakes occurred in 1896 on separate faults along a seismic lineation within the South Iceland seismic zone (Scholz, 1990b, p. 211-212). Similar sequences occurred in 1784, and 1732 to 1734. The historical record of earthquakes along the Nankai trough, Japan, includes three clusters of large earthquakes a few years apart in 1096 and 1099, 1360 and 1361, and 1944 and 1946 (Scholz, 1990b, p. 242-245). These events ruptured adjacent segments of the subduction zone. Similarly, the 1857 and 1906 earthquakes on the San Andreas fault could be considered a temporal cluster of large events on adjacent seismogenic segments of the fault. Although spatial rupture patterns of clustered events defy simple description, it appears

that large earthquakes can occur on the same fault or related faults closely spaced in time in a variety of tectonic settings.

Clusters of large earthquakes may be analogous to patterns of foreshocks, mainshocks and aftershocks, but on a longer time scale. Many geologic structures, including faults, exist at a variety of length scales, from microscopic to continental. It is reasonable to expect patterns of seismicity at different time scales as well. For example, short-term patterns of seismicity, such as aftershock sequences, may reflect characteristic times for local strain release, whereas longer temporal patterns may characterize the time scale of regional strain release. Indeed, Thatcher (1989) has documented cyclic bursts of regional seismicity along subduction zones. We propose a similar pattern of seismic "supercycles" along the southern half of the San Andreas fault. In this model, elastic strain accumulates continuously along the fault at a rate equivalent to the late Holocene slip rate and is released unevenly, in episodes of seismic activity. One or more large earthquakes, a "cluster," occurs during the latter part of a supercycle, after centuries of relative seismic quiescence.

Clusters of earthquakes may result from incomplete strain release during large earthquakes. Inversions of seismic waveforms and observations of surface slip indicate that the amount of slip on a fault surface varies spatially in large earthquakes (Wald, 1992; Rubin and McGill, 1992; Grant and Donnellan, submitted). Over time, the slip must even out and slip gaps, or asperities, must fail if the fault slip rate is to stay constant (Wald, 1992). Sequential earthquakes, i.e. a cluster, may occur until local accumulated strain is entirely relieved and the fault can "heal". Fault healing, perhaps due to mineralization at depth along fractures opened to pore fluids during an earthquake, may proceed simultaneously with strain accumulation during a period of quiescence, until stresses exceed the strength of the healed fractures,

or a rupture propagating from a distant section of the fault triggers renewed seismicity.

Regardless of the model used to describe earthquake recurrence, the irregular pattern of large prehistoric earthquakes on the southern half of the San Andreas fault has major implications for the validity of assumptions underlying several earthquake forecasting models. Many of these models were developed from studies of the San Andreas fault, including the Carrizo Plain, and then applied to other faults. The characteristic earthquake model (Schwartz and Coppersmith, 1984) is one example. This model assumes the existence of a Carrizo "segment" of the San Andreas fault (Rundle, 1988; Sykes and Nishenko, 1984; Stuart, 1986) that breaks only in repeated, similar, great earthquakes several centuries apart. However, the idea that the San Andreas can be divided into discrete fault segments with characteristic properties is questionable. Unlike the Wasatch fault zone, which is segmented along discrete faults (Schwartz and Coppersmith, 1984), there is no simple basis for determining segment boundaries along most of the San Andreas with the exception of the continuously creeping section in central California. Paleoseismic data and physical fault models suggest variability rather than regularity in seismic slip. Slider-block models of strike-slip fault behavior over multiple earthquake cycles show that the locus of peak slip shifts back and forth over several blocks (King, 1991). Each block has the same physical, i.e. characteristic, properties throughout the experiment, yet the blocks behave differently over several earthquake cycles. If the blocks are an appropriate model system for the San Andreas, the behavior of fault segments may vary with time.

Furthermore, calculations of earthquake probabilities for the Carrizo and Mojave "segments" are questionable because they are based on

"characteristic" properties of each segment, and a time-predictable model (WGCEP, 1988). A characteristic property attributed to the San Andreas fault in the Carrizo Plain is great strength (Sykes and Seeber, 1985; Stuart, 1986; Rundle, 1988; Sieh *et al.*, 1989). If the strength of a fault "segment" is defined by the repeat time of large earthquakes, then the Carrizo is not inherently stronger than the Mojave. The longest interval in the Carrizo Plain in this millenium is ~1450 to 1857. At Pallett Creek it is not much shorter - ~1480 to 1812. Furthermore, if the properties of a fault segment are defined by the amount of slip and length of rupture during large earthquakes, then the Carrizo segment may be similar to the Mojave segment. Salyards *et al.* (1992) measured approximately 6 m of slip across the San Andreas fault zone during each of the 1812 and 1857 earthquakes at Pallett Creek. In the Carrizo Plain, slip varied from 6.6 to 10 m on the surficial trace of the fault during the 1857 earthquake (Grant and Donnellan, submitted). Slip in earlier events is not known accurately enough for comparison. Both segments of the fault appear to have ruptured during great earthquakes similar to the 1857 earthquake, and during smaller (?) events such as C or E, and the 1812 earthquake. Thus, inherently greater strength of the Carrizo segment of the fault is not supported by recent data.

If the temporal pattern of large earthquakes on the San Andreas is irregular, and if the amount of surficial slip is only roughly proportional to the time between earthquakes (Salyards *et al.*, 1992; Grant and Donnellan, submitted), then the time-predictable model (Shimazaki and Nakata, 1980) would forecast earthquakes with large uncertainties. Calculations of earthquake probability and forecasts should incorporate models of irregular earthquake occurrence. A clustered earthquake model is only one of several possible models which could fit the small set of paleoseismic data. The

model describes temporal patterns of past earthquakes at only 3 discrete sites along the southern San Andreas fault. Nonetheless, it is an improvement over theoretical models of regular earthquake recurrence proposed for the Carrizo Plain (Sieh *et al.*, 1989). As more dates become available, our ability to detect patterns of past earthquakes will improve and increase our confidence in forecasting future earthquakes.

In applying our model to forecast earthquakes, the challenge lies in recognizing the presence of an earthquake cluster at the end of a seismic "supercycle". The time since the last earthquake in the Carrizo Plain (136 years) is approximately the same as the maximum calculated recurrence time within the event B, C, D, E cluster, but much less than the 350 to 450 years between event B and the 1857 earthquake. Is the Carrizo Plain within an earthquake cluster at the end of a supercycle and therefore likely to rupture again soon, perhaps triggered by a Parkfield earthquake? Or is it between earthquake clusters in mid-cycle with a low probability of an event as predicted by the Working Group on California Earthquake Probabilities (1988)? We can speculate that the low level of background seismicity in the Carrizo Plain implies that this section of the San Andreas is between earthquake clusters and has a low probability of rupture. If temporal clusters of earthquakes are indeed a dominant feature of seismic cycles, then the San Bernardino and Coachella Valley sections of the San Andreas may be more likely than the Carrizo Plain to generate large earthquakes in the near future. The southernmost part of the San Andreas has not ruptured historically and may have been between earthquake clusters for several centuries. Recent seismicity may indicate that the southern San Andreas fault is approaching a new cluster of earthquake activity.

Acknowledgments: We thank Leonard Bidart for permission to excavate Bidart Brothers property. Heidi Anderson, Manuel Berberian, Stefanie Brachfeld, Linda Maepa and Mike Slates contributed in the field. D&L Construction excavated the trenches. Topographic data was collected with a Wild TC2000 purchased with a grant from the W.M. Keck Foundation. Samples were dated at the NSF Accelerator Facility at the University of Arizona and were partially funded by NSF grant EAR85-12761. We thank reviewers for helpful suggestions that led to improvements of the manuscript. This work was supported by USGS NEHRP grants 14-08-0001-G1370, 14-08-0001-G1789, 1434-93-G-2331 and a graduate fellowship from Leighton and Associates. This is Caltech Division of Geological and Planetary Sciences contribution #5250.

References

- Blong, R.J. and R. Gillespie (1978). Fluvially transported charcoal gives erroneous ^{14}C ages for recent deposits, *Nature*, **271**, 739-741.
- Bonilla, M. G. and J.J. Lienkaemper (1990). Visibility of fault strands in exploratory trenches and timing of rupture events, *Geology*, **18**, 153-156.
- Clark, M. (1972). Surface rupture along the Coyote Creek fault. In *The Borrego Mountain Earthquake of April 9, 1968. U. S. Geol. Surv. Prof. Paper 787*, 55-86.
- Fumal, T. E., S. K. Pezzopane, R. J. Weldon II and D. P. Schwartz (1993). A 100-year average recurrence interval for the San Andreas fault at Wrightwood, California, *Science*, **259**, 199-203.
- Grant, L. B. and A. Donnellan (submitted). 1855 and 1991 surveys of the San Andreas fault: implications for fault mechanics, *Bull. Seism. Soc. Am.*
- Grant, L. B. and K. Sieh (1993). Stratigraphic evidence for seven meters of

- dextral slip on the San Andreas fault during the 1857 earthquake in the Carrizo Plain, in press *Bull. Seism. Soc. Am.*
- Huang, J. and D. L. Turcotte (1990). Evidence for chaotic fault interactions in the seismicity of the San Andreas fault and Nankai trough, *Nature*, **348**, 234-236.
- Jacoby, G., P. Sheppard and K. Sieh (1988). Irregular recurrence of large earthquakes along the San Andreas fault - Evidence from trees, *Science*, **241**, 196-199.
- King, C. (1991). Multi-cycle slip distribution along a laboratory fault, *J. Geophys. Res.*, **96**, 14377- 14381.
- Matsuda, T., Y. Ota, M. Ando and N. Yonekura (1980). Fault mechanism and recurrence time of major earthquakes in southern Kanto district, Japan, as deduced from coastal terrace data, *Geol. Soc. Amer. Bull.*, **89**, 1610-1618.
- Meisling, K. and K. E. Sieh (1979). Possible emplacement history of a sandblow structure at Pallett Creek, California, in *Geological Excursions in the Southern California area*, P.L. Abbott, ed., San Diego State University, Dept. Geol. Science, San Diego Calif., 63-66.
- Meisling, K. E. and K. E. Sieh (1980). Disturbance of trees by the 1857 Fort Tejon earthquake, California, *J. Geophys. Res.*, **85**, 3225-3238.
- Nelson, A. R. (1992). Discordant ^{14}C ages from buried tidal-marsh soils in the Cascadian subduction zone, southern Oregon coast, *Quaternary Research*, **38**, 74-90.
- Prentice, C. S. and K. Sieh (1989). A paleoseismic site along the Carrizo segment of the San Andreas fault, central California, *Eos, Trans, Amer. Geophys. Union*, **70**, 1349.

- Rubin, C. R. and S. F. McGill (1992). The June 28, 1992 Landers earthquake: slip distribution and variability along a portion of the Emerson fault, *Eos, Trans. Amer. Geophys. Union*, **73** no. 43, 362.
- Rundle, J. B. (1988). A physical model for earthquakes 2. Application to Southern California, *J. Geophys. Res.* **93**, 6255-6274.
- Salyards, S. L., K. E. Sieh and J. L. Kirschvink (1992). Paleomagnetic measurement of non-brittle coseismic deformation across the San Andreas fault at Pallett Creek, southern California, *J. Geophys. Res.* **97**, 12457-12470..
- Scholz, C. H. (1990). Earthquakes as chaos, *Nature*, **348**, 197-198.
- Scholz, C. H. (1990b). *The mechanics of earthquakes and faulting*, Cambridge University Press.
- Schwartz, D. P. and K. J. Coppersmith (1984). Fault behavior and characteristic earthquakes: Examples from the Wasatch and San Andreas fault zones, *J. Geophys. Res.* **89**, 5681-5698.
- Shimazaki, K. and T. Nakata (1980). Time-predictable recurrence model for large earthquakes, *Geophys. Res. Let.*, **7**, 279-282.
- Sieh, K. E. (1978). Slip along the San Andreas fault associated with the great 1857 earthquake, *Bull. Seism. Soc. Am.*, **68**, 1421-1448.
- Sieh, K. E. (1986). Slip rate across the San Andreas fault and prehistoric earthquakes at Indio, California (abstract), *Eos Trans. AGU*, **67**, 1200.
- Sieh, K. E. and R. H. Jahns (1984). Holocene activity of the San Andreas fault at Wallace Creek, California, *Geol. Soc. Am. Bull.* **95**, 883-896.
- Sieh, K. E., M. Stuiver and D. Brillinger (1989). A more precise chronology of earthquakes produced by the San Andreas fault in Southern California, *J. Geophys. Res.* **94**, 603-623.

- Smith, B. N. and S. Epstein (1971). Two categories of $^{13}\text{C}/^{12}\text{C}$ ratios for higher plants, *Plant Physiol.*, **47**, 380-384.
- Stuart, W. D. (1986) Forecast model for large and great earthquakes in Southern California, *J. Geophys. Res.* **91**, 13771-13786.
- Stuiver, M. and P.J. Reimer (1986). Computer program CALIB, *Radiocarbon*, **28**, 1022-1033.
- Sykes, L. R. and S. P. Nishenko (1984). Probabilities of occurrence of large plate rupturing earthquakes for the San Andreas, San Jacinto, and Imperial faults, California, *J. Geophys. Res.* **89**, 5905-5927.
- Sykes, L. R. and L. Seeber (1985). Great earthquakes and great asperities, San Andreas fault, southern California, *Geology*, **13**, 835-838.
- Thatcher, W. (1989). Earthquake recurrence and risk assessment in circum-Pacific seismic gaps, *Nature*, **341**, 432-434.
- Wald, D. J. (1992). Rupture characteristics of California earthquakes, Ph.D. thesis, California Institute of Technology, Pasadena.
- Ward, S. N. (1992). An application of synthetic seismicity in earthquake statistics: the middle America trench, *J. Geophys. Res.*, **97**, 6675-6682.
- Weldon, R. J. II (1991). Active tectonic studies in the United States, 1987-1990, in U.S. National Report to International Union of Geodesy and Geophysics 1987-1990, *Rev. of Geophys.*, 890-906.
- Wesnousky, S. G. (1986). Earthquakes, Quaternary faults, and seismic hazard in California, *J. Geophys. Res.* **91**, 12587-12631.
- Working Group on California Earthquake Probabilities (1988). Probabilities of large earthquakes occurring in California on the San Andreas fault, *U. S. Geol. Surv. Open File Report* , **88-398**.

Appendix A

Notes on Plant Species in the Carrizo Plain and Temblor Range

Plant information summarized below was obtained from the following references:

Twisselman, Ernest C., *A Flora of Kern County, California*, Wasmann Journal of Biology, vol. 25, nos. 1 and 2, Spring and Fall 1967, The University of San Fransisco. (illustrated by Eben and Gladys McMillan).

Barbour, Michael G. and Jack Major, eds., *Terrestrial Vegetation of California*, California Native Plant Society, Special Publication Number 9, Univ. of Calif. Davis, 1988.

Hubert, E. and K. Kakiba-Russell (1991). *Carrizo Plain Natural Area: A checklist of vascular plants*, California Energy Commission.

Common or occasional shrubs, subshrubs or trees of the saltbush, grassland, subshrub, juniper or juniper oak plant communities distributed in the Elkhorn Plain and foothills of the Temblor Range include:

Eastwoodia elegans (eastwoodia)

Ericameria/Haplopappus linearifoila (linear-leaved goldenbush)

Haplopappus acradenius ssp bracteosus (pale-leaf goldenbush)

Gutierrezia bracteata (matchweed, snakeweed)
Cleome isomeris or *Isomeris arborea* (bladderpod)
Atriplex polycarpa (common saltbush)
Atriplex spinifera (spiny saltbush)
Ceratoides/Eurotia lanata (winter fat)
Juniperus californica (Calif. juniper)
Ephedra californica (mormon tea)
Quercus douglasii (blue oak) scarce in Elkhorn
Yucca whipplei ssp. *caespitosa* (yucca)
Eriogonum fasciculatum ssp. *polifolium* (gray Calif. buckwheat)
Astrogalus oxyphysus (Diablo loco)

Of the above, *Atriplex polycarpa* and *Juniperus californica* were once more common.

Eben McMillan (personal communication 1992) thinks that *Eastwoodia*, saltbush and juniper are the longest lived species in my field area. *Ephedra* may also live a long time. He thinks the bushes live longer than the junipers, based on his observations of individual plants over a lifetime. In 70 years of observation, he has seen no change in several of the junipers, so he suspects they live at least 200 years, and probably longer. Juniper fence posts over a hundred years old are still in pretty good condition, so they resist weathering fairly well. (Note: at least one juniper survey marker remains from 1855 Freeman survey!) *Eastwoodia* is the most common shrub in my field area. He thinks that no viable seeds from *Eastwoodia* have ever been found, "so it must live a long time." Saltbush also grows a long time and resprouts after it has been burned, unlike the junipers.

Twisselman: North slopes of Temblor canyon have Douglas oaks and Calif. junipers. The southern slopes have upper Sonoran grasslands and scattered shrubs. "A modified form of the Lower Sonoran grassland occurs at high elevations in the arid southern Temblor Range." (p. 70), and only one shrub, *Atriplex polycarpa*, is "at all widespread" in the Lower Sonoran Grassland community (p.91). He also describes a Douglas Oak Woodland plant community "in favorable places in the Temblor Range" (p.96), with *Quercus Douglasii*, *Quercus lobata* and *Juniperus californica*. Along the east side of the Temblor Range, the most common shrubs are *Haplopappus linearifolius* and *Eriogonum fasciculatum* ssp. *polifolium*. *Eastwoodia* is also mentioned. The west side of the Temblor Range is not described.

Eastwoodia is part of the Upper Sonoran subshrub association in the Temblor Range, and is limited in distribution to local, highly specialized plant communities on hot dry slopes where it often grows in colonies. It is a member of the Aster tribe of the Sunflower family. *Juniperus californica* forms a distinctive local plant association in the Temblor Range. It was used by early settlers for fence posts ("many of which are still in service") and corrals. "...Extremely slow growing in the wild.." p.172.

Barbour and Major: "In stable, old communities, creosote bushes or clones may attain ages of several thousand years as a consequence of vegetative segmentation" (p.837). *Atriplex polycarpa* is found in some creosote bush scrub communities. Barbour and Major include it on a list of "important long-lived species" (p.844) Studies of *Quercus douglasii* saplings and small trees in the Santa Lucia Range show them to be 60 - 100 years old (p.395). Juniper is found in pack rat middens which are 8000 to 29000 years

old, in the Mojave desert.(p170). In the Temblor Range, *Juniperus californica* occurs in association with *Eriophyllum confertiflorum*, *Ephedra californica* and *viridis*, and *Yucca whipplei* (p.818). About half of all chaparral species can resprout from a root crown burl. The burls can be 250+ years in age (p.447).

Appendix B

Description of Section Corner Monuments and Distances Between Selected Monuments

This appendix contains a description and brief history of section markers near the San Andreas fault in the northern Carrizo Plain, San Luis Obispo county, California, from the southeastern edge of the Bidart fan to a few kilometers northwest of Wallace Creek (see location figures in chapter 3) in T30S R20E and T31S R20E. The area was originally surveyed and monumented by James E. Freeman in 1855 and 1856, prior to the Fort Tejon earthquake in 1857. The survey covered California Valley and extended to the base of the "Broken Mountains," or Temblor Range. Since the San Andreas fault lies slightly west of the range front, several section lines spanned the fault. Very little development has occurred in the Carrizo Plain since the original survey, and therefore very few surveys have been made since the original ones.

Most of the Temblor Range and Elkhorn Plain were first surveyed several decades after the 1857 earthquake, in 1871 and 1893. These surveys frequently mentioned section markers at the boundaries of Freeman's surveys, and noted that several markers were lost. Records of the original surveys, and some resurveys were obtained from the Bureau of Land Management (BLM), Cadastral Survey office, Sacramento, California. (The existence of 1855 and 1856 Carrizo Plain surveys was brought to my attention by Larry Vredenburg of the BLM office in Bakersfield, California).

Government surveys are recorded by the BLM on microfiche. The microfiche contain reproductions of original field notes, typed transcriptions of field notes, and survey plattes. The histories of the section markers discussed herein were obtained primarily from the BLM microfiche records.

Private surveys made by licensed surveyors in San Luis Obispo county, California, must be filed with the county Survey Records Office. I searched for records of resurveys in T30S R20E and T31S R20E. There are NO recorded resurveys on file with the county. A title search was also done to look for resurveys. No resurveys were mentioned, except for the subdivision of California Valley in 1960. If resurveys were ever recorded with the county, the records were probably destroyed by a 1981 fire (personal communication, Jack Hunter, Pacific Coast Engineering, San Luis Obispo, CA.). Section markers A and B (see below) have obviously been remonumented. A California Valley subdivision map on file with the county shows an "iron pipe" at both A and B. The subdivision field notes were destroyed by fire. Thus, except for the California Valley subdivision, very few private resurveys have been made, and these surveys have not been recorded.

Surveying convention and most government surveying standards require that degraded monuments be replaced in exactly the same location. "Lost" monuments, however, are proportionally reset and may not be replaced in their original locations. Thus, a section marker which has been remonumented, but not recorded, may have been reset proportionally, and is not reliable. Original monuments, although degraded, are most reliable.

A description of each marker, and its recorded history, follows. Information is included for markers which were not used in the study but were researched for possible use. Photographs of monuments D, E, H and J are in appendix C. Directions are given to monuments which are most

difficult to find. All township and range lines are referenced to the Mount Diablo Meridian, California. Topographic quadrangle maps are USGS 7.5' series, California.

All field data was collected jointly with Andrea Donnellan, in 1991. Descriptions are transcribed from my notes. I researched the history of the markers.

Monument :A

Location: T30S R20E, corner of sections 20,21,28,29; McKittrick Summit Quad

Description/History: Established by James Freeman in 1856. He placed a pint of charcoal at the base of a mound and marked it with a post. In 1893 Carpenter reported finding a post, 4 inches square, firmly set and marked, but no mound. He accepted the post as Freeman's original monument. In 1991, Grant and We found a cylindrical metal pipe, 7 cm diameter, capped with a plate marked "TWP30 SR20E sec 20 sec 21 sec 28 sec 29 54". We accept this as the current monument. Surveyed by We in 1991. A hollow iron pipe, 5 cm diameter, is located 5.5cm away, bearing 278 degrees. 2 cm N30E from the monument is a 4cm by 4 cm square weathered wood "fragment." All three markers are located approximately 20 cm away from a square wooden fence corner post, visible from Elkhorn Road. There is no record of remonumentation of this section corner on file with the San Luis Obispo (SLO) County Surveyors Office. The county has a numbering system for reset monuments. SLO County monument #54 is located far from the Carrizo Plain, and there is no record of remonumentation of A in 1954. Monument A has obviously been reset since 1893. Since the distance between A and B, which span the San Andreas fault, is almost precisely one mile (Table B-1), monument A was probably not reset in its original location. (A and B may

have been reset from Q, which is not in its original position. See monument Q, below.)

Monument B:

Location:T30S R20E, corner of sections 29,28,33,32; McKittrick Summit Quad

Description/History: A 6.5 cm diameter cylindrical metal pipe is located beneath an east-west trending barbed wire fence, approximately 18 cm west of a charred square wooden fence post. The pipe is capped with a plate engraved "TWP30 R20E sec 28 sec 29 sec 32 sec 33 55." Surveyed by Grant and Donnellan in 1991. A smaller cylindrical iron pipe is located between the monument and the fence post. In 1991, the monument was buried under approximately 1 m of decaying tumble weeds. To reach monument, drive southeast on Elkhorn Road from 7-Mile Road. Turn right on Simmler/Soda Lake/San Diego Crk Rd. and proceed south to the first section fence line. Park and walk west along the fence to the (broken) intersection with the N-S fence. Look for square post. Clear tumble weeds.

As with monument A, there is no record of remonumentation on file with San Luis Obispo County. The monument was originally established in late 1855 or early 1856 by Freeman. He placed a pint of charcoal, a post, and a mound at the corner. I found no other reference to this corner. It was probably not reset in its original location.

Monument C:

Location: T30S R20E, southern corner of sections 32 and 33, southern boundary of township; McKittrick Summit Quad

Description/History: Originally set by Freeman when he was establishing the township boundaries in 1855. He placed a pint of charcoal and a post in a mound. The corner is marked on Carpenter's 1893 plat, but is not described in his notes - or if it is, I couldn't find it! In 1983 DeJarnatt found a "deeply

embedded mound of stone 2 1/2 feet diameter, no marks visible" near a telephone pole and accepted it as the best available evidence of the corner location. He remonumented the corner with an iron pipe extending 6" above ground in a stone mound, with a magnet at the base and a brass cap engraved with the section corners and townships. We found his marker labelled with township, range sections and "US Dept. of the Interior Bureau of Land Management. Cadastral Survey," approximately 1 foot southwest of a telephone pole west of Simmler/Soda Lake/San Diego Creek road. Surveyed by Grant and Donnellan in 1991. This monument may be in the original location. However, we consider its location suspect because monuments B and A to the north are thought mislocated, and because the 1983 mound may have been established when the telephone lines were set.

Monument D:

Location:T30S R20E, southern corner of sections 33 and 34, southern boundary of township; McKittrick Summit Quad

Description/History: Established in 1855 by James E. Freeman. He placed charcoal at the base of a mound and placed a post in the mound to mark the corner. In 1893 Carpenter found the original monument and described it as a post, 4 inches square, firmly set and marked. DeJarnatt found an old, tilted, wooden stake or post in 1983 and accepted it as the original marker.

Therefore he did not remonument it. We found, and surveyed, a decayed 30 cm high wooden post, 12 cm maximum width at its base, tilted northward. It is located beneath a north-south trending barbed wire fence south of a 3 1/2 foot high square wooden fence post. To reach the monument, drive 2/10ths of a mile southeast of the Wallace Creek section line fence cattle guard on Elkhorn Road. Stop. Walk downstream (toward the valley) along a ~10-ft-deep gully to a north-south fence. Find the wooden post a few meters south

of the thalweg. We accept this monument as Freeman's original section corner!

Monument E:

Location:T30S R20E, southern corner of sections 34 and 35, southern boundary of township; McKittrick Summit Quad

Description/History: Established by James E. Freeman in 1855. On the bank of a channel, he placed a post in a "mound," with a charred stake at the base. It was found in 1893 by Carpenter. He described it as a juniper post 4 inches square, marked, 2 1/2 feet above ground **in a mound of stone 1 foot high** (emphasis mine). The 1955 USGS McKittrick Summit topographic quadrangle map shows a section corner marker found at the expected location. There is no record of remonumentation on file with San Luis Obispo county or the BLM. I tried to obtain a description of the section marker from the field notes of the USGS cartographers who field checked the topographic map. The original notes were disposed of in the 1980's.

In 1991 we found a diffuse mound of stones approximately 1/2 foot high on the side of an incised stream channel. We searched the area repeatedly for a more prominent and/or better preserved candidate monument, finding none. We also searched the channel walls and neighboring plateau for similar diffuse mounds of stones, finding no comparable candidates nearby. There are no fences, fenceposts or roads within several hundred yards of the candidate monument. After discussions with Daniel Manion, the "Monumentation Specialist" with the San Luis Obispo County Surveyors Office, we concluded that the candidate mound of stones is probably the original monument. There is no record of remonumentation. We returned to survey it. We placed a plastic tomato stake at our best estimate of the center of the mound, allowing for a few

centimeters of downhill creep of the stones. The survey was centered on the tomato stake.

To reach monument E, drive southeast on Elkhorn Rd. Turn left (north) on a dirt road between Phelan Creeks and Phelan fan (Chapter 2). The road crosses the boundary between sections 2 and 3, T31S, R20E. Proceed northeast until a fence corner is found. Walk approximately half a mile due west of the road. Good luck!

Monument F:

Location:T30S R20E, southern corner of sections 35 and 36, southern boundary of township; McKittrick Summit Quad

Description / History: Post, mound and charred stake set by Freeman in 1855. Found by John Reed in 1871. Found in 1893 by Carpenter. He described it as a marked juniper post, 4 inches square, 3 feet above ground in a mound of stone 1 1/2 feet high. In 1991 we found several candidate weathered posts in the approximate vicinity, but no mounds. The best candidate is an old wooden post, 3 1/2 inches square, rising 4 inches above ground. However, we could not determine which, if any, of the posts might have been the original. Crooked fences nearby suggest that the section corner has been lost. This section corner is on the boundary between Kern and San Luis Obispo counties. There is no record of a monument on file with SLO county. We consider the monument to be lost.

Monument G:

Location: T31S R20E, corner of sections 1,2,11,12. Painted Rock Quad.

Description/History: Established by James E. Freeman in 1856. He set a post in a mound above a deposit of charcoal. No further reference found, except on USGS 1959 topographic quad. map which shows section corner found, and an elevation of 2265 feet. We were unable to locate the monument on three

separate trips. We surveyed a reference marker approximately .1 mile south of the expected location of the true corner. The reference marker consists of a cairn of 2 rocks of maximum dimensions 30 cm and 20 cm, under a fence trending approximately N2-5W. The fence is relatively new (10-20 years old?) and changes trend several times. The true corner is probably lost.

Monument H:

Location: On the range line between T31S R20E and R21E. Southeast corner of sec 1, northwest corner of sec 12, T31S R20E. Painted Rock Quad.

Description/History: Established by James E. Freeman in 1855 with a post, a mound and a charred stake. Found by Howard Carpenter in 1893. He described a post, 4 inches square, firmly set, 2 feet above the ground surface, marked with a 2 foot high mound 4 1/2 feet in diameter. In 1991 we found a 6 foot high square (18cm x 17cm) wooden post a bend in a barbed wire fence. The fence does not extend to the north. It extends southward across the valley, in an apparently straight line along the rangeline, and N58W toward corner F, zigzagging markedly. Both fences have some weathered posts which look like old juniper branches. Three weathered (juniper?) posts from an abandoned fence line trend toward the existing fence corner. Approximately 53 cm from the corner post, under the N58W trending fence, is a 1 inch diameter rusted iron pipe and a 1 1/2 inch square wooden post extending 1 inch above ground.

There is no record of remonumentation of the corner. The abandoned fence line and weathered posts in the current fence, the unusual height of the corner post, and the iron pipe, indicate that this location has marked a local boundary for many years. We suspect that the original monument was located at the large post, the iron pipe, or between them. We surveyed both the iron pipe, our preferred choice for the original monument location, and

the base of the large corner post. (There is only a few centimeters difference in the north-south distance between either monument and corner J, a mile to the south.)

Monument I:

Location: T31S R20E, corner of sections 11, 12, 13 and 14. Painted Rock Quad.

Description/History: Established in 1856 by James Freeman, with charcoal, a post and a mound. No further record. Shown as found on USGS 1959 topographic quad, with an elevation of 2108 feet. I searched 1966 air photos. Not visible. A section-line fence was built after 1966 photos and prior to 1989. Searched for evidence of section corner along the fence and away from the fence. No monument was found. We occupied and surveyed a "new" cylindrical fence post near the apparent location of the corner.

Monument J:

Location: T31S R20E, southeast corner of sec. 12, northwest corner of sec. 13. On the rangeline between T31S R20E and T31S R21E. Painted Rock Quad.

Description/History: Established by James Freeman in 1855 with a post, a mound and a charred stake. Found by Harris in 1874, no description. No further record, except that it is marked as found on the 1959 topo. map. A fence runs along the apparent rangeline. It extends northward to monument H and southward across southern California Valley. The fence near the expected location of monument J is relatively new. The fence posts are cylindrical, wooden and unweathered, except for one slightly weathered, square wooden post. In 1991 there were several weathered planks scattered near the post. The planks looked older than any of the fence posts. At the base of the older square post is a boulder of at least 35 cm diameter. The boulder is partially buried by dirt from the steep slope. Several surveys of the Temblor Range and southern Carrizo Plain during the late 1800's used

boulders rather than posts to mark section corners, as allowed by the Manual of Surveying Instructions. The boulder is obviously not Freeman's original monument. However, it appears to mark a locally accepted section corner. Since the original monument survived the earthquake (mentioned by Harris in 1874) and has not been reset by a recorded survey, we think it is very likely that the boulder marks the location of the original, decayed monument, and therefore we accept it as the best location of the section corner.

Monument L1:

Location: T31S R20E southeast corner of sec13, northeast corner of section 24, on the rangeline between R20E and R21E. Painted Rock Quad.

Description/History: Established by James Freeman in 1855. In 1983 DeJarnatt found an iron pipe which he accepted as the best representation of the corner. He found the pipe by traversing from a corner 4 miles to the west. He did not find any intermediate section corner or quarter section corner monuments. DeJarnatt remonumented the corner. We found his monument, labelled "US Dept. of the Interior Cadastral Survey Bureau of Land Management 1983" with the township, range and section numbers. The monument is within the San Andreas fault zone. It is very unlikely that it is in the same location as Freeman's 1855 monument (see L, below). We surveyed it for reference.

Monument L:

Location: near T31S R20E southeast corner of sec13, northeast corner of section 24, on the rangeline between R20E and R21E. South of L1.

Description/History: Origin unknown. Since the 1855 monument would have been destroyed if it was originally placed in the San Andreas fault zone, we searched the area near monument L1 for candidate markers outside the fault zone. Since DeJarnatt traversed 4 miles to L1, we hypothesized that he might have intersected the rangeline north or south of the actual corner. We

searched the area near monument L and found a rusted iron pipe about 100 meters to the south of monument L1, next to a 6 foot high square wooden fence post. The post has a round metal washer inscribed KU 631. We surveyed the pipe for comparison with monument L. Results of the survey indicate that L is not located at the original corner. Since L1 is in the fault zone, for this study we consider the original corner "lost."

Monument N:

Location: T31S R20E, corner of sections 23,24,25 and 26. Painted Rock Quad.

Description/History: Established by Freeman in 1855 or 1856 with charcoal, a post and a mound. In 1983 DeJarnatt found an old wooden post which he accepted as the corner. He marked the post with a nail and washer. DeJarnatt placed an iron pipe with a brass cap and magnet 2 feet away from the post. We found We found DeJarnatt's marker. Not surveyed because there are no monuments within a mile which might be in their original locations.

Monument Q:

Location: T30S R20E , corner of sections 21,22,27 and 28. McKittrick Summit Quad.

Description/History: Established by Freeman in 1855 or 1856 with charcoal, a post and a mound. It was apparently found by Reed in 1871, but he did not describe it. It was not found by Carpenter in 1893. He considered it lost. He reset it with a sandstone 16x10x4 inches by measuring from monument D (2 miles to the south, on the opposite side of the San Andreas). Therefore, it is not in its original position. No further record. It is not on the 1959 topo. map.

Monument R:

Location: T30S R0E, corner of sections 27,28, 33 and 34. McKittrick Summit Quad.

Description/History: Established by Freeman in 1856 with charcoal, a post and a mound. Carpenter looked for it in 1893 but did not find it, and did not reset it. It is not shown on the 1959 topographic map. We found a cairn of 2 boulders, approximately 1 foot diameter each, at the base of a fence corner post. The cairn was probably placed between monuments Q and D to reset the corner.

Monument S:

Location: T30S R20E, corner of sections 26, 27, 34 and 35. McKittrick Summit Quad.

Description/History: Established in 1855 or 1856 by Freeman with charcoal, a post and a mound. Apparently found by Reed in 1871, but no description. Carpenter found it in 1893. He described it as a 4 inch square post, 3 feet above ground, marked. It is not shown on the 1959 topo. map, so we did not look for it.

Monument T:

Location: T31S R20E, corner of sections 2,3,10 and 11.

Description/History: Established by Freeman in 1856 with charcoal, a post and a mound. No further record. Not shown on the 1959 topo. map. The expected location of the corner has been buried by a recent debris flow (containing tires and home appliances). We searched for a monument. The corner is lost.

Monument W:

Location:T31S R20E, southeastern corner of section 24, northeastern corner of section 25. On the rangeline between R20E and R21E. Painted Rock Quad.

Description/History: Established by Freeman in 1855 with a charred stake, a mound and a post. No further record. Not shown on the 1959 topo. map. There is a road intersection and cattle guard at the approximate location of the

corner. We surveyed an arbitrary point on the edge of the road for measuring the relative distance to L and L1.

Monument α :

Location: T31S R20E, southeast corner of section 25, northeast corner of section 36, along the rangeline between R20E and R21E. Painted Rock Quad.

Description/History: Established by Freeman in 1855. No further record discovered with cursory search. The 1959 topo map shows the marker. We looked for it in the field. If it exists, it is buried by an impenetrable thicket of decayed tumbleweeds. At the suspected corner, the east-west fenceline is straight. The north-south fence is offset sinistrally by at least a meter (probably several meters).

DISTANCES SURVEYED WITH GPS IN 1991

Line	Horizontal Distance(m)	Δ mile (1609.265m)	Comment
A-B	1608.903	-0.362	
B-C	1617.659	8.394	
C-D	1627.750	18.48	
D-E	1616.713	7.448	
G-I	1442.258	-166.687	G is not the corner
I-J	1609.794	0.530	
H-J	1608.064	-1.201	
J-L	1769.946	160.196	L is not the corner
L-W	1541.487	-67.778	L & W not corners
L1-W	1639.076	29.811	L1, W, not corners

Appendix C

Photographs

This appendix contains photographs to augment data presented in chapters 2, 3 and 4.

Photo C-1: Sharp contact between the scoured margins of channel A-B and the unconsolidated gravel fill exposed in trench 4 on the Phelan fan. View is toward the northeast (upstream). The channel is cut into lithified late Pleistocene siltstone and sandstone beds of unit Qpf. Unit Qpf contrasts markedly with the loose imbricated gravel channel fill (unit Qa1). Scraper is 3 inches wide.

C-3



Photo C-2: Steep-walled channel ≥ 4 meters deep, cut across Elkhorn Road by runoff from storms in March 1991. Theresa Roberts is standing on Elkhorn Road, which runs perpendicular to the channel. This channel was cut in less than two weeks. The channels in the Phelan fan were also cut by stormwater erosion, and subsequently filled with gravels over a time period of several decades, perhaps centuries.

C-5



Photo C-3: View of the piercing line excavation proceeding toward the fault (southwest) from trench 4, on the Phelan fan. The paint brush is slightly below the piercing line. Several nails with colored flags and numbered tags are imbedded in the wall of trench 4. Tag number 32 marks an exposure of the red and black burned horizon.



Photo C-4: Further excavation of the piercing line from trench 4 toward the San Andreas fault. One of the meter sticks is slightly below the piercing line. A root cast forms a 45 degree angle with the meter stick and the piercing line. No faults are visible in the exposure. View toward the fault (southwest) from trench 4.

C-9



Photo C-5: Nails with flagging and numbered white tags mark the trend of the piercing line southwest of trench 3 on the Phelan fan. View is toward the southwest, away from the fault zone.



Photo C-6: Photograph of the fault zone in trench 5 on the Phelan fan. View is toward the northwest. Flagged nails at an elevation of 70 cm (arbitrary datum) mark the top of a bed that correlates with the angular unconformity on the opposite trench wall (see figure 2-8). The angular unconformity is not apparent in this exposure.

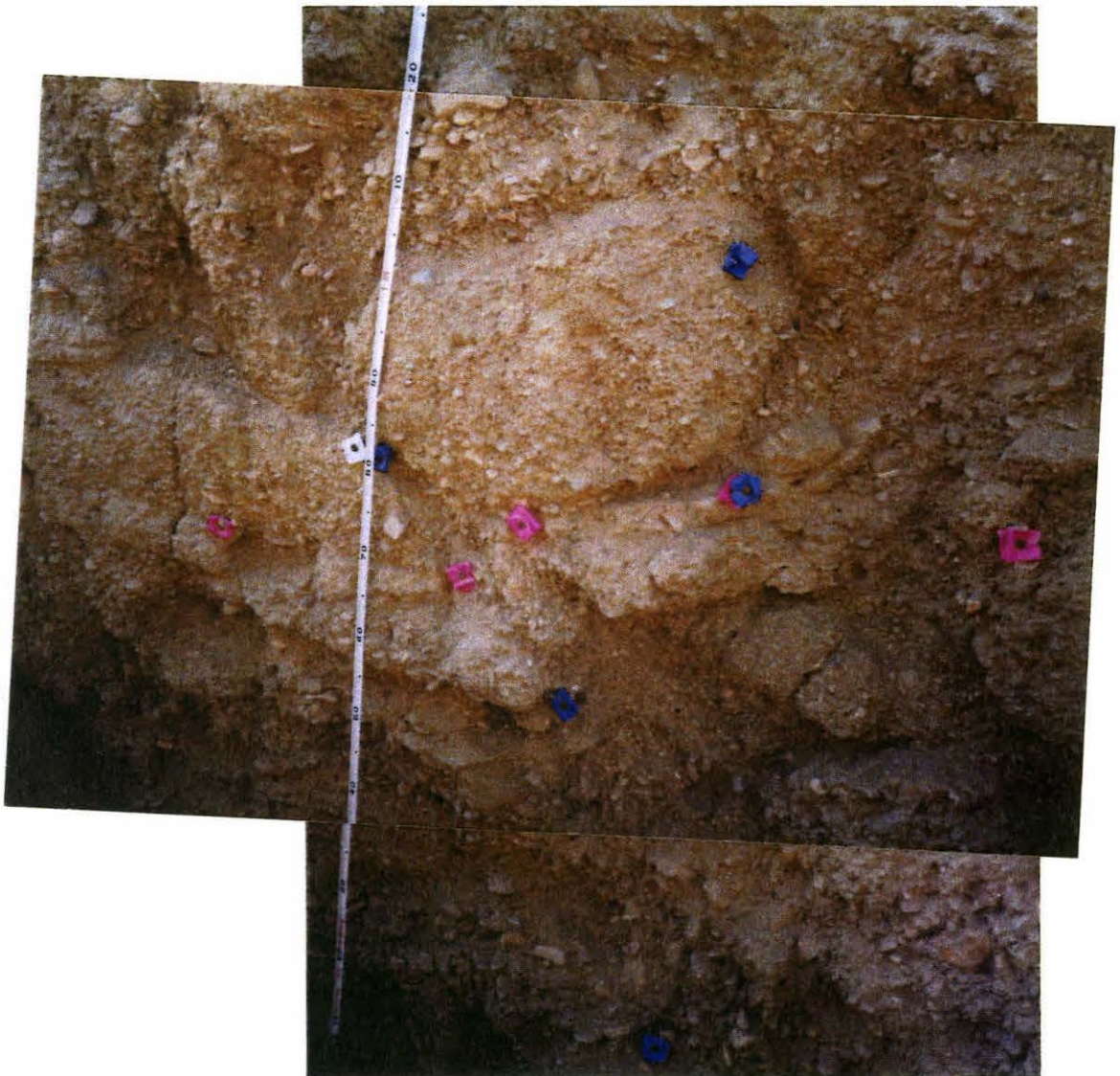


Photo C-7: Monument D, T30S R20E sections 33, 34, and T31S R20E sections 3, 4 in the Carrizo Plain, west of the San Andreas fault. The monument is the weathered, inclined post below the barbed wire fence. The notebook at the base of the marker is approximately 6 inches by 9 inches. View toward the west.

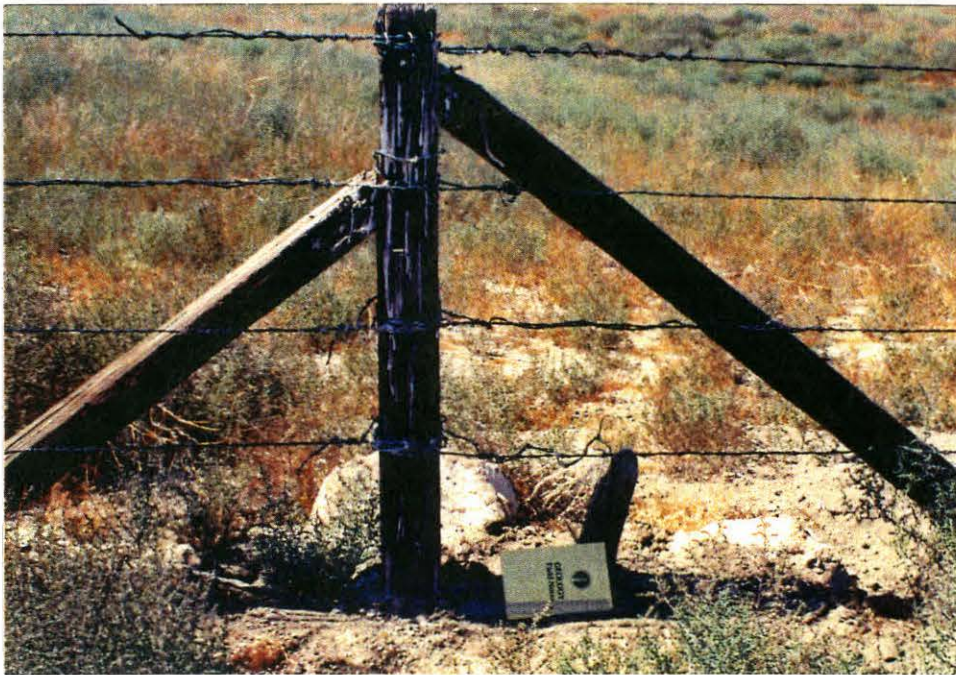


Photo C-8: Photo of monument E, T30S R20E sections 34, 35 and T31S R20E sections 2, 3 in the Carrizo Plain east of the San Andreas fault. The field notebook is approximately 6 inches by 9 inches. A 1 foot ruler is at the outer margin of the monument mound. A flagged "tomatoe" stake marks the estimated center of the monument.



Photos C-9: top) View toward the northeast of the approximate location of corner H at the common eastern corner of sections 1 and 12, T31S R20E in the foothills of the Temblor Range, east of the San Andreas fault. The taller wooden post marked with a ribbon is the locally accepted corner monument. A small iron pipe and stake in the grass west of the post (barely visible) may be the original corner location. The error in the location of the actual corner is the distance between the post and pipe.

bottom) View south from monument H toward monument J in the Panorama Hills. Old cedar fence posts are visible along the current fence. Older, abandoned fence posts west of the current fence are aligned with the current corner post, suggesting that the post marks the location of a section corner in continuous use for a "long" time.



Photo C-10: View of an excavated boulder and relatively new corner post on a hillside at the suspected location of the common eastern corner of sections 12 and 13, T31S R20E, in the Panorama Hills. The boulder and post are defined as monument J. Field notebook is approximately 6 inches by 9 inches.

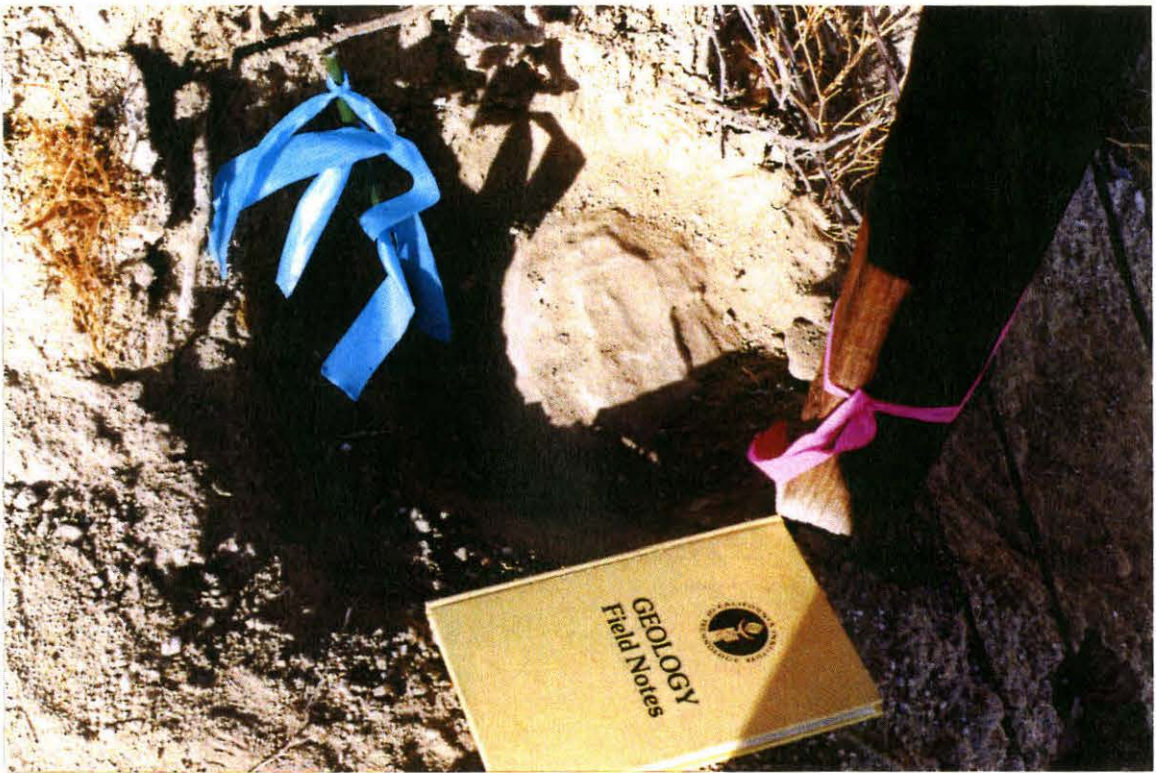


Photo C-11: View downstream, toward the southwest of a channel on the Bidart fan. The channel is offset approximately 7 m by the San Andreas fault. Stefanie Brachfeld is standing on the fault zone. The fault is aligned with Stefanie and the bush. Note the excellent exposure of geomorphic features due to the nearly complete absence of vegetation. Bidart Trench 2 was excavated next to this offset. Figures 2-2 and 4-3 are topographic maps of this offset.



Photo C-12: Photograph of the paleosol at the surface of unit 8 in trench 2 on the Bidart fan. The base of the ruler marks the approximate base of the soil. It is 2.5 cm thick at this location. The texture of the organic-rich soil contrasts with the massive sand of unit 7 above it, and the laminated silt and sand of unit 8 below the soil horizon.



Photo C-13: View of the surface of a fresh debris flow on the Bidart fan, April 1991. Pieces of detrital wood are embedded in the sediment. The surface of the flow is smooth. A few weeks after this photo was taken grasses sprouted and began forming a thin soil on the surface of the flow. Lens cap is 5 cm in diameter.

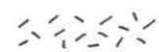
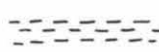




Appendix D



Legend for Plates



LITHOLOGY

 clay

 massive }
 laminated } silt


 massive }
 laminated } sand, fine to medium

 massive }
 laminated } sand, medium to coarse

 massive }
 laminated } granules

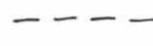
 pebbles

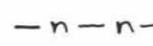
 cobbles


 boulders, to scale

CONTACTS

 sharp


 approximately located

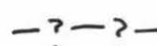
 gradational over n centimeters

 uncertain

FAULTS

 definite

 approximately located


 uncertain location or existence

MISCELLANEOUS SYMBOLS

■ carbon sample location

~~~~~ organic mat or soil horizon

∫ 7 m roots

 rodent burrow

————— fire scar

κ powdery precipitate in fractures.